SOME DYNAMIC AND AEROELASTIC PROBLEMS OF PLATE AND SHELL STRUCTURES

by

YECHIEL SHULMAN

S.B.(Aero. Eng.), Massachusetts Institute of Technology, 1954
S.B.(Ind.Manag.), Massachusetts Institute of Technology, 1954
S.M.(Aero. Eng.), Massachusetts Institute of Technology, 1954

SUBMITTED IN PARTIAL FULFILLMENT OF THE
REQUIREMENTS FOR THE DEGREE OF
DOCTOR OF SCIENCE

MASSACHUSETTS INSTITUTE OF TECHNOLOGY

JUNE 1959

Signature of Author_____
Dept. of Aeronautics and Astronautics, May 18, 1959

Certified by_____
Thesis Supervisor

Accepted by_____
Chairman, Departmental Committee on Graduate Students

SOME DYNAMIC AND AEROELASTIC PROBLEMS OF PLATE AND SHELL STRUCTURES

by

YECHIEL SHULMAN

Submitted to the Department of Aeronautics and Astronautics on May 18, 1959 in partial fulfillment of the requirements for the degree of Doctor of Science.

ABSTRACT

The theory of thin shells is examined and some simplified general expressions are presented. These reduce to Donnell's expressions in the case of circular cylindrical shells. An appropriate variational principle is formulated and the similarity to shallow-shell theory is shown. These results and those of the more exact Flügge shell theory are applied to the problem of free vibration of conical shells. Approximate solutions are obtained by variational methods using the various theories and various displacement and stress functions. Comparison of the results indicates that the method which utilizes a logarithmic transformation of the axial coordinate in conjunction with appropriate displacement expansion modes satisfying the geometrical boundary conditions yields results valid for both the membrane and bending cases and is capable of being used to obtain higher approximations. The results reveal that the influence of taper on membrane and bending frequencies of circular cylinders is opposite in nature, the former being increased, the latter-decreased by the taper.

The general problem of panel and shell flutter is reviewed and a physical explanation of the phenomenon is

offered. A general formulation is given, followed by a method of solution which is named here after Movchan and Houbolt, who apparently developed it independently. The Galerkin method is examined and its characteristics for this problem are discussed. This method is then applied in the solution of the flutter problem of cylindrical and conical shells. Extensive calculations indicate that by taking account of the previously neglected axial bending stiffness of the shell, the nature of the flutter mode is revealed and minimum flutter speeds are obtained, which are much lower than those obtained previously using 'medium shell' theory.

The effect of large thermal stresses on the frequencies of plates under generalized support conditions is investigated. It is shown that whereas before buckling occurs the effect of a rising temperature is to decrease the frequencies, the opposite effect is true after buckling has taken place. The role of the support conditions is stressed.

Thesis Supervisor: Raymond L. Bisplinghoff

Title: Professor of
Aeronautical Engineering

May 18, 1959

Professor Alvin Sloane
Secretary of the Faculty
Massachusetts Institute of Technology
Cambridge 39, Massachusetts

Dear Professor Sloane,

In accordance with the regulations of the faculty, I hereby submit a thesis entitled Some Dynamic and Aeroelastic Problems of Plate and Shell Structures in partial fulfillment of the requirements for the degree of Doctor of Science in Aeronautical Engineering.

Respectfully yours,

Yechiel Shulman

ACKNOWLEDGMENT

The author is indebted to Prof. R.L. Bisplinghoff, the thesis supervisor, for his invaluable advice, guidance and encouragement in conducting this investigation. The association with him has been a constant source of inspiration. Thanks are also due Prof. J. Dugundji and Prof. T.H.H. Pian for many helpful discussions and suggestions during various phases of this research.

Appreciation is expressed to members of the M.I.T. Aeroelastic and Structures Research Laboratory, who assisted in the preparation of this thesis and in particular to Miss Helen Petrides of the Computing Section, who so ably performed the calculations and to Miss Shirley Hogan who did the typing.

Finally, the author wishes to thank his wife for her patience with him throughout this period, and his parents, who made all this possible.

This work was done in part at the M.I.T. Computation Center, Cambridge, Mass. It was sponsored in part by the Office of Scientific Research, U.S. Air-Force, under contract No. AF 49(638), and in part by the Office of Naval Research, U.S. Navy, under contract No. Nonr-1841(22).

TABLE OF CONTENTS

LIST OF SYMBOLS

A_1, A_2	metrics of shell segment (2)*
[A]	stiffness matrix (3)
C^2	thickness parameter $(\frac{1}{12}[\frac{h}{R_o}]^2)$
C_*^2	thickness parameter $(\frac{1}{1-\nu^2} C^2)$
[C]	inertia matrix (3)
C_f	rotational stiffness of edge support (7)
D	bending rigidity
D_i	differential operators (2)
$[D^{(1)}]$	stiffness matrix (6)
$[D^{(2)}]$	aerodynamic matrix (6)
$[D^{(3)}]$	inertia matrix (6)
E	Young's modulus
F	stress function
G	shear modulus
GJ	torsional rigidity
G_1, G_2	functions defined in (3-60)
G_i i=1-4	functions defined in (7A)
H_i i=1-5	functions defined in (3-29) and (3-37)
$H_n^{(1)}$	Hankel function of the first kind, of order n
$H_n^{(2)}$	Hankel function of the second kind, of order n
I_n	modified Bessel function of the first kind, of order n
J_n	Bessel function of the first kind, of order n
K_n	modified Bessel function of the second kind, of order n

* Numbers in ( ) indicate the chapter in which the symbol appears.

K_i i=1-4	functions defined in (3-33)
L	height of cone (3). Wave length (4)
L( )	loading operator (4)
$L_i^{(0)}$, $L_i^{(1)}$	differential operators (5)
M	Mach number. Number of expansion modes (3)
M(∅)	differential operator (4)
M_1, M_2, M_{12}	moment resultants (2)
N_1, N_2, N_{12}	tangential stress resultants (2)
P	nondimensionalization factor (4). Number of expansion modes (7)
Q	bilinear concomitant (4)
Q_1, Q_2	shear stress resultants (2)
Q_i i=1-6 .	functions defined in (7A)
R	radius of cylinder (2,5). Radius of cone (3)
R_o	average radius of cone (3)
R_1, R_2	principal radii of curvature (2)
R_i i=1-5	functions defined in (7A)
S_i i=1-8	functions defined in (7A)
S( )	structural operator (4)
T_i i=1-4	functions defined in (7A)
T	Kinetic energy. Temperature. Tension in membrane (4)
U, U_o, U_1	Strain energy
V	Potential energy. Velocity of flow
$\overline{V}$, $\widetilde{V}$	nondimensional velocity
X	x-component of load
Y	y-variation of plate modes (7)
Y_n	Bessel function of the second kind, of order n
Z	z-component of load

a	speed of sound in air. Plate dimension (7)
a_m	speed of sound in material
a_i i=1-6	functions defined in (3A)
b_i i=1-10	functions defined in (3A)

b	plate dimension (7)
e_1, e_2, e_ζ	strain components (2)
$f(\delta)$	function of δ (3)
$f(x)$	generalized function (4)
g	functional dependence between real and imaginary parts of eigenvalue (4)
h	shell or plate thickness
k	wave number (4A). Reduced frequency (5)
k_y	lateral stiffness of edge support (7)
ℓ	length of cone along generator (3). Length of cylinder (5)
n	number of circumferential waves. Number of waves in buckling mode of plate (7)
Δp	aerodynamic load
q	generalized coordinate (7)
r	distance from vertex of cone (3,6). Radial distance from cylinder axis (5). Temperature ratio (7)
r_o, r_1	distance from vertex of cone to narrow and wide bases, respectively
t	time
u_1, u_2, u_3	displacement components of shell element
u, v, w	midsurface displacement components
x, y, z	cartesian coordinates

α	coefficients of thermal expansion. Semi-vertex angle of cone
α_1, α_2	midsurface metrics
β	logarithmic coordinate (3). $\sqrt{M^2-1}$ (5)
β_1	$\ln \delta_*$
$\gamma_{1\zeta}$, $\gamma_{2\zeta}$, γ_{12}	shear strain components
δ	conical parameter (3). Coefficient of lateral restraint (7)
δ_*	ratio of r_1 to r_o
Δ	conical parameter (3) $([\frac{\sin\alpha}{\bar{\lambda}}]^2)$
ϵ_1, ϵ_2	strain components

ζ	radial coordinate (2). Coefficient of rotational restraint (7)
Θ	circumferential angular coordinate
Θ	Θ-component of load
λ	cylinder aspect ratio $(\frac{\pi R_o}{L})$ (3). Plate aspect ratio $(\frac{a}{b})$ (7). Eigenvalue (4)
$\bar{\lambda}$	"modified" cylinder aspect ratio $(\lambda \frac{\cos\alpha}{f(\delta)})$ (3)
μ	mass ratio (4). $(\frac{1-\nu}{2})$ (3)
ν	Poisson's ratio
ξ	nondimensional length (4A,5)
ξ_1, ξ_2	curvilinear coordinates of shell (2)
Ξ_1, Ξ_2	ξ_1- and ξ_2- components of load
π	variational integral
ρ	material density
ρ_a	air density
σ	wave number (5)
ϕ	mode shape (4). Velocity potential (5.1) Displacement function (5.2)
$\varkappa_1$, $\varkappa_2$, $\varkappa_{12}$	curvature changes (2)
ψ	impulse-response function (5)
ω	circular frequency
Ω	frequency ratio (3). 'Modified' frequency (5)

Subscripts

a	air
m	$m^{\underline{th}}$ mode
o	condition at zero load
R	real
I	imaginary

OBJECT

It is the purpose of this investigation to study the following dynamic and aeroelastic problems: (a) the free vibration characteristics of truncated thin conical shells, (b) the phenomenon of shell flutter as applied to the cases of conical and cylindrical shells, (c) the vibration characteristics of plates in the presence of large thermal stresses.

CHAPTER 1

INTRODUCTION

One of the distinguishing characteristics of the fields of structures and aeroelasticity, as indeed of aeronautical technology in general, is the continuous change that these areas have been undergoing in the past decade. The transition from the subsonic to the supersonic flight regime and the emergence of large missiles have resulted in a host of new problems, which were brought about by the changing structural configurations on the one hand, and the new operational environments on the other. In addition, the necessity to rely on increasingly thinner, lighter, and thus more flexible structures has resulted in aeroelastic considerations becoming of increasing importance in the design of both aircraft and missiles.

Whereas in the past lifting surfaces have been long and narrow, present-day supersonic aircraft have low-aspect-ratio wings, which behave more like plates than beams. Whereas in the past the typical structure was of semi-monocoque design, the advent of ballistic missiles and spacecraft, with their extremely low structural weight requirements, means that relatively unreinforced thin shell structures are becoming of growing importance.

Ever striving towards higher performance and speeds, the engineer must now face not only different structural geometries, but entirely new problems. The effects of kinetic

heating and of high accelerations, structural and aerodynamic nonlinearities, aerothermoelastic coupling and time-varying parameters are all problems which currently occupy the attention of workers in the field, and are all direct results of these efforts. The importance of each of these effects will depend on the configuration and particular mission of the given vehicle. However, the magnitude of the complexities they bring about may be appreciated when one notes that the classical bending-torsion flutter problem is now being superseded by the multiple-degree-of-freedom flutter (possibly of finite amplitude), where the structural and possibly the environmental characteristics change rapidly with time, so that the flutter condition is not unique, but rather depends on the time history of the flight. Needless to say, this adds a new dimension to the problem.

In attempting to rationally analyze these new problems, use must be made of theoretical tools and techniques with which structural analysts and aeroelasticians have had little acquaintance up to now. In particular, familiarity with the linear and nonlinear plate and shell theories of elasticity has now become a must. On the other hand, the great simplification in accounting for the unsteady aerodynamic loads, provided by piston theory, facilitated the analyses of many problems and enabled a better understanding of others.

Of these new problems which were outlined by Bisplinghoff in his Wright Brothers Lecture [1]*, some have already been successfully investigated. Methods of analysis of thermal stresses in built up structures have been developed [2]. Thermal effects on structural stiffness have been the subject of a number of investigations [3,4,5,6]. New approaches to

---

* Numbers in [ ] refer to the numbered references at the end.

the concept of aeroelastic stability under the new conditions have been suggested [7]. Other problems, however, still remain to be solved.

The present work contains some theoretical investigations of cylindrical and conical shell flutter problems and an investigation of a particular plate problem.

In attempting to analyze the problem of aeroelastic instability of shells, it was soon discovered that not only has the "old" problem not been solved satisfactorily, i.e. the linear problem in the absence of thermal and acceleration effects, but that the solution of the free vibration problem of conical shells has also eluded success. It was therefore necessary to tackle these two problems before any other effects are to be incorporated in the analysis.

This investigation, then, develops in the following manner:

Chapter 2 is concerned with the development of a simple thin shell theory, and establishes the analytical tools required in the succeeding applications.

In Chapter 3 the free vibration problem of truncated conical shells is analyzed. Since the nature of the problem makes an approximate solution necessary, various methods of approach are used and compared with one another, and the optimum method is selected. Some results are presented and the way is shown by which higher approximations may be obtained.

Chapter 4 presents a comprehensive review of the phenomenon of panel flutter. It is shown that panel and shell flutter phenomena are fundamentally the same. Included are a physical description of the phenomenon, followed by a generalized formulation, discussion of its analytical aspects and methods of solution of the problem.

In Chapter 5 this discussion is applied to the cylindrical shell case, and the identity between the panel and shell

problems is established. Chapter 6 presents the application to the conical shell case. Numerical results are given in both cases.

The effects of thermal stresses are included in Chapter 7, where these effects are studied as they influence the vibration characteristics of plates, both in the linear and nonlinear range.

Finally, Chapter 8 presents the conclusions which may be drawn from this study.

CHAPTER 2

SOME DEVELOPMENTS IN THIN SHELL THEORY

2.1 Introduction

The fundamental developments of shell theory date back to the last century. However, the efforts to transform the subject from a primarily mathematical theory into an engineering tool have taken place relatively late. Recent trends in airframe design caused a shift in the interest of structural analysts and, to a lesser degree, of aeroelasticians, towards the problems of shell-type structures requiring use of this theory. Therefore this subject which has traditionally been taught as a branch of applied mathematics lately emerged as a course in aeronautical engineering. Many useful analytical tools have been developed for treatment of static and dynamic shell problems. Among these may be mentioned the work of Donnell [8], who developed a simplified theory for cylindrical shells, the work of Marguerre [9] on shallow shell theory, and others. Due to the environmental conditions of high-speed flight, thermal effects on shell structures have become of particular interest. Consequently all methods which are developed for treatment of shell problems must include these effects, which have become a part of the facts of life to the aeronautical engineer.

In this chapter, some tools useful in the analysis of shell problems are presented, following along Vlasov's [52] development. These are later applied in the following chapters to the solution of some specific problems in shell structures.

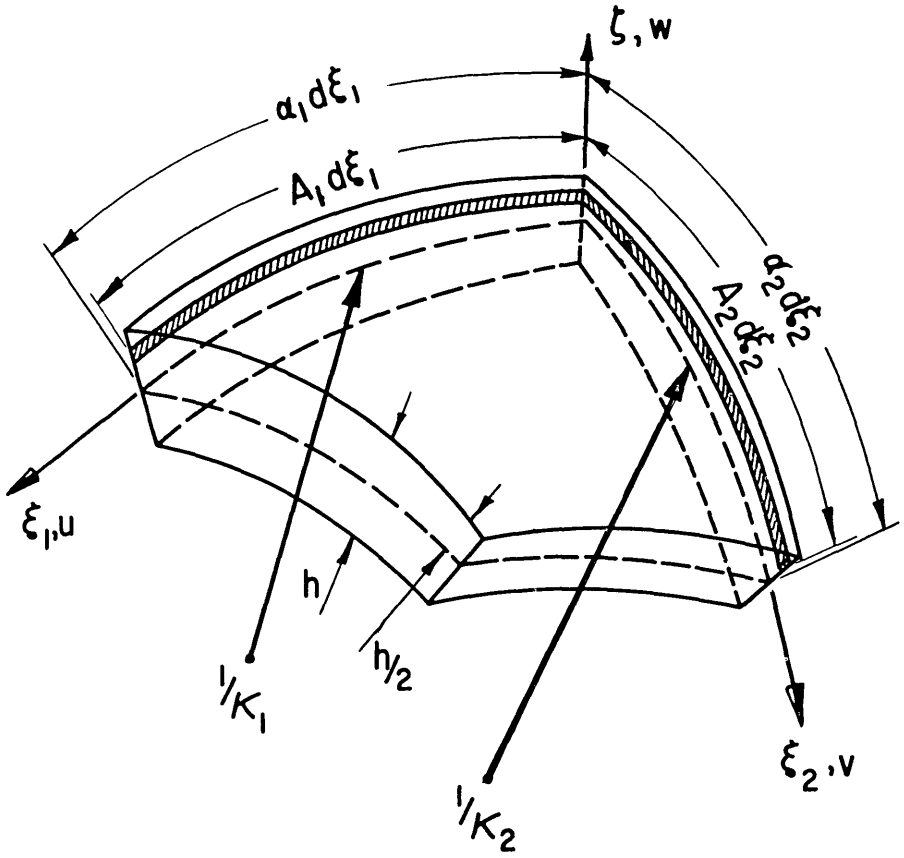

FIG. 2.1 SHELL COORDINATE SYSTEM

2.2 Fundamental Equations of Thin Shells

We consider a thin shell described by a system of orthogonal curvilinear coordinates, ξ_1 and ξ_2, which coincide with the lines of curvature of the middle surface, and the coordinate ζ, measured along the outer normal to it, as shown by Fig. 2.1.

In this coordinate system, the strain components at any point in the shell $P(\xi_1, \xi_2, \zeta)$ are given by,

$$e_1 = \frac{1}{A_1}\left[\frac{\partial u_1}{\partial \xi_1} + \frac{u_2}{A_2}\frac{\partial A_2}{\partial \xi_2} + u_3\frac{\partial A_1}{\partial \zeta}\right] \tag{2-1a}$$

$$e_2 = \frac{1}{A_2}\left[\frac{\partial u_2}{\partial \xi_2} + \frac{u_1}{A_1}\frac{\partial A_1}{\partial \xi_1} + u_3\frac{\partial A_2}{\partial \zeta}\right] \tag{2-1b}$$

$$\gamma_{12} = \frac{A_2}{A_1}\frac{\partial}{\partial \xi_1}\left(\frac{u_2}{A_2}\right) + \frac{A_1}{A_2}\frac{\partial}{\partial \xi_2}\left(\frac{u_1}{A_1}\right) \tag{2-1c}$$

$$e_\zeta = \frac{\partial u_3}{\partial \zeta} \tag{2-2a}$$

$$\gamma_{1\zeta} = A_1\frac{\partial}{\partial \zeta}\left(\frac{u_1}{A_1}\right) + \frac{1}{A_1}\frac{\partial u_3}{\partial \xi_1} \tag{2-2b}$$

$$\gamma_{2\zeta} = A_2\frac{\partial}{\partial \zeta}\left(\frac{u_2}{A_2}\right) + \frac{1}{A_2}\frac{\partial u_3}{\partial \xi_2} \tag{2-2c}$$

where u_1, u_2, u_3 are the displacements along ξ_1, ξ_2, ζ, respectively. A_1^2 and A_2^2 are the first fundamental magnitudes of the surface parallel to the middle surface at a distance ζ from it. The relationship between A_1^2, A_2^2, the first fundamental magnitudes of the middle surface α_1^2, α_2^2, and the principal radii of curvature R_1, R_2, are,

$$A_1 = \alpha_1\left(1 + \frac{\zeta}{R_1}\right) \tag{2-3a}$$

$$A_2 = \alpha_2\left(1 + \frac{\zeta}{R_2}\right) \tag{2-3b}$$

If we adopt the Kirchhoff-Love hypothesis that normals to the undeformed surface remain unstretched normals to the deformed surface, than Eqs.(2-2) are equal to zero, since the normal and transverse shear strains must vanish.

If the assumption is now made that the shell thickness is much smaller than either of the principal radii of curvature, and that terms of the form u_i/R_i $(i = 1,2)$ are negligible compared with those of the form $\alpha_i^{-1}\,\partial u_3/\partial \xi_i$ $(i = 1,2)$, then Equations (2-2) yield the following expressions for the displacements at $P(\xi_1,\xi_2,\zeta)$ in terms of u,v,w the middle surface displacements at $P_o(\xi_1,\xi_2, 0)$,

$$u_1 = u - \frac{\zeta}{\alpha_1}\frac{\partial w}{\partial \xi_1} \tag{2-4a}$$

$$u_2 = v - \frac{\zeta}{\alpha_2}\frac{\partial w}{\partial \xi_2} \tag{2-4b}$$

$$u_3 = w \tag{2-4c}$$

Substitution of Eqs.(2-4) into Eqs.(2-1) yields the expressions for the strain components,

$$e_1 = \epsilon_1 + \varkappa_1 \zeta \tag{2-5a}$$

$$e_2 = \epsilon_2 + \varkappa_2 \zeta \tag{2-5b}$$

$$\gamma_{12} = \gamma + \varkappa_{12}\zeta \qquad (2\text{-}5c)$$

where the strain components ϵ_1, ϵ_2, γ and curvature changes $\varkappa_1$, $\varkappa_2$, $\varkappa_{12}$ on the middle surface are given by,

$$\epsilon_1 = \frac{1}{\alpha_1}\frac{\partial u}{\partial \xi_1} + \frac{v}{\alpha_1\alpha_2}\frac{\partial \alpha_1}{\partial \xi_2} + \frac{w}{R_1} \qquad (2\text{-}6a)$$

$$\epsilon_2 = \frac{1}{\alpha_2}\frac{\partial v}{\partial \xi_2} + \frac{u}{\alpha_1\alpha_2}\frac{\partial \alpha_2}{\partial \xi_1} + \frac{w}{R_2} \qquad (2\text{-}6b)$$

$$\gamma = \frac{\alpha_1}{\alpha_2}\frac{\partial}{\partial \xi_2}\left(\frac{u}{\alpha_1}\right) + \frac{\alpha_2}{\alpha_1}\frac{\partial}{\partial \xi_1}\left(\frac{v}{\alpha_2}\right) \qquad (2\text{-}6c)$$

$$\varkappa_1 = -\frac{1}{\alpha_1}\frac{\partial}{\partial \xi_1}\left(\frac{1}{\alpha_1}\frac{\partial w}{\partial \xi_1}\right) - \frac{1}{\alpha_1\alpha_2^2}\frac{\partial \alpha_1}{\partial \xi_2}\frac{\partial w}{\partial \xi_2} \qquad (2\text{-}7a)$$

$$\varkappa_2 = -\frac{1}{\alpha_2}\frac{\partial}{\partial \xi_2}\left(\frac{1}{\alpha_2}\frac{\partial w}{\partial \xi_2}\right) - \frac{1}{\alpha_2\alpha_1^2}\frac{\partial \alpha_2}{\partial \xi_1}\frac{\partial w}{\partial \xi_1} \qquad (2\text{-}7b)$$

$$\varkappa_{12} = -\frac{\alpha_2}{\alpha_1}\frac{\partial}{\partial \xi_1}\left(\frac{1}{\alpha_2^2}\frac{\partial w}{\partial \xi_2}\right) - \frac{\alpha_1}{\alpha_2}\frac{\partial}{\partial \xi_2}\left(\frac{1}{\alpha_1^2}\frac{\partial w}{\partial \xi_1}\right) \qquad (2\text{-}7c)$$

Equations (2-6) are the same as those given by Wang [10], for example, but Eqs.(2-7) are different in that they do not contain any u and v terms. This is a direct result of the assumption made earlier, which is believed to be valid for thin shells.

If in addition we make the assumption that the Gaussian curvature of the shell ($K_G = R_1^{-1} R_2^{-1}$) is small, then the compatibility relation between the strain components including thermal effects, is,

$$\frac{\partial}{\partial\xi_1}\left\{\frac{1}{\alpha_1}\left[\frac{\partial(\alpha_2\epsilon_2)}{\partial\xi_1} - \epsilon_1\frac{\partial\alpha_2}{\partial\xi_1} - \gamma\frac{\partial\alpha_1}{\partial\xi_2}\right]\right\}$$

$$+ \frac{\partial}{\partial\xi_2}\left\{\frac{1}{\alpha_2}\left[\frac{\partial(\alpha_1\epsilon_1)}{\partial\xi_2} - \epsilon_2\frac{\partial\alpha_1}{\partial\xi_2} - \gamma\frac{\partial\alpha_2}{\partial\xi_1}\right]\right\} \tag{2-8}$$

$$- \frac{\partial^2\gamma}{\partial\xi_1\partial\xi_2} + \alpha_1\alpha_2\left[\frac{\chi_2}{R_1} + \frac{\chi_1}{R_2}\right]$$

$$+ \alpha\left\{\frac{\partial}{\partial\xi_1}\left[\frac{\alpha_2}{\alpha_1}\frac{\partial T}{\partial\xi_1}\right] + \frac{\partial}{\partial\xi_2}\left[\frac{\alpha_1}{\alpha_2}\frac{\partial T}{\partial\xi_2}\right]\right\} = 0$$

where α is the coefficient of thermal expansion and T the temperature change.

The relationship between the stress resultants and the moments shown in Fig. 2.2, and the strains and curvature changes, including thermal effects, are given by,

The stress resultants,

$$N_1 = \frac{Eh}{1-\nu^2}\left[\epsilon_1 + \nu\epsilon_2 - \alpha(1+\nu)T^{(0)}\right] \tag{2-9a}$$

$$N_2 = \frac{Eh}{1-\nu^2}\left[\epsilon_2 + \nu\epsilon_1 - \alpha(1+\nu)T^{(0)}\right] \tag{2-9b}$$

$$N_{12} = N_{21} = Gh\gamma \tag{2-9c}$$

The moments,

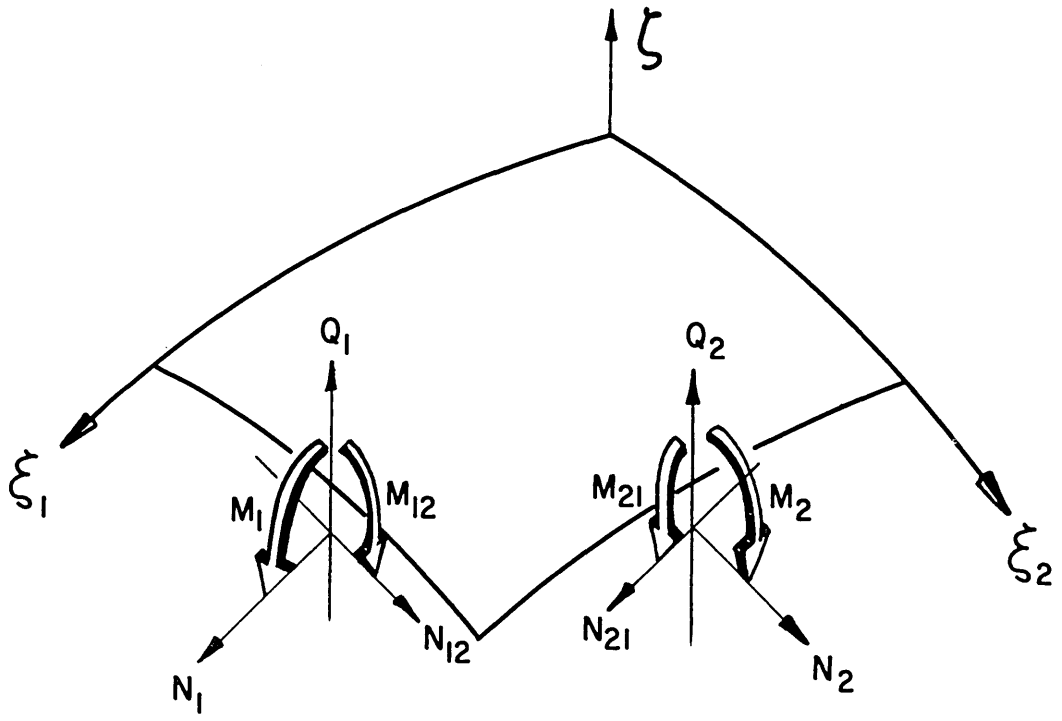

FIG.2.2 STRESS RESULTANTS & MOMENTS ON SHELL ELEMENT

$$M_1 = D\,[\varkappa_1 + \nu\,\varkappa_2 - \alpha(1+\nu)\,T^{(1)}] \qquad (2\text{-}10a)$$

$$M_2 = D\,[\varkappa_2 + \nu\,\varkappa_1 - \alpha(1+\nu)\,T^{(1)}] \qquad (2\text{-}10b)$$

$$M_{12} = M_{21} = \frac{D(1-\nu)}{2}\,\varkappa_{12} \qquad (2\text{-}10c)$$

where,

$$T^{(0)} = \frac{1}{h}\int_{-h/2}^{h/2} T\,d\zeta \qquad (2\text{-}11a)$$

$$T^{(1)} = \frac{1}{h^3}\int_{-h/2}^{h/2} T\zeta\,d\zeta \qquad (2\text{-}11b)$$

are the zeroth and the first moment of the temperature distributions across the shell thickness. For a thin shell the temperature distribution may, in most cases, be regarded as constant across the shell, in which case,

$$T^{(0)} = T \qquad (2\text{-}12a)$$

$$T^{(1)} = 0 \qquad (2\text{-}12b)$$

The equations of equilibrium which are consistent with the stated assumptions are given by,

$$\frac{\partial}{\partial\xi_1}(\alpha_2 Q_1) + \frac{\partial}{\partial\xi_2}(\alpha_1 Q_2) - \alpha_1\alpha_2\left(\frac{N_1}{R_1} + \frac{N_2}{R_2}\right) + \alpha_1\alpha_2 Z = 0 \qquad (2\text{-}13a)$$

$$\frac{\partial}{\partial \xi_1}(\alpha_2 N_1) + \alpha_1 \frac{\partial N_{12}}{\partial \xi_2} + 2N_{12}\frac{\partial \alpha_1}{\partial \xi_2} - N_2 \frac{\partial \alpha_2}{\partial \xi_1} + \alpha_1 \alpha_2 \Xi_1 = 0 \qquad (2\text{-}13b)$$

$$\frac{\partial}{\partial \xi_2}(\alpha_1 N_2) + \alpha_2 \frac{\partial N_{12}}{\partial \xi_1} + 2N_{12}\frac{\partial \alpha_2}{\partial \xi_1} - N_1 \frac{\partial \alpha_1}{\partial \xi_2} + \alpha_1 \alpha_2 \Xi_2 = 0 \qquad (2\text{-}13c)$$

$$\frac{\partial}{\partial \xi_1}(\alpha_2 M_1) + \alpha_1 \frac{\partial M_{12}}{\partial \xi_2} + 2M_{12}\frac{\partial \alpha_1}{\partial \xi_2} - M_2 \frac{\partial \alpha_2}{\partial \xi_1} - \alpha_1 \alpha_2 Q_1 = 0 \qquad (2\text{-}13d)$$

$$\frac{\partial}{\partial \xi_2}(\alpha_1 M_2) + \alpha_2 \frac{\partial M_{12}}{\partial \xi_1} + 2M_{12}\frac{\partial \alpha_2}{\partial \xi_1} - M_1 \frac{\partial \alpha_1}{\partial \xi_2} - \alpha_1 \alpha_2 Q_2 = 0 \qquad (2\text{-}13e)$$

It should be noted that as compared with the equilibrium equations given in Ref. [10], for example, the components due to transverse shear in the tangential equilibrium equations, Eqs. (2-13b,c) are omitted. This is necessary in order to be consistent with the assumptions concerning the thickness of the shell and its Gaussian curvature.

An examination of the omitted terms would show that they are of the order $(\frac{h}{R_i})^3$, whereas the other terms in these equations are of order $-\frac{1}{R_i}(\frac{h}{R_i})$. Since the initial assumption $N_{12} = N_{21}$ implies that $(\frac{h}{R_i})^2 \ll 1$, then consistency demands that these terms should properly be omitted. Otherwise, the result is that higher order terms are retained in one equation while omitted in another of the same order.

The formulation of the problem is completed with the statement of the boundary conditions. At each edge of the shell the boundary conditions may be mixed, i.e. they may involve both displacements and forces. However, only one condition in each of the following alternative pairs may be specified.

They are, at the boundary ξ_i = constant,

$$N_i = \overline{N_i} \quad \text{or} \quad u_i = \overline{u_i} \qquad i = 1,2 \qquad (2\text{-}14a)$$

$$N_{ij} = \overline{N_{ij}} \quad \text{or} \quad u_j = \overline{u_j} \qquad i \neq j \qquad (2\text{-}14b)$$

$$Q_i + \frac{\partial M_{ij}}{\partial \xi_j} = \overline{Q_i} \quad \text{or} \quad w = \overline{w} \qquad (2\text{-}14c)$$

$$M_i = \overline{M_i} \quad \text{or} \quad \frac{\partial w}{\partial \xi_i} = \overline{\frac{\partial w}{\partial \xi_i}} \qquad (2\text{-}14d)$$

2.3 Stress Function and Shallow-Shell Theory

In the important case when there exist no tangential forces, $\Xi_1 = \Xi_2 = 0$, then similar to the plate problem, a great simplification is possible in the equations by the introduction of an appropriate Airy stress function. However, unlike the plate case, for which the tangential and transverse equilibrium equations are independent of one another, in the shell case, due to its curvature, the two effects are coupled, so that a set of two equations must be solved simultaneously.

Defining the differential operators of Eqs. (2-7) as,

$$D_1(w) = \frac{1}{\alpha_1}\frac{\partial}{\partial \xi_1}\left(\frac{1}{\alpha_1}\frac{\partial w}{\partial \xi_1}\right) + \frac{1}{\alpha_1 \alpha_2^2}\frac{\partial \alpha_1}{\partial \xi_2}\frac{\partial w}{\partial \xi_2} \qquad (2\text{-}15a)$$

$$D_2(w) = \frac{1}{\alpha_2}\frac{\partial}{\partial \xi_2}\left(\frac{1}{\alpha_2}\frac{\partial w}{\partial \xi_2}\right) + \frac{1}{\alpha_2 \alpha_1^2}\frac{\partial \alpha_2}{\partial \xi_1}\frac{\partial w}{\partial \xi_1} \qquad (2\text{-}15b)$$

$$D_3(w) = \frac{\alpha_2}{\alpha_1}\frac{\partial}{\partial \xi_1}\left(\frac{1}{\alpha_2^2}\frac{\partial w}{\partial \xi_2}\right) + \frac{\alpha_1}{\alpha_2}\frac{\partial}{\partial \xi_2}\left(\frac{1}{\alpha_1^2}\frac{\partial w}{\partial \xi_1}\right) \qquad (2\text{-}15c)$$

then the curvature changes are given by,

$$\varkappa_1 = - D_1(w) \tag{2-16a}$$

$$\varkappa_2 = - D_2(w) \tag{2-16b}$$

$$\varkappa_{12} = - D_3(w) \tag{2-16c}$$

We note that the differential operator appearing in Eq. (2-8) is equivalent to the operator ∇^2 in the curvilinear coordinate system ξ_1, ξ_2, i.e.,

$$\nabla^2 w = \frac{1}{\alpha_1\alpha_2}\left[\frac{\partial}{\partial\xi_1}\left(\frac{\alpha_2}{\alpha_1}\frac{\partial w}{\partial\xi_1}\right) + \frac{\partial}{\partial\xi_2}\left(\frac{\alpha_1}{\alpha_2}\frac{\partial w}{\partial\xi_2}\right)\right] = D_1(w) + D_2(w) \tag{2-17}$$

A stress function F is now defined in the following manner,

let,

$$N_1 = D_2(F) \tag{2-18a}$$

$$N_2 = D_1(F) \tag{2-18b}$$

$$N_{12} = - \frac{1}{2} D_3(F) \tag{2-18c}$$

With this definition the system of equations reduces to the following pair of equations,

$$\nabla^4 F - Eh\left[\tilde{\nabla}^2 w - \alpha\nabla^2 T^{(0)}\right] = 0 \tag{2-19a}$$

$$D\left[\nabla^4 w + \alpha(1+\nu)\nabla^2 T^{(1)}\right] + \tilde{\nabla}^2 F - Z = 0 \tag{2-19b}$$

where the operator $\tilde{\nabla}^2(\ )$ is defined by,

$$\tilde{\nabla}^2(\ ) = \frac{1}{R_2} D_1(\ ) + \frac{1}{R_1} D_2(\ ) \tag{2-20}$$

The transverse shears are given by,

$$Q_1 = - \frac{D}{\alpha_1} \frac{\partial}{\partial \xi_1} [\nabla^2 w + \alpha(1+\nu)T^{(1)}] \tag{2-21a}$$

$$Q_2 = - \frac{D}{\alpha_2} \frac{\partial}{\partial \xi_2} [\nabla^2 w + \alpha(1+\nu)T^{(1)}] \tag{2-21b}$$

The shell problem has now been reduced to the solution of the two simultaneous equations, Eqs. (2-19), subject to the boundary conditions, Eqs. (2-14). It is easily seen that for the case of zero curvature, namely for a plate, the operator $\tilde{\nabla}^2(\ )$ vanishes and we obtain the familiar compatibility and equilibrium equations,

$$\nabla^4 F + Eh\alpha\nabla^2 T^{(0)} = 0 \tag{2-22a}$$

$$D[\nabla^4 w + \alpha(1+\nu)\nabla^2 T^{(1)}] - Z = 0 \tag{2-22b}$$

An interesting aspect of this simplified thin shell theory is that it results in a set of equations which are similar to those obtained using shallow-shell theory.

Reference [9] gives the following two equations for linear shallow-shell theory,

$$\nabla^4 F + Eh\alpha\nabla^2 T - EhD_4(w) = 0 \qquad (2\text{-}23a)$$

$$D\nabla^4 w + D_4(F) - Z = 0 \qquad (2\text{-}23b)$$

where,

$$D_4(\ ) = -\frac{\partial^2 z}{\partial y^2}\frac{\partial^2(\ )}{\partial x^2} - \frac{\partial^2 z}{\partial x^2}\frac{\partial^2(\ )}{\partial y^2} + 2\frac{\partial^2 z}{\partial x \partial y}\frac{\partial^2(\ )}{\partial x \partial y} \qquad (2\text{-}24)$$

and where x,y are the cartesian coordinates on the shell's projection, and z is its height above the projection.

It is seen that Eqs. (2-23) are of the same form as Eqs. (2-19). However, the latter refer to the shell coordinates and therefore may be expected to be more accurate for shells whose gradient is relatively large.

For the case of a cylindrical segment, if we define,

$$y = R\theta \qquad (2\text{-}25)$$

then both theories yield identical results. This indicates that Donnell's theory, which, as shown in the next section, is the application to the cylindrical case of the shell theory presented here, possesses an accuracy identical with that of shallow-shell theory.

2.4 Variational Principles

The concept of a variational principle, besides being a concise expression from which the various equations governing the problem may be derived, is also a powerful tool for the approximate analysis of boundary-value problems in Elasticity and many other fields.

The two most well-known variational methods are those associated with the principles of minimum potential energy and minimum complementary energy. The former states that the displacements which satisfy the geometrical boundary conditions, and which are obtained by minimizing the variational integral are those that satisfy the equilibrium equations. In this case the integral is a function of the displacements only. The latter states that the stresses which satisfy the force boundary conditions, and which are obtained by minimizing the variational integral are those that satisfy the compatibility equations. In this case the integral is a function of the stresses only. The choice of each method depends on the particular problem.

For the shell problem as formulated above, where the equations of equilibrium and compatibility are coupled with each other, these methods may sometimes be at a disadvantage, since the use of either one would tend to "favor" the corresponding member of Eqs. (2-19). Another principle which might be used in this case is one where the minimization of the integral results in stress and displacement functions which satisfy both the equilibrium and compatibility equations simultaneously. Such a variational method is provided by Reissner's principle [11].

The form of the variational integral applicable to the shell theory developed above is,

$$\begin{aligned}\pi = \iint \Bigg\| \frac{D}{2} \Big\{ [\nabla^2 w]^2 + \frac{1-\nu}{2} [D_3{}^2(w) - 4D_1(w)D_2(w)] \\ + 2\alpha(1+\nu)T^{(1)}\nabla^2 w \Big\} - \frac{1}{2Eh} \Big\{ [\nabla^2 F]^2 + \frac{1+\nu}{2} \\ [D_3{}^2(F) - 4D_1(F)D_2(F)] + 2\alpha(1+\nu)T^{(0)}\nabla^2 F \Big\} \\ + [\tilde{\nabla}^2 F - Z]w \Bigg\| \alpha_1\alpha_2 d\xi_1 d\xi_2\end{aligned} \tag{2-26}$$

As an example, in the case of a circular cylindrical shell, for which,

$$\begin{aligned} \xi_1 &= x & \alpha_1 &= 1 & R_1 &= \infty \\ \xi_2 &= \theta & \alpha_2 &= R & R_2 &= R \end{aligned} \tag{2-27}$$

application of the condition $\delta\pi = 0$ results in the following set of equations,

$$\frac{1}{Eh}\nabla^4 F + \alpha\nabla^2 T^{(0)} - \frac{1}{R}\frac{\partial^2 w}{\partial x^2} = 0 \tag{2-28a}$$

$$D[\,\nabla^4 w + \alpha(1+\nu)\nabla^2 T^{(1)}\,] + \frac{1}{R}\frac{\partial^2 F}{\partial x^2} - Z = 0 \tag{2-28b}$$

These are immediately recognized to be Donnell's equations including thermal effects.

The close affinity between this shell theory and shallow-shell theory is illustrated further by the comparison between Eq. (2-26) and the corresponding variational integral for shallow shells which, in its non-linear form, is given by,

$$\begin{aligned} \pi_{s.s.} = \iint \Bigg\{ & \frac{D}{2}\Big\{[\nabla^2 w]^2 + 2(1+\nu)[w_{xy}{}^2 - w_{xx}w_{yy}] \\ & + 2\alpha(1+\nu)T^{(1)}\nabla^2 w\Big\} - \frac{1}{2Eh}\Big\{[\nabla^2 F]^2 \\ & + 2(1+\nu)[F_{xy}{}^2 - F_{xx}F_{yy}] + 2\alpha EhT^{(0)}\nabla^2 F\Big\} \\ & + [D_4(F) - Z]w \\ & + \Big\{\frac{1}{2}F_{xx}w_y{}^2 + \frac{1}{2}F_{yy}w_x{}^2 - 2F_{xy}w_x w_y\Big\}\Bigg\} dxdy \end{aligned} \tag{2-29}$$

In the comparison, the last term, which accounts for the non-linear terms in von-Kármán's large deflection equations, should of course be omitted.

CHAPTER 3

VIBRATIONS OF CONICAL SHELLS

3.1 Introduction

The emergence of missiles in recent years has focused the attention of engineers to the static and dynamic behavior of their particular structural components. Most of this attention was directed at problems concerned with circular cylindrical shells. Some attention was also given to the static behavior of conical shells, but relatively little to the investigation of their dynamic behavior. Since truncated conical shell structures (or tapered cylinders) play an important part in the design of missile structures, knowledge of their vibration characteristics is necessary not only for its own sake, but also as a prerequisite to a rational aeroelastic analysis of such structures.

The reasons for the dearth of work done on this subject may be due to the fact that unlike the circular cylinder case, where exact solution of the problem is possible, the cone problem is not as amenable to an exact solution. This fact led the few investigators who have tackled this problem to the use of approximate methods whose results not only differ but are applicable to limited cases only.

The work of Federhofer [12], for example, who used a power series expansion for the assumed mode shapes, probably provides a good first approximation for cones of wide vertex angles, which approach a concentric circular plate in the

limit. Due to the employment of these mode shapes, however, the accuracy of the results when the other limiting case of circular cylinders is approached cannot be expected to be good, unless a large number of mode shapes is used, since the cylindrical mode shapes are trigonometric in nature.

Goldberg [13], in a recent paper, limited his investigation to axisymmetric motion, and then considered those modes having no circumferential displacement components. The problem was solved using power series. Obviously the results are limited to this single case only.

Grigolyuk [14] attacked the more general problem, while using mode shapes which reduce to the cylindrical shapes in the limit. The results are claimed to apply to cones of arbitrary vertex angle, but since a single mode was used, no estimate is available of the accuracy.

Herrmann and Mirsky [15] investigated, in essence, the effect of taper on the vibrations of cylindrical shells using the cylinder's trigonometric mode shapes. Their results showed that the frequencies of the tapered shells are invariably higher than those of the corresponding untapered ones, for length-to-radius ratios greater than 3, approximately. The analysis used a single expansion mode in each displacement component so that in this case too, no estimate is available of its accuracy. In addition, the choice of modes coupled with the over-accuracy in the expression for the strain components resulted in quite complicated expressions involving sine-integral and cosine-integral functions for the elements in the resulting 3 x 3 characteristic determinant. These drawbacks which are common with those of Ref. [14], make an extension of this analysis to include more modes quite inefficient from a computational standpoint.

The object of this chapter is to study the primarily flexural vibration characteristics of conical shells with small vertex angles (tapered cylindrical shells) for the

purpose of obtaining more reliable results than the ones obtained so far. This is done by using shell theories of differing complexity, by using various methods of solution and by employing different assumed displacement and stress functions. By comparing the various results with each other the effect of the different assumptions and approaches used may be assessed and a choice of the most appropriate method for use in getting higher approximations may be made. The various shell theories used include shallow shell theory, the "first approximation" shell theory presented in the previous chapter, and Flügge's [16] shell theory. The methods of solution include use of Reissner's principle, Eq.(2-26) and the principle of minimum potential energy, in conjunction with various assumed displacement and/or stress functions.

3.2 Shallow-Shell Approximation

The simplest approach to the problem is through use of shallow-shell theory. This theory is by no means applicable to all cases, since its underlying assumptions limits its use to shell segments whose maximum gradient is small compared to unity. However, through some ingenuity it may be applied to problems which at first seem to be beyond its realm.

The vibration problem of the circular cylinder is a case in point. For asymmetric motion, the vibration modes vary sinusoidally around the circumference. If one is primarily interested in those modes for which the motion is essentially transverse in character, then one may consider the half-wave bounded by two nodal generators as a shallow-shell segment. The application of the theory to this segment yields frequencies which are in good agreement with more exact results, when the number of circumferential waves n is greater than 2.

This idea is now extended to the truncated conical shell. A shell segment bounded by two nodal generators is considered,

as shown in Fig. 3.1. Using an approximation similar to the one used for cylinders, the cone's height above its projection is given by,

$$z = \frac{R}{2}\left[\left(\frac{\pi}{2n}\right)^2 - \left(\frac{y}{R}\right)^2\right] \tag{3-1}$$

where for cones the shell radius R varies linearly along its length.

The origin is chosen at the midpoint between the wide and narrow bases and x is measured along the axis positive towards the wide base. The radius R is then given by,

$$R = R_o + x\tan\alpha \tag{3-2}$$

where R_o is the average radius and α the semi-vertex angle.

From Eqs.(3-1) and (3-2) the curvatures are obtained,

$$\frac{\partial^2 z}{\partial y^2} = -\left(R_o + x\tan\alpha\right)^{-1} \tag{3-3a}$$

$$\frac{\partial^2 z}{\partial x \partial y} = \left(R_o + x\tan\alpha\right)^{-1}\theta\tan\alpha \tag{3-3b}$$

$$\frac{\partial^2 z}{\partial x^2} = -\left(R_o + x\tan\alpha\right)^{-1}(\theta\tan\alpha)^2 \tag{3-3c}$$

where,

$$\theta = \left(R_o + x\tan\alpha\right)^{-1} y \tag{3-4}$$

The Rayleigh-Ritz method is now used in conjunction with the shallow-shell variational principle given by Eq.(2-29).

For a simply supported shell, due to the asymmetry of the problem with respect to x, the following 2-mode assumed

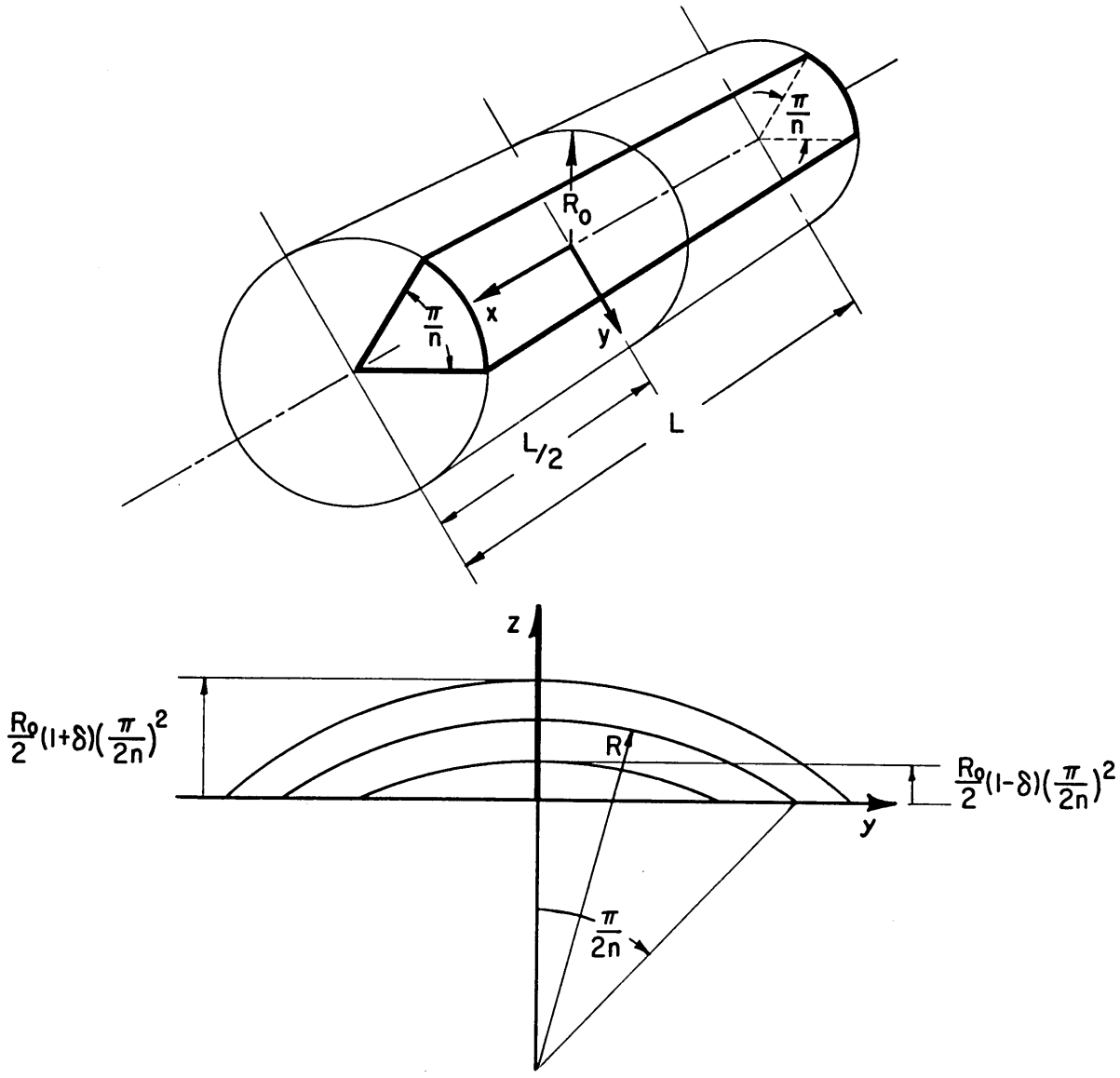

FIG. 3.1 SHALLOW SHELL SEGMENT

functions for w and F are taken,

$$w = [w_1 \cos\tfrac{\pi}{L}x + w_2 \sin 2\tfrac{\pi}{L}x]\cos n\theta \; e^{i\omega t} \tag{3-5a}$$

$$F = [F_1 \cos\tfrac{\pi}{L}x + F_2 \sin 2\tfrac{\pi}{L}x]\cos n\theta \; e^{i\omega t} \tag{3-5b}$$

where L is the cone height, i.e. the length of its projection on the XY plane.

If the θ-y relation as given by Eq.(3-4) is retained, then the evaluation of the variational integral will yield terms involving the sine-integral and cosine-integral functions, similar to those obtained in Ref. [15]. This is a direct consequence of the use of the simple trigonometric functions given by Eqs.(3-5). Since this investigation tries to avoid this complexity and in view of the fact that only a first approximation is sought at this point, then, for small α the differential dy will be approximated by,

$$dy \simeq R_o d\theta \tag{3-6}$$

Equations (3-3) and (3-5), using Eq.(3-6), are now substituted into the integral,

$$\pi = \int_{-L/2}^{L/2} \int_{-\pi/2n}^{\pi/2n} \Big\{ \frac{D}{2} \Big([\nabla^2 w]^2 + 2(1-\nu)[w_{xy}^2 - w_{xx}w_{yy}] \Big) - \frac{1}{2Eh} \Big([\nabla^2 F]^2 + 2(1+\nu)[F_{xy}^2 - F_{xx}F_{yy}] \Big) + \frac{1}{2}\rho h \dot{w}^2 - [F_{xx}z_{yy} + F_{yy}z_{xx} - 2F_{xy}z_{xy}]\, w \Big\} R_o \, d\theta \, dx \tag{3-7}$$

Performing the variations,

$$\frac{\partial \pi}{\partial w_i} = \frac{\partial \pi}{\partial F_i} = 0 \qquad (i = 1,2) \tag{3-8}$$

a set of four homogeneous simultaneous algebraic equations in the coefficients w_1, w_2, F_1, F_2 is obtained. The characteristic determinant is given by,

$$\begin{vmatrix} (\lambda^2+n^2)^2 C_*^2 - \bar{\omega}^2 & -\lambda^2 c_{12} & 0 & \lambda^2 c_{14} \\ \lambda^2 c_{12} & (\lambda^2+n^2)^2 & -\lambda^2 c_{23} & 0 \\ 0 & \lambda^2 c_{23} & (4\lambda^2+n^2)^2 C_*^2 - \bar{\omega}^2 & -4\lambda^2 c_{34} \\ -\lambda^2 c_{14} & 0 & 4\lambda^2 c_{34} & (4\lambda^2+n^2)^2 \end{vmatrix} = 0 \tag{3-9}$$

where,

$$\lambda = \frac{\pi}{L} R_o \tag{3-10a}$$

$$\bar{\omega}^2 = \frac{\rho}{E} R_o^2 \omega^2 \tag{3-10b}$$

$$C_*^2 = \frac{1}{12(1-\nu^2)} \left(\frac{h}{R_o}\right)^2 \tag{3-10c}$$

and where the c_{ij}'s are given, for small α, by,

$$c_{12} = \left[1 + 1.145\left(\frac{\tan\alpha}{\lambda}\right)^2 + .588\left(\frac{\tan\alpha}{\lambda}\right)^4\right] \tag{3-11a}$$

$$c_{14} = \left(\frac{\tan\alpha}{\lambda}\right)\left[1.415 + 2.205\left(\frac{\tan\alpha}{\lambda}\right)^2 + .134\left(\frac{\tan\alpha}{\lambda}\right)^4\right] \tag{3-11b}$$

$$c_{23} = \left(\frac{\tan\alpha}{\lambda}\right)\left[1.415 + 1.373\left(\frac{\tan\alpha}{\lambda}\right)^2 + .134\left(\frac{\tan\alpha}{\lambda}\right)^4\right] \tag{3-11c}$$

$$c_{34} = [1 + .903(\frac{\tan\alpha}{\lambda})^2 + .318(\frac{\tan\alpha}{\lambda})^4] \qquad (3\text{-}11d)$$

Solution of the set, Eqs.(3-9), will yield two values for $\bar{\omega}^2$, which correspond to the lowest two frequencies of the shell, for the particular n. By omitting the second terms in the assumed functions, Eqs.(3-5), an explicit expression for the lowest frequency is obtained,

$$\bar{\omega}^2 = \frac{\lambda^4 c_{12}^2}{(n^2+\lambda^2)^2} + C_*^2(n^2+\lambda^2)^2 \qquad (3\text{-}12)$$

For $\alpha = 0$, Eqs.(3-9) reduce to the cylindrical set and yield the lowest two natural frequencies for the equivalent cylinder of length L and radius R_o,

$$\bar{\omega}_{cyl}^{(m)2} = \frac{[m\lambda]^4}{(n^2+[m\lambda]^2)^2} + C_*^2(n^2+[m\lambda]^2)^2 \qquad (3\text{-}13)$$

Eq.(3-12), therefore, gives the first approximation to the effect of taper on the cylinder's lowest natural frequency for the particular n($n > 2$).

It is seen that the effect of taper in the first approximation reveals itself only through the membrane terms, and it always raises the shell frequency.

It is evident that the nature of the approximations used in this case renders an extension of this method to include higher modes with an apparent improvement in results, as quite unrealistic. Therefore, we turn next to the use of the shell theory developed in the previous chapter.

3.3 Use of Displacement and Stress Functions

In the rest of the chapter we return to the original

conception of the shell. We consider a thin, truncated conical shell of height L and of semi-vertex angle α. Each point on the middle surface is located by the coordinates r, θ, where r is the distance from the vertex and θ is the circumferential angle. r_o and r_1 are the distances from the vertex to the narrow and wide bases, respectively (Fig. 3.2).

In this coordinate system, we have,

$$\xi_1 = r \qquad \alpha_1 = 1 \qquad R_1 = \infty$$
$$\xi_2 = \theta \qquad \alpha_2 = r\sin\alpha \qquad R_2 = \frac{r}{\cot\alpha} \tag{3-14}$$

$$D_1(\ ) = \frac{\partial^2(\ )}{\partial r^2} \tag{3-15a}$$

$$D_2(\ ) = \frac{1}{r^2\sin^2\alpha}\frac{\partial^2(\ )}{\partial\theta^2} + \frac{1}{r}\frac{\partial(\ )}{\partial r} \tag{3-15b}$$

$$D_3(\ ) = \frac{2}{r\sin\alpha}\frac{\partial}{\partial\theta}\left[\frac{\partial(\ )}{\partial r} - \frac{1}{r}(\ )\right] \tag{3-15c}$$

$$\nabla^2(\ ) = \frac{1}{r}\frac{\partial}{\partial r}\left[r\frac{\partial(\ )}{\partial r}\right] + \frac{1}{r^2\sin^2\alpha}\frac{\partial^2(\ )}{\partial\theta^2} \tag{3-15d}$$

$$\tilde{\nabla}^2(\ ) = \frac{\cot\alpha}{r}\frac{\partial^2(\ )}{\partial r^2} \tag{3-15e}$$

Equations (2-19), with the force Z as the inertia load and in the absence of thermal effects, take the form,

$$\nabla^4 F - Eh\frac{\cot\alpha}{r}w_{rr} = 0 \tag{3-16a}$$

$$D\nabla^4 w + \frac{\cot\alpha}{r}F_{rr} + \rho h\ddot{w} = 0 \tag{3-16b}$$

Similar to the case of a cylinder, Eqs.(3-16) can be reduced to a single eighth-order equation in w.

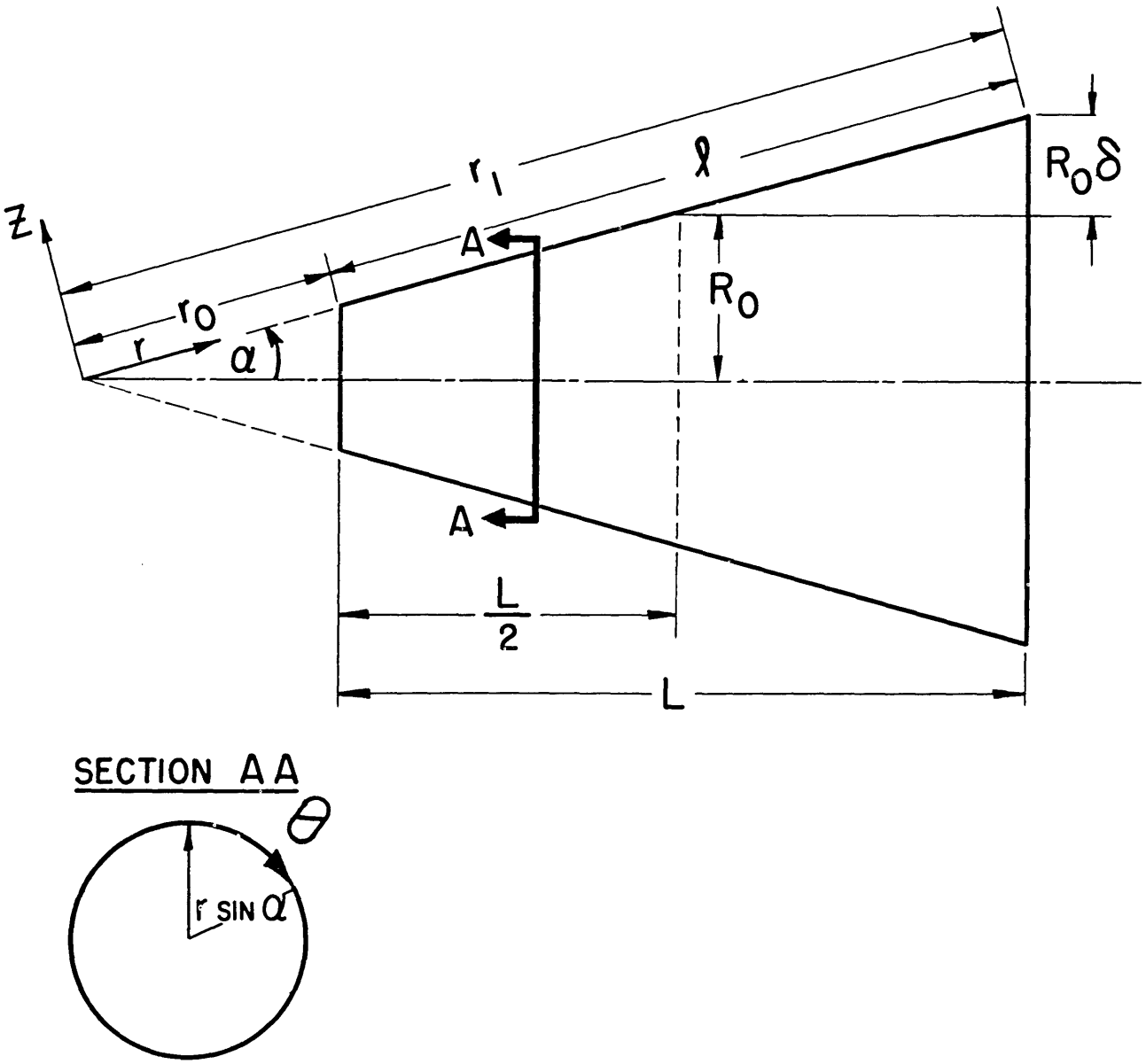

FIG. 3.2 CONICAL SHELL COORDINATE SYSTEM

We note that for this coordinate system the following identity is valid,

$$[r^4\nabla^4(\ )]_{rr} = r^2\nabla^4[r^2(\ )_{rr}] \tag{3-17}$$

If Eq.(3-16a) is multiplied by r^4, then differentiated twice with respect to r, and Eq.(3-16b) is multiplied by r^3, operated on by $\nabla^4(\ )$ and then multiplied by r^2, then using Eq.(3-17), F can be eliminated between the two resulting equations to yield,

$$r^2\nabla^4[r^3(D\nabla^4 w + \rho h\ddot{w})] + Eh\cot^2\alpha[r^3 w_{rr}]_{rr} = 0 \tag{3-18}$$

It can be easily verified that Eq.(3-18) reduces to the corresponding equation for the cylinder when $\alpha = 0$.

So far, Eqs.(3-16) or (3-18) have not been solved in closed form in terms of tabulated functions. It is therefore necessary to resort to approximate methods of solution.

First, we introduce a coordinate transformation which replaces r by ln r. This causes the equidimensional portions of each equation to become derivatives with constant coefficients. This simplifies the computational labor considerably, since, as will be seen later, the integrations result in simple algebraic and exponential expressions rather than Si and Ci functions. Physically, this transformation has the effect of shifting the peak of the mode shape away from the midpoint, as is to be expected in this asymmetrical (about the midpoint) problem.

Therefore, let,

$$r = r_o e^{\beta} \tag{3-19}$$

Also, define,

$$\bar{\theta} = \theta \sin\alpha \tag{3-20}$$

Substituting Eqs.(3-19) and (3-20) into Eqs.(3-15) we have,

$$D_1(\ ) = \frac{1}{r^2}\left[\frac{\partial^2(\ )}{\partial\beta^2} - \frac{\partial(\ )}{\partial\beta}\right] \tag{3-21a}$$

$$D_2(\ ) = \frac{1}{r^2}\left[\frac{\partial^2(\ )}{\partial\bar{\theta}^2} + \frac{\partial(\ )}{\partial\beta}\right] \tag{3-21b}$$

$$D_3(\ ) = \frac{2}{r^2}\frac{\partial}{\partial\bar{\theta}}\left[\frac{\partial(\ )}{\partial\beta} - (\ )\right] \tag{3-21c}$$

$$\nabla^2(\ ) = \frac{1}{r^2}\left[\frac{\partial^2(\ )}{\partial\beta^2} + \frac{\partial^2(\ )}{\partial\bar{\theta}^2}\right] \tag{3-21d}$$

$$\tilde{\nabla}^2(\ ) = \frac{\cot\alpha}{r}\left[\frac{\partial^2(\ )}{\partial\beta^2} - \frac{\partial(\ )}{\partial\beta}\right] \tag{3-21e}$$

The Rayleigh-Ritz method will now be employed, using the variational integral, Eq.(2-26).

Due to the fact that the shell is a body of revolution, the variation of the functions w and F around the circumference is periodic, with wave number n, namely,

$$w(\beta,\theta,t) = \bar{w}(\beta)\cos n\theta\ e^{i\omega t} \tag{3-22a}$$

$$F(\beta,\theta,t) = \bar{F}(\beta)\cos n\theta\ e^{i\omega t} \tag{3-22b}$$

Substituting Eqs.(3-21) and (3-22) into Eq.(2-26) (with T = 0) and integrating with respect to θ, we get,

$$\delta\pi = \delta \int_0^{\beta_1} \left\| \frac{D}{2}\left(e^{-2\beta}\right)\left\{ [\bar{w}''-\bar{n}^2\bar{w}]^2 + 2(1-\nu)[\bar{n}^2(\bar{w}'-\bar{w})^2 \right.\right.$$

$$\left. - (\bar{w}''-\bar{w}')(\bar{w}'-\bar{n}^2\bar{w})]\right\} - \frac{1}{2Eh}\left(e^{-2\beta}\right)\left\{ [\bar{F}''-\bar{n}^2\bar{F})^2 \right. \tag{3-23}$$

$$\left. + 2(1+\nu)[\bar{n}^2(\bar{F}'-\bar{F})^2-(\bar{F}''-\bar{F}')(\bar{F}'-\bar{n}^2\bar{F})]\right\}$$

$$+ r_o\cot\alpha e^{-\beta}(\bar{F}''-\bar{F}')\bar{w} - r_o{}^4\frac{\rho h}{2}\omega^2 e^{2\beta}\bar{w}^2 \Big\| d\beta = 0$$

where,

$$\beta_1 = \ln \frac{r_1}{r_o} \tag{3-24a}$$

$$\bar{n} = \frac{n}{\sin\alpha} \tag{3-24b}$$

$$(\ )' = \frac{d(\ )}{d\beta} \tag{3-24c}$$

For a 'simply supported' shell the boundary conditions at the edges are,

At $\beta = 0,\ \beta_1$,

$$N_r = \frac{e^{-2\beta}}{r_o{}^2}\,[\bar{F}'-\bar{n}^2\bar{F}] = 0 \tag{3-25a}$$

$$v = 0 \tag{3-25b}$$

$$\bar{w} = 0 \tag{3-25c}$$

$$M_r = D \frac{e^{-2\beta}}{r_o^2} [\bar{w}''+(\nu-1)\bar{w}' - \bar{n}^2\bar{w}] = 0 \qquad (3\text{-}25d)$$

It now remains to choose appropriate forms for the functions $\bar{w}$ and $\bar{F}$.

An assumed function for $\bar{w}$, which satisfies two of the boundary conditions, Eqs.(3-25c-d), is given by,

$$\bar{w}(\beta) = \tilde{w}\, e^{\frac{1-\nu}{2}\beta} \sin\frac{\pi}{\beta_1}\beta \qquad (3\text{-}26)$$

The choice of the stress function is a little more difficult. Since no explicit expression for v in terms of either $\bar{F}$ or $\bar{w}$ (or both) exists in this case, the boundary condition on v, Eq.(3-25b) cannot be written in terms of the two functions, and therefore cannot be satisfied exactly. In the following, three different choices for $\bar{F}$ are made, each satisfying different requirements, the results to be compared with each other.

(a) <u>The Stress Function Satisfies the Force Boundary Condition</u>

For our first choice, we assume a function $\bar{F}$ such that Eq.(3-25a) is satisfied. Such a function is given by,

$$\bar{F}(\beta) = EhR_o\tilde{F} \left[\sin\frac{\pi}{\beta_1}\beta + \frac{\pi}{\beta_1}\frac{1}{\bar{n}^2}\cos\frac{\pi}{\beta_1}\beta\right] \qquad (3\text{-}27)$$

The procedure to be followed is the same as in the shallow-shell case, namely, to substitute Eqs.(3-26) and (3-27) into Eq.(3-23), which, after the integration, becomes a quadratic form in the amplitudes $\tilde{w}$ and $\tilde{F}$. Then, application of the minimum condition results in two homogeneous simultaneous equations of the form,

$$[C_*^2 H_1 - \bar{\omega}^2 H_2]\tilde{w} + (1-\delta)\cos\alpha H_3 \tilde{F} = 0 \qquad (3\text{-}28a)$$

$$-(1-\delta)\cos\alpha H_3 \tilde{w} + H_4 \tilde{F} = 0 \qquad (3\text{-}28b)$$

where the H_i's are the various integrated terms. H_1 and H_2, which depend on the form of $\bar{w}$ only, will remain the same for all three cases. However, H_4 which depends on $\bar{F}$ and H_3 which depends on both $\bar{w}$ and $\bar{F}$, will take different forms in each case.

We have, then,

$$H_1 = \frac{1-\delta_*{}^{2(\mu-1)}}{\mu-1} \frac{[n^2+\bar{\lambda}^2(1-\mu^2\Delta)]^2 + 4\mu\bar{\lambda}^2\Delta[\bar{\lambda}^2-(1-\mu)n^2]}{\bar{\lambda}^2[1+(1-\mu)^2\Delta]} \qquad (3\text{-}29a)$$

$$H_2 = \frac{\delta_*{}^{2(\mu+1)} - 1}{\mu+1} \frac{(1-\delta)^4}{\bar{\lambda}^2[1+(1+\mu)^2\Delta]} \qquad (3\text{-}29b)$$

and for this case,

$$H_3{}^{(a)} = \frac{1-\delta_*{}^{\mu-1}}{\mu-1} \frac{2(1-\frac{\sin^2\alpha}{n^2}) + (1-\mu)\Delta}{1 + (\frac{1-\mu}{2})^2\Delta} \qquad (3\text{-}30a)$$

$$H_4{}^{(a)} = [1-\delta_*{}^{-2}] \frac{(n^2+\bar{\lambda}^2)^2(1+\frac{2\sin^2\alpha}{n^2}) - 4(1+\nu)\bar{\lambda}^4\Delta}{\bar{\lambda}^2(1+\Delta)} \qquad (3\text{-}30b)$$

where,

$$\bar{\lambda} = \frac{\pi\sin\alpha}{\beta_1} = \lambda \frac{\cos\alpha}{f(\delta)} \qquad (3\text{-}31a)$$

$$\Delta = \left[\frac{\sin\alpha}{\bar{\lambda}} \right]^2 \tag{3-31b}$$

$$\delta = \frac{L}{2R_o}\tan\alpha = \frac{\text{Radius of wide base - Average radius}}{\text{Average radius}} \tag{3-31c}$$

$$\delta_* = \frac{1+\delta}{1-\delta} = \frac{r_1}{r_o} = \frac{\text{Radius of wide base}}{\text{Radius of narrow base}} \tag{3-31d}$$

$$f(\delta) = \ln \delta_* = \frac{1}{\delta}\tanh^{-1}\delta = 1+\frac{\delta^2}{3}+\frac{\delta^4}{5}+..... \tag{3-31e}$$

$$\mu = \frac{1-\nu}{2} \tag{3-31f}$$

For a nontrivial solution, the determinant of the coefficients in Eqs.(3-28) must vanish. Expanding the determinant we get an explicit expression for the frequency,

$$\bar{\omega}^2 = \cos^2\alpha\, K_1 K_2^{(a)} + C_*^2 K_3 K_4 \tag{3-32}$$

where,

$$K_1 = \frac{1+\mu}{\mu}\,\frac{1}{(1-\delta)^2}\,\frac{\delta_*^{2\mu}-1}{\delta_*^{2(\mu+1)}-1} \tag{3-33a}$$

$$K_2^{(a)} = \left\{ \frac{[1+\delta][1-\delta_*^{\mu-1}]}{\mu-1} \right\}^2 \left\{ \frac{\mu}{[\delta_*^{2\mu}-1]\delta} \right\} \left\{ \frac{\bar{\lambda}^4[1+(1-\mu)\Delta][1+\frac{3}{2}(1+2\mu)\Delta][1-\frac{\bar{\lambda}^2\Delta}{n^2}]}{[n^2+\bar{\lambda}^2]^2[1+2\frac{\bar{\lambda}^2}{n^2}\Delta] - 8(1-\mu)\bar{\lambda}^4\Delta} \right\} \tag{3-33b}$$

$$K_3 = \frac{\mu+1}{\mu-1}\,\frac{1}{(1-\delta)^4}\,\frac{\delta_*^{2(\mu-1)}-1}{\delta_*^{2(\mu+1)}-1} \tag{3-33c}$$

$$K_4 = \left\{1+\frac{4\mu\Delta}{1+(1-\mu)^2\Delta}\right\}\left\{[n^2+\bar{\lambda}^2(1-\mu^2)]^2+4\mu\bar{\lambda}^2\Delta[\bar{\lambda}^2-(1-\mu)n^2]\right\} \qquad (3\text{-}33d)$$

It can be easily shown that as the cone approaches a cylinder of radius R_o, i.e. as $\alpha \to o$, $\cos^2\alpha \to 1$, and,

$$\lim_{\alpha\to 0} K_1 = 1 \qquad (3\text{-}34a)$$

$$\lim_{\alpha\to 0} K_2 = \frac{\lambda^4}{(n^2+\lambda^2)^2} \qquad (3\text{-}34b)$$

$$\lim_{\alpha\to 0} K_3 = 1 \qquad (3\text{-}34c)$$

$$\lim_{\alpha\to 0} K_4 = (n^2+\lambda^2)^2 \qquad (3\text{-}34d)$$

and Eq.(3-32) reduces to the frequency formula for the cylinder, Eq.(3-13) (with m = 1).

It is clear that one can obtain a second approximation to the frequency by assuming two (or more) modes satisfying the same boundary conditions instead of the single mode expression for $\bar{w}$ and $\bar{F}$. Such modes would be of the form,

$$\bar{w} = e^{\frac{1-\nu}{2}\beta} \sum_m \bar{w}_m \sin\frac{m\pi}{\beta_1}\beta \qquad (3\text{-}35a)$$

$$F = \sum_m F_m\left(\sin\frac{m\pi}{\beta_1}\beta + \frac{m\pi}{\beta_1}\frac{1}{\bar{n}^2}\cos\frac{m\pi}{\beta_1}\beta\right) \qquad (3\text{-}35b)$$

However, this will not be pursued any further, as our purpose is to explore other approaches in order to arrive at the optimum method to be used. Let us just remark that Eq.(3-32) shows that in this case taper affects both the membrane and

the bending terms, in contrast with Eq.(3-12) where the taper affected the membrane terms only.

(b) The Stress Function Satisfies the Compatibility Equation

The second approach to the problem follows Marguerre's method. In this method, the assumed function for $\bar{w}$ as given by Eq.(3-26) is substituted into the compatibility relation, Eq.(3-16a), and the stress function $\bar{F}$ is solved for in terms of $\bar{w}$, subject to the boundary conditions. Since compatibility is thus assured, one must use the principle of minimum potential energy, rather than Reissner's principle, in order to satisfy the equilibrium equation and to solve for the frequency.

In this case the stress function $\bar{F}$ is required to satisfy the force boundary condition - Eq.(3-26a) and also the condition that $\epsilon_\theta = 0$ at the edges. The latter condition is not identical to the condition expressed by Eq.(3-25b) but is a close approximation to it. This expression for $\bar{F}$ was obtained first by Mushtari and Sachenkov [17] in their investigation of the cone buckling problem. It is used here for comparison purposes only, since it is quite unwieldy and practically incapable of being extended to include more modes.

The result of the steps described above yields the following expression for $\bar{F}$,

$$\bar{F} = EhR_o\tilde{w}\frac{\cos\alpha}{1-\delta}\Big(e^{(1+\mu)\beta}\Big[a_1\sin\frac{\pi}{\beta_1}\beta + a_2\sin\alpha\cos\frac{\pi}{\beta_1}\beta\Big] + \frac{\bar{\lambda}}{4}\Big[a_3e^{\bar{n}\beta}+a_4e^{-\bar{n}\beta}+a_5e^{(\bar{n}+2)\beta}+a_6e^{(2-\bar{n})\beta}\Big]\Big) \tag{3-36}$$

where the constants a_i are functions of n, $\bar{\lambda}$, α and μ, and are defined in Appendix 3A.

Equation (3-36) which defines $\bar{F}$ in terms of $\bar{w}$, and

Eq.(3-26) which defines $\bar{w}$, are now substituted into the energy integral, which, after the integration, becomes a quadratic form in the amplitude $\tilde{w}$, of the form,

$$\pi_p = [C_*^2 H_1 - \bar{\omega}^2 H_2 + (1-\delta)^2 \cos^2\alpha \; H_5] \; \tilde{w}^2 \qquad (3\text{-}37)$$

where H_5 is a function of the various parameters. Application of the minimum condition results in the frequency equation,

$$\bar{\omega}^2 = \cos^2\alpha \; K_1 K_2^{(b)} + C_*^2 K_3 K_4 \qquad (3\text{-}38)$$

where K_1, K_3, K_4, are given by Eq.(3-33), and where now,

$$K_2^{(b)} = \bar{\lambda}^2[1 + (1+\mu)^2\Delta] \left\| \; b_6 + \frac{\mu n \sin\alpha}{\delta_*^{2\mu}-1} \left(\delta_*^{2\mu}\left[\frac{b_4-b_5}{b_7} - \left(1+\frac{2\sin\alpha}{n}\right)\frac{b_4}{b_{10}}\right] + \frac{b_4+b_5}{b_8} - \left(1-\frac{2\sin\alpha}{n}\right)\frac{b_4}{b_9}\right) \right\| \qquad (3\text{-}39)$$

where the b_i's are defined in Appendix 3A.

It is seen that the frequency expression given by Eq.(3-38) differs from the previously obtained expression, given by Eq.(3-32), in the membrane term. This, of course, is to be expected, since the bending term depends on $\bar{w}$ only, which is common to both cases. The present expression, as the previous one, reduces to the cylindrical expression when $\alpha \longrightarrow o$. The expressions for $\bar{w}$ and $\bar{F}$ in both cases reduce to their cylindrical counterparts as well.

Since the results of this method are quite unwieldy for practical use, a third much simpler case is now worked

out.

(c) A Stress Function Approximating Case (b)

If the expression for the stress function given by Eq.(3-31) is examined as to the order of magnitude of the various terms, it turns out that the leading term is,

$$\bar{F} = EhR_o \tilde{F}\, e^{(1+\mu)\beta} \sin\frac{\pi}{\beta_1}\beta \tag{3-40}$$

Accordingly, we take this expression for $\bar{F}$ as our third choice, hoping to obtain a simpler, yet relatively accurate frequency equation. Eq.(3-40) reduces to the cylindrical expression in the limit, but it does not satisfy the remaining boundary conditions, Eqs.(3-25a-b).

Since in this case $\bar{F}$ is considered as an independent function, rather than being a solution of the compatibility equation, we use the same method as employed in case (a). This results in a set of equations identical to Eqs.(3-28), where in this case,

$$H_3^{(c)} = \frac{1-\delta_*^{2\mu}}{\mu} \tag{3-41a}$$

$$H_4^{(c)} = \frac{\delta_*^{2\mu}-1}{\mu}\,\frac{1}{\bar{\lambda}^2(1+\mu^2\Delta)}\left\{ n^2 + \bar{\lambda}^2[1-(1+\mu)^2\Delta] \right\}^2 + 4\bar{\lambda}^{-2}\Delta[\bar{\lambda}^2(1+\mu+4\mu^2) + n^2\mu(1+\mu)] \tag{3-41b}$$

The frequency expression is given by,

$$\bar{\omega}^2 = \cos^2\alpha\, K_1 K_2^{(c)} + C_*^2\, K_3 K_4 \tag{3-42}$$

where,

$$K_2^{(c)} = \frac{\bar{\lambda}^4[1+\mu^2\Delta][1+(1+\mu)^2\Delta]}{\left\{n^2 + \bar{\lambda}^2[1-(1+\mu)^2\Delta]\right\}^2 + 4\bar{\lambda}^2\Delta[n^2\mu(1+\mu)+\bar{\lambda}^2(1+\mu+4\mu^2)]} \quad (3\text{-}43)$$

Here again, $K_2^{(c)}$ is the factor differing from cases (a) and (b).

Comparing the membrane term in the frequency expressions, which is different in each of the three cases, we observe that cases (a) and (c) are much simpler than case (b) for practical calculations. The question of relative accuracy will be resolved in Section (3.6), where the results of all methods employed in the solution of this problem will be compared for some representative cases.

3.4 Use of Displacement Functions

The frequency expressions obtained thus far are based on shell theories in which certain assumptions are inherent regarding the tangential displacements of the shell. Both theories completely ignore the tangential inertia effect, and in addition, use of shallow shell theory was seen to involve difficulties stemming from the fact that the width of the shell segment is not constant. If one attempts to overcome this difficulty by using a polar, rather than cartesian coordinate system, then all the advantage of this simple theory is lost, since the expressions become similar to those of the "first-approximation" shell theory. The latter theory, besides neglecting tangential inertia, also neglected certain terms on the basis of the assumptions of small Gaussian cur-

vature and a small thickness-to-radius-of-curvature ratio.

Let us examine these approximations in our case. Firstly, the Gaussian curvature is indeed zero, since $R_1^{-1} = 0$, so there is no problem there. The validity of the other two assumptions for cylindrical shells has been borne out. For conical shells, however, due to the fact that they narrow down towards the top, the membrane effect gains in importance so that the lowest vibration mode, in which we are interested, involves considerable u and v displacements, which may be, perhaps, equal in importance to the usually dominant w displacement. For this reason an approach which utilizes all three displacement components and retains all the neglected terms might be appropriate in this case. This would certainly have been true had we considered an almost complete cone (a truly complete cone presents difficulties due to the singularity at the apex). Here, however, we consider a thin shell which is closer in shape to a cylinder than to a complete cone. Therefore it seems that the higher order thickness effects and perhaps even the tangential inertia effects may be neglected. However, an important advantage of an approach utilizing displacement functions is that the geometrical boundary conditions can be satisfied exactly, unlike the approach used earlier.

Since the assumed functions to be used reduce to the cylindrical mode shapes for $\alpha = o$, the validity of the method is probably good only for small values of δ, (which is the parameter indicating how close to a complete cone the shell gets). One should be careful to put a limit on the value of δ beyond which the validity of the results should be questioned. This value will probably depend on the number of expansion modes used, but it certainly cannot be very close to unity, the value defining a complete cone. For shells resembling complete cones, rather than tapered cylinders, expansion modes in terms of power series may be more appro-

priate for use.

In the following development, two approaches will be used so that the effect of the neglected terms may be determined. The first approach takes all of these terms into account by using Flügge's shell theory, and it also employs assumed modes satisfying all the boundary conditions. The second approach uses the approximate shell theory, to which tangential inertia effects are added, together with a set of simplified assumed modes satisfying the geometrical boundary conditions only. Both approaches employ the Rayleigh-Ritz method.

(a) Flügge's Theory and Displacement Functions Satisfying all the Boundary Conditions

This theory improves on the shell theory presented in Chapter 2 by including certain higher order terms in the expressions for the curvature changes. The expressions for the middle surface strains are the same. Using Eq.(3-14) the strains, given by Eqs.(2-6), become,

$$\epsilon_r = \frac{\partial u}{\partial r} \tag{3-44a}$$

$$\epsilon_\theta = \frac{1}{r}\frac{\partial v}{\partial \theta} + \frac{u}{r} + \frac{\cot\alpha}{r} w \tag{3-44b}$$

$$\gamma = \frac{1}{r}\frac{\partial u}{\partial \theta} + r\frac{\partial}{\partial r}\left(\frac{v}{r}\right) \tag{3-44c}$$

For this theory, the strain energy is given by,

$$U = U_o + U_1 \tag{3-45}$$

where U_o is the value given by the simplified theory,

$$U_o = \int_{r_o}^{r_1} \int_0^{2\pi} \left\| \frac{Eh}{2(1-\nu^2)} [\epsilon_r{}^2 + \epsilon_\theta{}^2 + 2\nu\epsilon_r\epsilon_\theta + \frac{1-\nu}{2}\gamma^2] \right.$$

(3-46)

$$\left. + \frac{D}{2}\left\{ [\nabla^2 w]^2 + \frac{1-\nu}{2}[D_3(w)^2 - 4D_1(w)D_2(w)] \right\} \right\| r\sin\alpha d\theta dr$$

and where U_1 is the additional term due to Flügge's theory, given by,

$$U_1 = \int_{r_o}^{r_1} \int_0^{2\pi} \frac{D}{2} \frac{\cot\alpha}{r} \left\| -2D_1(w)[\frac{\partial u}{\partial r} + \frac{\nu}{r}\frac{\partial v}{\partial \theta}] + 2D_2(w) \right.$$

$$[\frac{u}{r} + \frac{\cot\alpha}{r} w] - \frac{1-\nu}{2} D_3(w)[3r\frac{\partial}{\partial r}(\frac{v}{r}) - \frac{1}{r}\frac{\partial u}{\partial \theta}]$$

(3-47)

$$+ \frac{\cot\alpha}{r}[\frac{u}{r} + \frac{\cot\alpha}{r} w]^2 + \frac{\cot\alpha}{r}\frac{1-\nu}{2}\left\{ 3[r\frac{\partial}{\partial r}(\frac{v}{r})]^2 \right.$$

$$\left. \left. + [\frac{1}{r}\frac{\partial u}{\partial \theta}]^2 \right\} \right\| r\sin\alpha d\theta dr$$

The kinetic energy is simply,

$$T = \frac{\rho h}{2} \int_{r_o}^{r_1} \int_0^{2\pi} [\ \dot{u}^2 + \dot{v}^2 + \dot{w}^2\ ]\ r\sin\alpha d\theta dr \qquad (3\text{-}48)$$

Following the transformation defined by Eq.(3-19), the assumptions,

$$u(\beta,\theta,t) = \bar{u}(\beta)\cos n\theta\ e^{i\omega t} \qquad (3\text{-}49a)$$

$$v(\beta,\theta,t) = \bar{v}(\beta)\sin n\theta\ e^{i\omega t} \qquad (3\text{-}49b)$$

$$w(\beta,\theta,t) = \bar{w}(\beta)\cos n\theta\ e^{i\omega t} \qquad (3\text{-}49c)$$

and integration around the circumference, the energy integrals take the form,

$$U_o = \frac{\pi \sin\alpha}{2} \int_0^{\beta_1} \Big\| \frac{Eh}{1-\nu^2}[\bar{u}'^2 + (\bar{u}+\cot\alpha\bar{w}+\overline{n\nu})^2 + 2\nu\bar{u}'(\bar{u} + \cot\alpha\bar{w}+\overline{n\nu}) + \frac{1-\nu}{2}(\bar{v}'-\bar{v}-\overline{nu})^2] + Dr_o^{-2}e^{-2\beta}\Big\{(\bar{w}''-\bar{n}^2\bar{w})^2 + 2(1-\nu)[\bar{n}^2(\bar{w}'-\bar{w})^2 - (\bar{w}''-\bar{w}')(\bar{w}'-\bar{n}^2\bar{w})]\Big\} \Big\| d\beta \quad (3\text{-}50)$$

$$U_1 = \frac{\pi\cos\alpha}{2} Dr_o^{-2} \int_0^{\beta_1} e^{-2\beta} \Big\| -2(\bar{w}''-\bar{w}')(\bar{u}'+\nu\overline{nv}) + 2(\bar{w}' - \bar{n}^2\bar{w})(\bar{n}+\cot\alpha\bar{w}) + (1-\nu)\bar{n}(\bar{w}'-\bar{w})[3(\bar{v}'-\bar{v}) + \overline{nu}] + \cot\alpha(\bar{n}+\cot\alpha\bar{w})^2 + \cot\alpha\frac{1-\nu}{2}[3(\bar{v}'-\bar{v})^2 + \bar{n}^2\bar{u}^2] \Big\| d\beta \quad (3\text{-}51)$$

$$T = -\rho h\omega^2 \frac{\pi}{2} \sin\alpha\, r_o^2 \int_0^{\beta_1} [\bar{u}^2 + \bar{v}^2 + \bar{w}^2]\, e^{2\beta} d\beta \quad (3\text{-}52)$$

The sum of Eqs.(3-50)-(3-52) is analogous to Eq.(3-23) used in the previous section. It is seen that besides replacing $\bar{F}$ by $\bar{u}$ and $\bar{v}$ it includes the tangential inertia terms.

In terms of the displacements, the boundary conditions are given as,

At $\beta = 0, \beta_1$,

$$N_r = \frac{Eh}{1-\nu^2}\frac{e^{-\beta}}{r_o}[\bar{u}'+\nu\bar{u}+\nu\overline{n}\bar{v}+\nu\cot\alpha\bar{w}] = 0 \qquad (3\text{-}53a)$$

$$\bar{v} = 0 \qquad (3\text{-}53b)$$

$$\bar{w} = 0 \qquad (3\text{-}53c)$$

$$M_r = \frac{D}{r_o^2}e^{-2\beta}[\bar{w}''-(1-\nu)\bar{w}'-\nu(\overline{n}-\cot^2\alpha)\bar{w}-\cot\alpha(\bar{u}'+\nu\bar{u})] = 0 \qquad (3\text{-}53d)$$

A set of displacement functions satisfying Eqs.(3-53) are given by,

$$\bar{u}(\beta) = \tilde{u}\, e^{-\nu\beta}\cos\frac{\pi}{\beta_1}\beta \qquad (3\text{-}54a)$$

$$\bar{v}(\beta) = \tilde{v}\sin\frac{\pi}{\beta_1}\beta \qquad (3\text{-}54b)$$

$$\bar{w}(\beta) = \frac{\tilde{w}}{\cos\alpha}e^{\mu\beta}\sin\frac{\pi}{\beta_1}\beta \qquad (3\text{-}54c)$$

Equations (3-54) are now substituted into Eqs.(3-50)-(3-52) and the minimum condition is applied,

$$\frac{\partial(U+T)}{\partial\tilde{u}} = \frac{\partial(U+T)}{\partial\tilde{v}} = \frac{\partial(U+T)}{\partial\tilde{w}} = 0 \qquad (3\text{-}55)$$

The resulting characteristic determinant is then given by,

$$\begin{vmatrix} a_{uu}+b_{uu}C^2-c_{uu}\tilde{\omega}^2 & a_{uv} & a_{uw}+b_{uw}C^2 \\ a_{uv} & a_{vv}+b_{vv}C^2-c_{vv}\tilde{\omega}^2 & a_{vw}+b_{vw}C^2 \\ a_{uw}+b_{uw}C^2 & a_{vw}+b_{vw}C^2 & a_{ww}+b_{ww}C^2-c_{ww}\tilde{\omega}^2 \end{vmatrix} = 0 \qquad (3\text{-}56)$$

where the $a_{u_iu_j}$ are the elements due to the membrane terms and are given by,

$$a_{uu}= G_1(\nu)\left\| \bar{\lambda}^2[1+\Delta(\frac{1+2\Delta\nu^2}{1+\Delta\nu^2} - 2\nu^2)] + n^2 \frac{1-\nu}{2} \frac{1+2\Delta\nu^2}{1+\Delta\nu^2} \right\| \qquad (3\text{-}57a)$$

$$a_{uv} =G_1(\nu/2) \frac{n\bar{\lambda}}{2} \left\| 1 + \nu[1 - \frac{\Delta^{\frac{1}{2}} + (2-3\nu-\nu^2)\Delta}{1 + (\frac{\nu}{2})^2\Delta \quad 4}] \right\| \qquad (3\text{-}57b)$$

$$a_{uw}= G_2(\frac{\mu-\nu}{2}) \bar{\lambda}\nu \frac{1 + \frac{\mu-\nu}{2}(1-\nu^2)\Delta}{1 + (\frac{\mu-\nu}{2})^2\Delta} \qquad (3\text{-}57c)$$

$$a_{vv}= n^2 + \frac{1-\nu}{2} \bar{\lambda}^2 (1+\Delta) \qquad (3\text{-}57d)$$

$$a_{vw}= G_1(\mu/2) \frac{n}{1 + (\frac{\mu}{2})^2\Delta} \qquad (3\text{-}57e)$$

$$a_{ww}= G_2(\mu) \frac{1}{1 + \mu^2\Delta} \qquad (3\text{-}57f)$$

The $b_{u_iu_j}$ are the elements due to the bending terms and are given by,

$$b_{uu} = \frac{\cos^2\alpha G_1(1+\nu)}{(1-\delta)^2}\left[\, n^2\,\frac{1-\nu}{2} + \bar{\lambda}^2\Delta\,\right]\left[\,\frac{1+2\Delta(1+\nu)^2}{1+\Delta(1+\nu)^2}\,\right] \qquad (3\text{-}58a)$$

$$b_{uw} = \frac{\bar{\lambda}G_1(1-\frac{\mu-\nu}{2})}{(1-\delta)^2[1+\Delta(1-\frac{\mu-\nu}{2})^2]}\Big\|\ \bar{\lambda}^2\left[\,1 + \frac{\Delta}{2}(5\nu-3\mu-7\mu\nu+\nu^2)\,\right]$$

$$- \frac{n^2}{2}[1-\nu-\Delta(1+\nu^2)(1-\tfrac{\mu-\nu}{2})] - \Delta(1-\tfrac{\mu-\nu}{2}) \qquad (3\text{-}58b)$$

$$\left\{1 + \bar{\lambda}^2\Delta^2[1 + \nu(3\nu-6\mu+3\mu^2-2\mu\nu)]\right\}\Big\|$$

$$b_{vv} = \frac{3\cos^2\alpha}{(1-\delta)^2}\,G_1(1)\,\frac{1-\nu}{2}\,\bar{\lambda}^2 \qquad (3\text{-}58c)$$

$$b_{vw} = \frac{n}{(1-\delta)^2}\,G_1(1-\tfrac{\mu}{2})\,\frac{3-\nu}{2}\,\bar{\lambda}^2\left[\,\frac{1 + \Delta(1-\frac{\mu}{1-\nu/3})}{1 + \Delta(1-\frac{\mu}{2})^2}\,\right] \qquad (3\text{-}58d)$$

$$b_{ww} = \frac{G_1(1-\mu)}{\cos^2\alpha(1-\delta)^2[1+(1-\mu)^2\Delta]}\Big\|\ [n^2-\cos^2\alpha-\mu^2\bar{\lambda}^2\Delta]^2$$

$$+ 2\bar{\lambda}^2\Big\{n^2[1-\Delta\mu(1-\mu)] + \Delta(1+\mu)\Big\} + \bar{\lambda}^4\Big\{\,1 + \qquad (3\text{-}58e)$$

$$+4\Delta[1 - \nu(1-\mu) - \mu(2-\tfrac{3}{2}\mu)] + 2\Delta^2(1-2\nu-3\mu+\tfrac{5}{2}\mu^2+2\mu\nu)(1-\mu)^2\Big\}\Big\|$$

The $c_{u_iu_i}$ are the elements due to the inertia terms and are given by,

$$c_{uu} = G_2(1-\nu)\ (1-\delta)^2\ \frac{1 + 2(1-\nu)^2\Delta}{1 + (1-\nu)^2\Delta} \tag{3-59a}$$

$$c_{vv} = G_2(1)\ (1-\delta)^2\ \frac{1}{1+\Delta} \tag{3-59b}$$

$$c_{ww} = G_2(1+\mu)\ (1-\delta)^2\ \frac{1}{\cos^2\alpha[1+(1+\mu)^2\Delta]} \tag{3-59c}$$

where,

$$\tilde{\omega}^2 = (1-\nu^2)\bar{\omega}^2 \tag{3-60a}$$

$$c^2 = (1-\nu^2)c_*^2 = \frac{1}{12}\left(\frac{h}{R_o}\right)^2 \tag{3-60b}$$

$$G_1(\ ) = \frac{1 - e^{-2\beta_1(\ )}}{2\beta_1(\ )} \tag{3-60c}$$

$$G_2(\ ) = \frac{e^{2\beta_1(\ )} - 1}{2\beta_1(\ )} = e^{2\beta_1(\ )}G_1(\ ) \tag{3-60d}$$

The solution of Eq.(3-56) yields three frequencies, the lowest of which is of interest to us.

It is seen that this approach results in quite involved expressions for the elements in the characteristic determinant. It is clear that any extension to include more expansion modes becomes prohibitively laborious, so that it is questionable whether such an extension should even be attempted, We therefore turn now to the second approach, in an attempt to obtain more managable expressions.

(b) "First Approximation" Shell Theory and Simple Displacement Functions

This approach employs the thin shell theory of Chapter 2.

If Eqs.(3-54) were to be used for the assumed displacement functions, then the resulting characteristic determinant would be similar to Eq.(3-56) except for the vanishing of the $b_{u_i u_j}$'s , save b_{ww} (in b_{ww} the $\cos^2\alpha$ term would be missing from the first bracket). This would still leave us with quite involved expressions for the elements. Therefore we seek another set of displacement functions which would ameliorate this situation.

In a free vibration problem the minimum requirement of the Rayleigh-Ritz method is that the assumed functions satisfy the geometrical boundary conditions only, rather than both the geometrical and force boundary conditions. This requirement is met, in this case, by taking trigonometric functions, in the variable β, for the assumed displacements. Due to the relative simplicity of these functions, the expressions may be written in a general manner, for an arbitrary number of assumed modes.

Let,

$$\bar{u}(\beta) = \sum_{m=1}^{M} \tilde{u}_m \cos\frac{m\pi}{\beta_1}\beta \qquad (3\text{-}61a)$$

$$\bar{v}(\beta) = \sum_{m=1}^{M} \tilde{v}_m \sin\frac{m\pi}{\beta_1}\beta \qquad (3\text{-}61b)$$

$$\bar{w}(\beta) = \sum_{m=1}^{M} \tilde{w}_m \frac{1}{\cos\alpha} \sin\frac{m\pi}{\beta_1}\beta \qquad (3\text{-}61c)$$

It is seen that each of the assumed modes for $\bar{v}$ and $\bar{w}$ satisfies the boundary conditions given by Eqs.(3-53b-c). The other boundary conditions will be satisfied on the average by the approximation. It is noted that as $\alpha \longrightarrow 0$,

$$\lim_{\alpha\to 0} \frac{\beta}{\beta_1} = \lim_{\alpha\to 0} \frac{\ln(1+ x/r_o)}{\ln(1+ \ell/r_o)} = \frac{x}{\ell} \qquad (3\text{-}62)$$

where x is the distance along the generator from the top base and ℓ is the length of the generator. Thus, Eqs.(3-61) reduce to the expressions for the cylinder in the limit.

Equations (3-61) are now substituted into Eqs.(3-50) and (3-52), resulting in the following expression for the total energy*,

$$\begin{aligned}
U_o + T = \frac{Eh\pi^2}{4\bar{\lambda}(1-\nu^2)} \sum_{m=1}^{M} \Bigg\| & [\bar{\lambda}^2(m^2+\Delta)+(\tfrac{1-\nu}{2})n^2]\tilde{u}_m^2 \\
& + [\bar{\lambda}^2(m^2+\Delta)(\tfrac{1-\nu}{2})+n^2]\tilde{v}_m^2 + \tilde{w}_m^2 + 2(\tfrac{1+\nu}{2})m\bar{\lambda}n\tilde{u}_m\tilde{v}_m \\
& + 2\nu m\bar{\lambda}\tilde{u}_m\tilde{w}_m + 2n\tilde{v}_m\tilde{w}_m - \frac{1}{f(\delta)(m^2+\Delta)}\Big\{ m^2\tilde{v}_m^2\tilde{\omega}_m^2 \\
& + (m^2+2\Delta)u_m^2 + \frac{m^2}{\cos^2\alpha}[\tilde{\omega}_m^2 - \frac{C^2}{(1-\delta^2)^2}(n^2+m^2\bar{\lambda}^{-2})^2]\tilde{w}_m^2\Big\} \Bigg\| \\
+ \frac{2Eh\pi^2}{\bar{\lambda}(1-\nu^2)} \sum_{m=1}^{M} \sum_{\bar{m}=2}^{\bar{m}\neq m} \Bigg[& \frac{m\bar{\lambda}}{\bar{m}^2-m^2}\Big\{\nu m\bar{\lambda}\tilde{u}_m\tilde{u}_{\bar{m}} + \frac{1-\nu}{2}\,\bar{m}\bar{\lambda}\tilde{v}_m\tilde{v}_{\bar{m}} \\
& + \frac{3-\nu}{2}\,n\tilde{v}_m\tilde{u}_{\bar{m}} + \tilde{w}_m\tilde{u}_{\bar{m}}\Big\}\begin{cases} \frac{\Delta^{\frac{1}{2}}}{\pi} & \text{odd} \\ 0 & \text{even} \end{cases} \qquad (3\text{-}63) \\
& + \frac{1}{(m^2-\bar{m}^2)^2+8\Delta(m^2+\bar{m}^2)+16\Delta^2} \Bigg\| \tilde{\omega}^2\Big\{ (m^2+\bar{m}^2+4\Delta)\tilde{u}_m\tilde{u}_{\bar{m}}
\end{aligned}$$

---

* In the following, the words 'odd' and 'even' refer to the sum $m + \bar{m}$.

$$+ 2n\bar{m}\left[\tilde{v}_m\tilde{v}_{\bar{m}} + \frac{1}{\cos^2\alpha}\tilde{w}_m\tilde{w}_{\bar{m}}\right]\Bigg\}\begin{Bmatrix}(1+\delta^2)\ \frac{\Delta^{\frac{1}{2}}}{\pi}\ \text{odd}\\ -\frac{\Delta}{f(\delta)}\quad\text{even}\end{Bmatrix} \qquad \text{(3-63 cont'd)}$$

$$+ \frac{c^2}{(1-\delta^2)^2}\frac{2n\bar{m}\tilde{w}_m\tilde{w}_{\bar{m}}}{\cos^2\alpha}\Bigg\{ n^4 + \frac{n^2\bar{\lambda}^2}{2}\left[(5-\nu)m^2 - (1-\nu)\bar{m}^2\right]$$

$$+ \frac{\bar{\lambda}^4\bar{m}^2}{2}\left[(1+\nu)m^2 + (1-\nu)\bar{m}^2\right]\Bigg\}\begin{Bmatrix}(1+\delta^2)\ \frac{\Delta^{\frac{1}{2}}}{\pi}\ \text{odd}\\ \frac{\Delta}{f(\delta)}\quad\text{even}\end{Bmatrix}\Bigg]$$

If the minimum condition is now applied,

$$\frac{\partial(U_o+T)}{\partial\tilde{u}_m} = \frac{\partial(U_o+T)}{\partial\tilde{v}_m} = \frac{\partial(U_o+T)}{\partial\tilde{w}_m} = 0 \qquad (3\text{-}64)$$

we obtain 3M homogeneous simultaneous algebraic equations in the amplitudes $\tilde{u}_m$, $\tilde{v}_m$, $\tilde{w}_m$, of the general form,

$$\tilde{u}_m\left\{\bar{\lambda}^2(m^2+\Delta) + \frac{1-\nu}{2}n^2 - \frac{m^2+2\Delta}{m^2+\Delta}\frac{\tilde{\omega}^2}{f(\delta)}\right\} + \tilde{v}_m\frac{1+\nu}{2}\bar{\lambda}mn + \tilde{w}_m\nu\bar{\lambda}m$$

$$- \frac{4\Delta^{\frac{1}{2}}}{\pi}\sum_{\bar{m}}^{\substack{m+\bar{m}\\ \text{odd}}}\left\{\nu\bar{\lambda}^2\tilde{u}_{\bar{m}} + \frac{3-\nu}{2}\frac{n\bar{m}\bar{\lambda}}{\bar{m}^2-m^2}\tilde{v}_{\bar{m}} + \frac{\bar{m}\bar{\lambda}}{\bar{m}^2-m^2}\tilde{w}_{\bar{m}}\right\} \qquad (3\text{-}65a)$$

$$+ \tilde{\omega}^2\sum_{\bar{m}}\frac{8[m^2+\bar{m}^2+4\Delta]\ \tilde{u}_{\bar{m}}}{(m^2-\bar{m}^2)^2+(8\Delta)(m^2+\bar{m}^2)+16\Delta^2}\begin{Bmatrix}(1+\delta^2)\ \frac{\Delta^{\frac{1}{2}}}{\pi}\ \text{odd}\\ -\frac{\Delta}{f(\delta)}\quad\text{even}\end{Bmatrix} = 0$$

$$\tilde{u}_m \frac{1+\nu}{2} nm\bar{\lambda} + \tilde{v}_m\left\{n^2 + \frac{1-\nu}{2}\bar{\lambda}^2(m^2+\Delta) - \frac{m^2}{m^2+\Delta}\frac{\tilde{\omega}^2}{f(\delta)}\right\} + n\tilde{w}_m$$

$$- \frac{4\Delta^{\frac{1}{2}}}{\pi} \sum_{\bar{m}}^{\substack{m+\bar{m}\\ \text{odd}}} \frac{3-\nu}{2} \frac{nm\bar{\lambda}}{m^2-\bar{m}^2} \tilde{u}_{\bar{m}} \qquad (3\text{-}65b)$$

$$+ \tilde{\omega}^2 \sum_{\bar{m}} \frac{16m\bar{m}\,\tilde{v}_{\bar{m}}}{(m^2-\bar{m}^2)^2+(8\Delta)(m^2+\bar{m}^2)+16\Delta^2} \begin{Bmatrix} (1+\delta^2)\frac{\Delta^{\frac{1}{2}}}{\pi} \text{odd} \\ -\frac{\Delta}{f(\delta)} \text{ even} \end{Bmatrix} = 0$$

$$\tilde{u}_m \nu\bar{\lambda}m + n\tilde{v}_m + \tilde{w}_m \left\{1 - \frac{m^2}{(m^2+\Delta)f(\delta)\cos^2\alpha}\left[\tilde{\omega}^2\right.\right.$$

$$\left.\left. - \frac{c^2}{(1-\delta^2)^2}(n^2+m^2\bar{\lambda}^2)^2\right]\right\} - \frac{4\Delta^{\frac{1}{2}}}{\pi} \sum_{\bar{m}}^{\substack{m+\bar{m}\\ \text{odd}}} \frac{\bar{\lambda}m}{m^2-\bar{m}^2} \tilde{u}_{\bar{m}}$$

$$+ \frac{1}{\cos^2\alpha} \sum_{\bar{m}} \frac{16m\bar{m}\quad \tilde{w}_{\bar{m}}}{(m^2-m^2)^2+(8\Delta)(M^2+m^2)+16\Delta^2} \left\| \tilde{\omega}^2 \begin{Bmatrix} (1+\delta^2)\frac{\Delta^{\frac{1}{2}}}{\pi} \text{odd} \\ -\frac{\Delta}{f(\delta)} \text{ even} \end{Bmatrix} \right. \qquad (3\text{-}65c)$$

$$+ \frac{c^2}{(1-\delta^2)^2}\left\{[n^2 + \bar{\lambda}^2(\frac{m^2+\bar{m}^2}{2})]^2\right.$$

$$\left.\left. - \nu\bar{\lambda}^4(\frac{m^2-\bar{m}^2}{2})^2\right\} \begin{Bmatrix} (1+\delta^2)\frac{\Delta^{\frac{1}{2}}}{\pi} \text{odd} \\ \frac{\Delta}{f(\delta)} \text{ even} \end{Bmatrix} \right\| = 0$$

The lowest frequency obtained from the solution of the characteristic determinant of Eqs.(3-65) is the required result.

For a single mode, M = 1, the determinant takes the form,

$$\begin{vmatrix} a_{uu}-c_{uu}\omega^2 & a_{uv} & a_{uw} \\ a_{uv} & a_{vv}-c_{vv}\omega^2 & a_{vw} \\ a_{uw} & a_{vw} & a_{ww}+b_{ww}c^2-c_{ww}\omega^2 \end{vmatrix} = 0 \qquad (3\text{-}66)$$

where,

$$a_{uu} = \bar{\lambda}^2(1+\Delta) + \frac{1-\nu}{2} n^2 \qquad (3\text{-}67a)$$

$$a_{uv} = \frac{1+\nu}{2} n\bar{\lambda} \qquad (3\text{-}67b)$$

$$a_{uw} = \nu\bar{\lambda} \qquad (3\text{-}67c)$$

$$a_{vv} = n^2 + \frac{1-\nu}{2} \bar{\lambda}^2(1+\Delta) \qquad (3\text{-}67d)$$

$$a_{vw} = n \qquad (3\text{-}67e)$$

$$a_{ww} = 1 \qquad (3\text{-}67f)$$

$$b_{ww} = \frac{(n^2+\bar{\lambda}^2)^2}{f(\delta)\cos^2\alpha(1-\delta^2)^2(1+\Delta)} \qquad (3\text{-}68)$$

$$c_{uu} = \frac{1+2\Delta}{1+\Delta} \frac{1}{f(\delta)} \qquad (3\text{-}69a)$$

$$c_{vv} = \frac{1}{1+\Delta} \frac{1}{f(\delta)} \qquad (3\text{-}69b)$$

$$c_{ww} = \frac{1}{1+\Delta} \frac{1}{f(\delta)} \frac{1}{\cos^2\alpha} \qquad (3\text{-}69c)$$

Comparison of Eqs.(3-57)-(3-59) with Eqs.(3-67)-(3-69) shows the remarkable simplicity of the latter expressions,

which are very similar to the expressions for a cylinder. The simplicity of these, as well as the cross coupling terms among the various modes, is an important advantage from a computational standpoint, since rapid calculations can be carried out for even a large number of assumed modes.

This result may be further simplified, if desired, by neglecting the tangential inertia terms. This simplification is expected to be valid for large n.

3.5 Exact Solutions

So far, all the results were obtained using approximate variational methods. This was necessary since no exact solutions to the equations of motion are available in the general case.

For some cases, however, exact solutions in terms of tabulated functions are possible. In this section solutions are given for two such cases. A search of the literature has failed to disclose any previous publications of these results.

(a) Torsional Vibrations Using Membrane Theory

We consider the case of axisymmetric deformations of the conical shell. Under this condition there are two distinct types of deformations, uncoupled from each other. One involves the transverse and longitudinal displacements w and u, the other involves the circumferential displacement v only, thus being a purely torsional mode. This situation is similar to the case of circular cylinders.

Using membrane theory, the equations of free vibrations are given by,

$$r^2\frac{d^2u}{dr^2} + r\frac{du}{dr} + [r^2\frac{\rho(1-\nu^2)\omega^2}{E} - 1]u + \nu\cot\alpha r\frac{dw}{dr} - \cot\alpha\, w = 0 \quad (3\text{-}70a)$$

$$\nu\cot\alpha\, r\frac{du}{dr} + \cot\alpha\, u - [r^2\frac{\rho(1-\nu^2)\omega^2}{E} - \cot^2\alpha]\, w = 0 \quad (3\text{-}70b)$$

$$r^2\frac{d^2v}{dr^2} + r\frac{dv}{dr} + [r^2\frac{\rho}{G}\omega^2 - 1]\, v = 0 \quad (3\text{-}71)$$

It is seen that Eqs.(3-70) involve u, w only, whereas Eq.(3-71) involves v only.

In Ref. [15] Eqs.(3-70) are solved for some special cases, e.g. for $\rho \propto r^{-2}$ etc., and as mentioned in Section 3.1, a power series approach is used to solve them in Ref. [13]. Equation (3-71) defines the torsional vibrations of the shell. Its general solution is given in terms of Bessel functions,

$$v = A\, J_1(\bar{\omega}\bar{r}) + B\, Y_1(\bar{\omega}\bar{r}) \quad (3\text{-}72)$$

where, $\bar{\omega} = \omega\ell\sqrt{\frac{\rho}{G}}$ = non-dimensional torsional frequency (3-73a)

$\bar{r} = \frac{r}{\ell}$ = non-dimensional length (ℓ = length along generator) (3-73b)

For a "simply-supported" shell, v = 0 at both edges. Then the mode shapes are given by,

$$v_m = A\left\{ J_1(\bar{\omega}_m\bar{r}) - \frac{J_1(\bar{\omega}_m\frac{1-\delta}{2\delta})}{Y_1(\bar{\omega}_m\frac{1-\delta}{2\delta})}\, Y_1(\bar{\omega}_m\bar{r}) \right\} \quad (3\text{-}74)$$

and the frequency equation is given by,

$$\frac{Y_1(\bar{\omega}_m \frac{1-\delta}{2\delta})}{J_1(\bar{\omega}_m \frac{1-\delta}{2\delta})} = \frac{Y_1(\bar{\omega}_m \frac{1+\delta}{2\delta})}{J_1(\bar{\omega}_m \frac{1+\delta}{2\delta})} \tag{3-75}$$

Eq.(3-75) is now written in the form,

$$\frac{Y_1(\frac{\bar{\omega}_m}{2\delta} - \frac{\bar{\omega}_m}{2})}{J_1(\frac{\bar{\omega}_m}{2\delta} - \frac{\bar{\omega}_m}{2})} = \frac{Y_1(\frac{\bar{\omega}_m}{2\delta} + \frac{\bar{\omega}_m}{2})}{J_1(\frac{\bar{\omega}_m}{2\delta} + \frac{\bar{\omega}_m}{2})} \tag{3-76}$$

As the cone approaches a cylinder $\delta \longrightarrow 0$ and the arguments become large. We have then,

$$\lim_{t \longrightarrow \infty} \frac{Y_1(t)}{J_1(t)} = \tan(t - \frac{3\pi}{4}) \tag{3-77}$$

Therefore, for $\delta \longrightarrow 0$,

$$\tan(\frac{\bar{\omega}_m}{2\delta} - \frac{3\pi}{4} - \frac{\bar{\omega}_m}{2}) = \tan(\frac{\bar{\omega}_m}{2\delta} - \frac{3\pi}{4} + \frac{\bar{\omega}_m}{2}) \tag{3-78}$$

and we have,

$$\bar{\omega}_m = m\pi \tag{3-79}$$

This is exactly the solution for the torsional vibrations of the cylindrical shell. It can also be shown that the mode shape reduces to the sinusoidal function of the cylinder.

On the other hand, for closed cones, $\delta = 1$. Eqs.(3-74) and (3-75) reduce in this case to,

$$v_m = A\, J_1(\bar{\omega}_m\, \bar{r}) \tag{3-80a}$$

$$J_1(\bar{\omega}_m) = 0 \tag{3-80b}$$

This interesting result means that the torsional frequency of the cone is independent of the vertex angle and depends only on its length. Therefore the result should be valid for circular plates as well. A quick check proves that this is actually the case. Furthermore, the torsional vibration frequency of the truncated cone equals that of a concentric circular plate whose outer radius equals the length of the complete cone and inner radius equals the distance from the vertex to the narrow base along the side.

A comparison of the results given here with those obtained by the approximate method of Section 3.4 will be made in Section 3.6.

(b) Flexural Vibrations Neglecting Membrane Effect

We next consider the case where the shell's deformations are primarily flexural in character. The equation of motion is given by Eq.(3-16b), where F_{rr} is replaced by N_θ,

$$D\nabla^4 w + \frac{\cot\alpha}{r} N_\theta + \rho\, h\, \ddot{w} = 0 \tag{3-81}$$

Using Eqs.(2-9b) and (3-44) to express N_θ in terms of the displacements and substituting into Eq.(3-81), we obtain,

$$D\nabla^4 w + \frac{Eh}{1-\nu^2} \frac{\cot\alpha}{r} \left[\frac{\cot\alpha}{r} w + \frac{u}{r} + \frac{1}{r}\frac{\partial v}{\partial \theta} + \nu \frac{\partial u}{\partial r}\right] + \rho h \ddot{w} = 0 \tag{3-82}$$

Obviously, this equation cannot be solved by itself, since it involves all three displacement components. An approximate form of this equation, which neglects the tangential displacements, considers axisymmetric motion only and neglects the first and second derivatives in w, was investigated by Ramakrishna [18] in his study of loudspeakers. This simplified equation takes the form,

$$r^2\frac{d^4w}{dr^4} + 2r\,\frac{d^3w}{dr^3} + \left(\frac{12\cot^2\alpha}{h^2} - \frac{\rho h}{D}\,\omega^2\,r^2\right) w = 0 \qquad (3\text{-}83)$$

He was unable to solve the equation exactly, however, and had to resort to the use of a Rayleigh-Ritz approach.

If the membrane terms are neglected altogether, Eq.(3-81) takes the form,

$$(\nabla^4 - \bar{\omega}^2)\, w = 0 \qquad (3\text{-}84)$$

where,

$$\bar{\omega}^2 = \sqrt{\frac{\rho h}{D}}\,\ell^2\,\omega^2 = \text{nondimensional bending frequency} \qquad (3\text{-}85a)$$

$$\nabla^2 w = \frac{1}{\bar{r}}\frac{\partial}{\partial \bar{r}}\left(\bar{r}\,\frac{\partial w}{\partial \bar{r}}\right) + \frac{1}{\bar{r}^2}\frac{\partial^2 w}{\partial \bar{\theta}^2} \qquad (3\text{-}85b)$$

While Eq.(3-84) does not purport to represent the true behavior of the shell, it has the advantage that it can be solved exactly and thus provide useful information on the shell's pure bending vibrations. By comparing the solutions of this case to those of a circular cylinder (where the membrane effects have also been neglected), an insight is gained into the effect of taper on the motion, as far as the bending

terms are concerned. The neglect of the membrane terms is justified when most of the strain energy is due to bending, which occurs when n is large and the thickness is not too small.

Equation (3-84) was solved by Partridge [19] in an approximate manner for a cone clamped at its narrow base. It is believed, however, that the solution is in error due to the particular choice of the coordinate system.

The solution to Eq.(3-84) is the sum of the solutions to each one of the equations,

$$(\nabla^2 - \bar{\omega})\ w = 0 \tag{3-86a}$$

$$(\nabla^2 + \bar{\omega})\ w = 0 \tag{3-86b}$$

and is given by,

$$\begin{aligned} w(\bar{r},\theta) = [&A_1 J_{\bar{n}}(\bar{\omega}^{\frac{1}{2}}\bar{r}) + A_2 J_{-\bar{n}}(\bar{\omega}^{\frac{1}{2}}\bar{r}) \\ &+ A_3 I_{\bar{n}}(\bar{\omega}^{\frac{1}{2}}\bar{r}) + A_4 I_{-\bar{n}}(\bar{\omega}^{\frac{1}{2}}\bar{r})]\ \cos n\theta \end{aligned} \tag{3-87}$$

The boundary conditions are,

At $\bar{r} = \frac{1-\delta}{2\delta},\ \frac{1+\delta}{2\delta}$

$$w = 0 \tag{3-88a}$$

$$M_r = \frac{D}{\ell^2}\left[\frac{\partial^2 w}{\partial \bar{r}^2} + \nu\left(\frac{1}{\bar{r}}\frac{\partial w}{\partial \bar{r}} + \frac{1}{\bar{r}^2}\frac{\partial^2 w}{\partial \bar{\theta}^2}\right)\right] = 0 \tag{3-88b}$$

Substitution of Eq.(3-87) in Eqs.(3-88) yields the 4 x 4 characteristic determinant from which the frequencies may be

obtained. Since tables of Bessel functions are available generally for integral orders, and since generality is not lost thereby, $\bar{n}$ is assumed as an integer, in which case $J_{-\bar{n}}$ is replaced by $Y_{\bar{n}}$ and $I_{-\bar{n}}$ is replaced by $K_{\bar{n}}$. In this case the determinant reads,

$$\begin{vmatrix} a_{11} & a_{12} & a_{13} & a_{14} \\ a_{21} & a_{22} & a_{23} & a_{24} \\ a_{31} & a_{32} & a_{33} & a_{34} \\ a_{41} & a_{42} & a_{43} & a_{44} \end{vmatrix} = 0 \qquad (3\text{-}89)$$

where,

$$a_{11} = J_{\bar{n}}(\bar{\omega}_o^{\frac{1}{2}}) \qquad a_{12} = Y_{\bar{n}}(\bar{\omega}_o^{\frac{1}{2}})$$
$$a_{13} = I_{\bar{n}}(\bar{\omega}_o^{\frac{1}{2}}) \qquad a_{14} = K_{\bar{n}}(\bar{\omega}_o^{\frac{1}{2}}) \qquad (3\text{-}90)$$

$$a_{21} = [\bar{n}(\bar{n}+1)(1-\nu) - \bar{\omega}_o]J_{\bar{n}}(\bar{\omega}_o^{\frac{1}{2}}) - (1-\nu)\bar{\omega}_o\, J_{\bar{n}-1}(\bar{\omega}_o^{\frac{1}{2}}) \qquad (3\text{-}91a)$$

$$a_{22} = [\bar{n}(\bar{n}+1)(1-\nu) - \bar{\omega}_o]Y_{\bar{n}}(\bar{\omega}_o^{\frac{1}{2}}) - (1-\nu)\bar{\omega}_o\, Y_{\bar{n}-1}(\bar{\omega}_o^{\frac{1}{2}}) \qquad (3\text{-}91b)$$

$$a_{23} = [\bar{n}(\bar{n}+1)(1-\nu) + \bar{\omega}_o]I_{\bar{n}}(\bar{\omega}_o^{\frac{1}{2}}) - (1-\nu)\bar{\omega}_o\, I_{\bar{n}-1}(\bar{\omega}_o^{\frac{1}{2}}) \qquad (3\text{-}91c)$$

$$a_{24} = [\bar{n}(\bar{n}+1)(1-\nu) + \bar{\omega}_o]K_{\bar{n}}(\bar{\omega}_o^{\frac{1}{2}}) + (1-\nu)\bar{\omega}_o\, K_{\bar{n}-1}(\bar{\omega}_o^{\frac{1}{2}}) \qquad (3\text{-}91d)$$

and where a_{3i} and a_{4i} are similar to a_{1i} and a_{2i}, respectively, with $\bar{\omega}_o$ replaced by $\bar{\omega}_1$, where,

$$\bar{\omega}_o = \bar{\omega} \left(\frac{1-\delta}{2\delta}\right)^2 \tag{3-92a}$$

$$\bar{\omega}_1 = \bar{\omega} \left(\frac{1+\delta}{2\delta}\right)^2 \tag{3-92b}$$

By a proper limiting process, it can be shown that as $\delta \longrightarrow 0$ these results reduce to the known results for a cylinder of length ℓ and radius R_o,

$$\bar{\omega}_{cyl} = \left(\frac{\ell n}{R_o}\right)^2 + \pi^2 \tag{3-93}$$

For $\delta = 1$, a complete cone, the mode shape is given by,

$$w = A \left[J_{\bar{n}}(\bar{\omega}^{\frac{1}{2}} \bar{r}) - \frac{J_{\bar{n}}(\bar{\omega}^{\frac{1}{2}})}{I_{\bar{n}}(\bar{\omega}^{\frac{1}{2}})} I_{\bar{n}}(\bar{\omega}^{\frac{1}{2}} \bar{r})\right] \cos n\theta \tag{3-94}$$

and the characteristic equation is,

$$\frac{I'_{\bar{n}}(\bar{\omega}^{\frac{1}{2}})}{I_{\bar{n}}(\bar{\omega}^{\frac{1}{2}})} - \frac{J'_{\bar{n}}(\bar{\omega}^{\frac{1}{2}})}{J_{\bar{n}}(\bar{\omega}^{\frac{1}{2}})} = \frac{2\bar{\omega}^{\frac{1}{2}}}{1-\nu} \tag{3-95}$$

For large values of $\bar{n}$ (small α or large n), the ratio of the $I_{\bar{n}}$'s approaches unity, and since the value of $\bar{\omega}^{1/2}$ is of the order of $\bar{n}$, a good approximation to $\bar{\omega}^{1/2}$ is obtained by the root of,

$$J_{\bar{n}}(\bar{\omega}^{\frac{1}{2}}) = 0 \tag{3-96}$$

For the ratio of the $J_{\bar{n}}$'s to be large and negative, the actual value of $\bar{\omega}^{1/2}$ must be slightly smaller than that given by Eq.(3-96).

From Eqs.(3-93) and (3-96), using Jahnke and Emde [20], we can calculate the ratio of the frequencies of the complete cone to that of the corresponding cylinder. An example is given in Table 3.1.

TABLE 3.1

FREQUENCY RATIO OF CONE TO CYLINDER FOR n = 6

α	5^o	10^o	15^o	17.5^o
$\bar{n}$	68.8	34.5	23.2	20.0
$\frac{\omega_{cone}}{\omega_{cyl}}$	.31	.35	.39	.40

It is evident that the flexural frequency of the complete cone is always less than that of the corresponding cylinder, if the membrane terms are neglected.

3.6 Comparison of the Methods

The lack of exact solutions to the problem in the general case has forced us to the use of various approximate methods of solution. Since it was shown that there exist a number of such approximate methods, the obvious question is what are the criteria of selection of one particular method over all others? Obviously, the most important consideration is whether the method approximates well the exact solution. In instances such as ours, where the exact solution is not known (except for some special cases), a clue to the quality of the results is provided by the convergence rate of higher approximations obtained by including more expansion modes. This leads to the criteria of how well is the method adapted

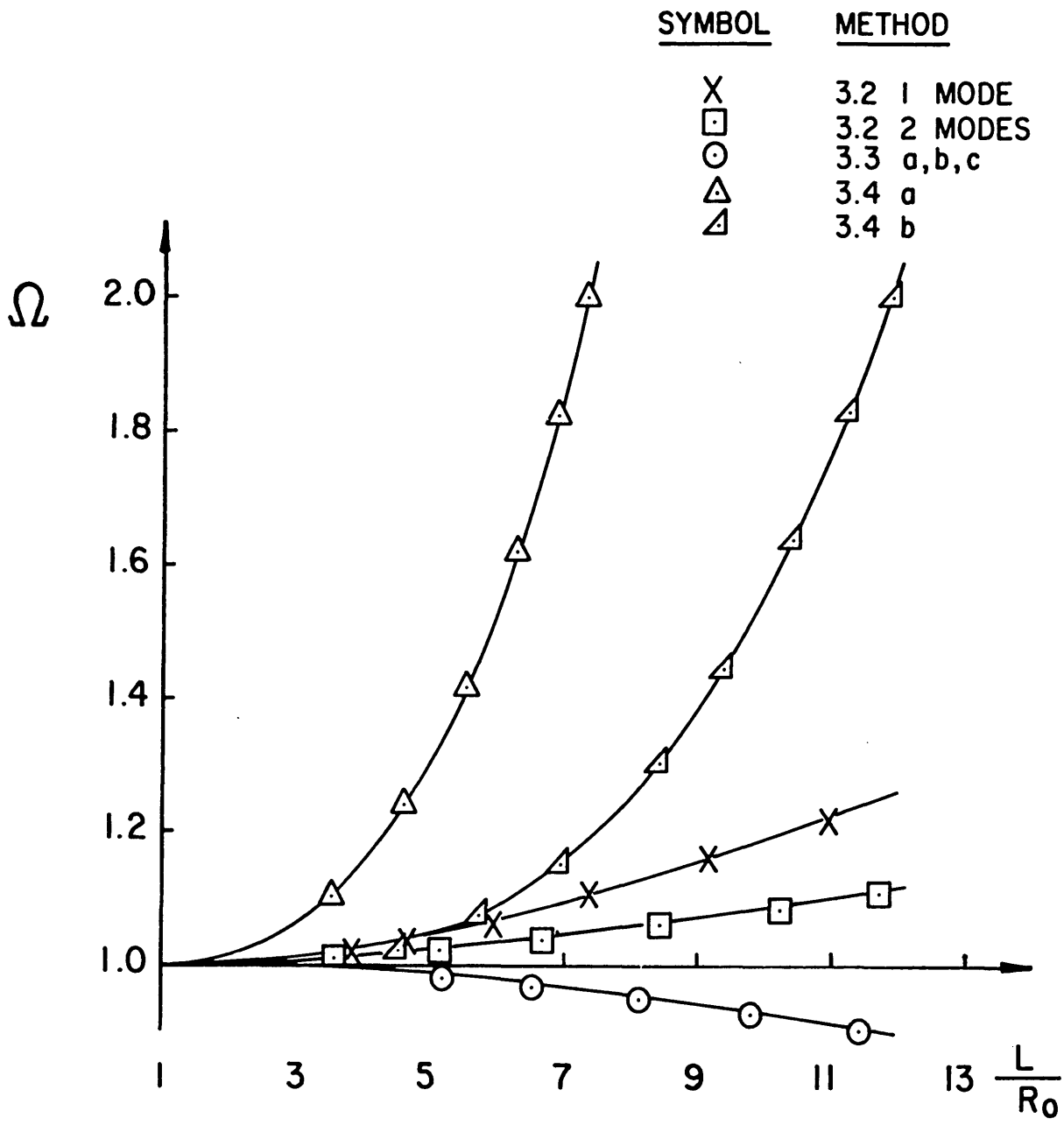

FIG. 3.3 COMPARISON OF FREQUENCY RATIOS BY DIFFERENT METHODS

(a) $n = 2$, $h/R = 0$, $\alpha = 5°$

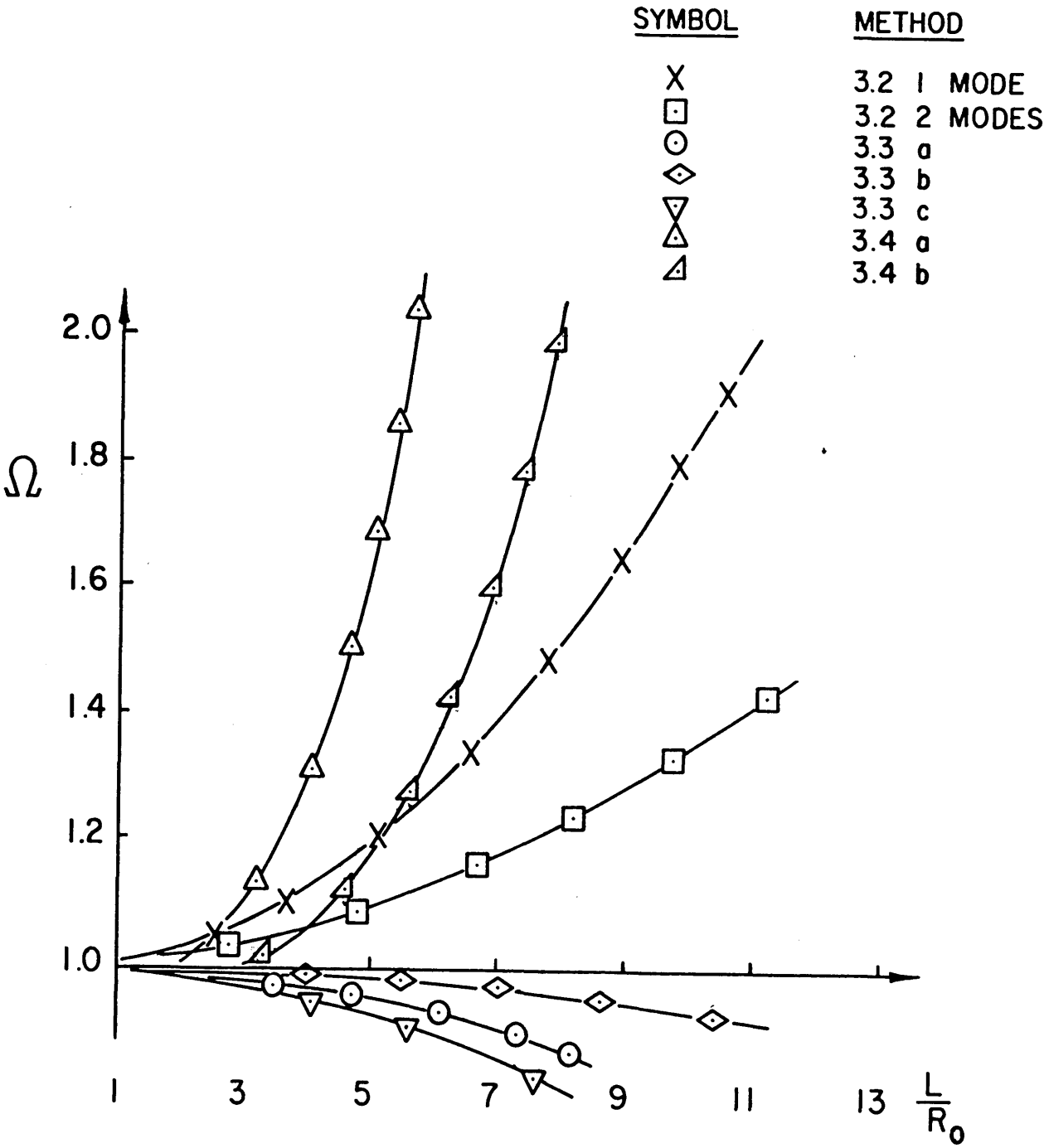

FIG. 3.3 (CONTINUED)

(b) $n = 2$, $h/R = 0$, $\alpha = 10°$

to the inclusion of more than one assumed mode and whether calculations can be made efficiently. An additional important consideration is the range of applicability of each method, namely, whether or not it accounts equally well for the membrane and bending effects. If the evaluation of each method is approached from this view point, the task of selection of the most appropriate method becomes a little easier.

First of all, it is necessary to determine whether all or most of the results reveal similar trends. If so, then it may be assumed that the same trend is exhibited by the true solution (unless all the approximate results are in error, which seems unlikely). If any of the methods reveals a trend contrary to that of the others, then the question of which is the correct trend must be settled by comparison with higher approximations. When the methods yielding the right trend have been established, then it is possible to apply the other criteria and to decide on the "best" method.

Another check on the method is provided by using it to solve the special case for which an exact solution is known, and comparing the two results. In our case, two factors are at work, namely, the membrane stresses and the flexural stresses, whose effects are coupled due to the curvature of the shell. Since we have been able to obtain two exact solutions for cases where either membrane or flexure effect exists but not both, we may assess the ability of the method to yield satisfactory solutions in each of these diverse cases, and therefore to determine how well it accounts for the two effects.

Although calculations were made for a wide range of the parameters, comparison of the results is made for three cases only. These represent situations where (a) No bending terms are present, (b) The strain energy due to bending is comparable with that due to stretching, (c) The bending effect predominates. Thus the three cases cover the whole range of

interest of this problem.

The results of the first case are shown in Fig. 3.3, wherein is plotted the quantity Ω, which is the ratio of the frequency of the cone to that of the corresponding cylinder having the same $\frac{L}{R_o}$ ratio, vs. this ratio, for the case $n = 2$, $\frac{h}{R_o} = 0$ and $\alpha = 5^o$ and 10^o. The various methods are identified by the number of the section in which they are developed. Fig. 3.4 shows the same results for the second case, for which $n = 4$, $\frac{h}{R_o} = \frac{1}{100}$ and $\alpha = 5^o$ and 10^o. Finally Fig. 3.5 gives the results for the third case, for which $n = 6$, $\frac{h}{R_o} = \frac{1}{30}$, $\alpha = 5^o$ and 10^o.

These plots reveal the fact that although in most cases similar trends are shown by all the methods, the results may differ widely. This is true not only of methods utilizing different theories, but also of variations within each approach due to the employment of different assumed modes. It is seen that for $\alpha = 5^o$, the results of the three methods employing stress and displacement functions are the same, but that for $\alpha = 10^o$ they vary considerably. Also, that the two methods employing pure displacement functions vary considerably in cases (a) and (b), but are quite close in case (c).

Fig. 3.3 shows that Methods 3.3 (stress and displacement functions) exhibit a trend opposite to that of the other methods. As will be shown later, on the basis of higher approximations, the membrane effect tends to increase the frequency of the cone compared to that of the cylinder, therefore Methods 3.3 show the wrong trend in this case.

Figs. 3.4 and 3.5 show that as bending effects become more important, Methods 3.2 (shallow-shell theory) yield an Ω of unity. The reason for this can be easily seen from Eq.(3-9), which shows that shallow-shell theory does not predict any difference in the bending term between the cone and the cyl-

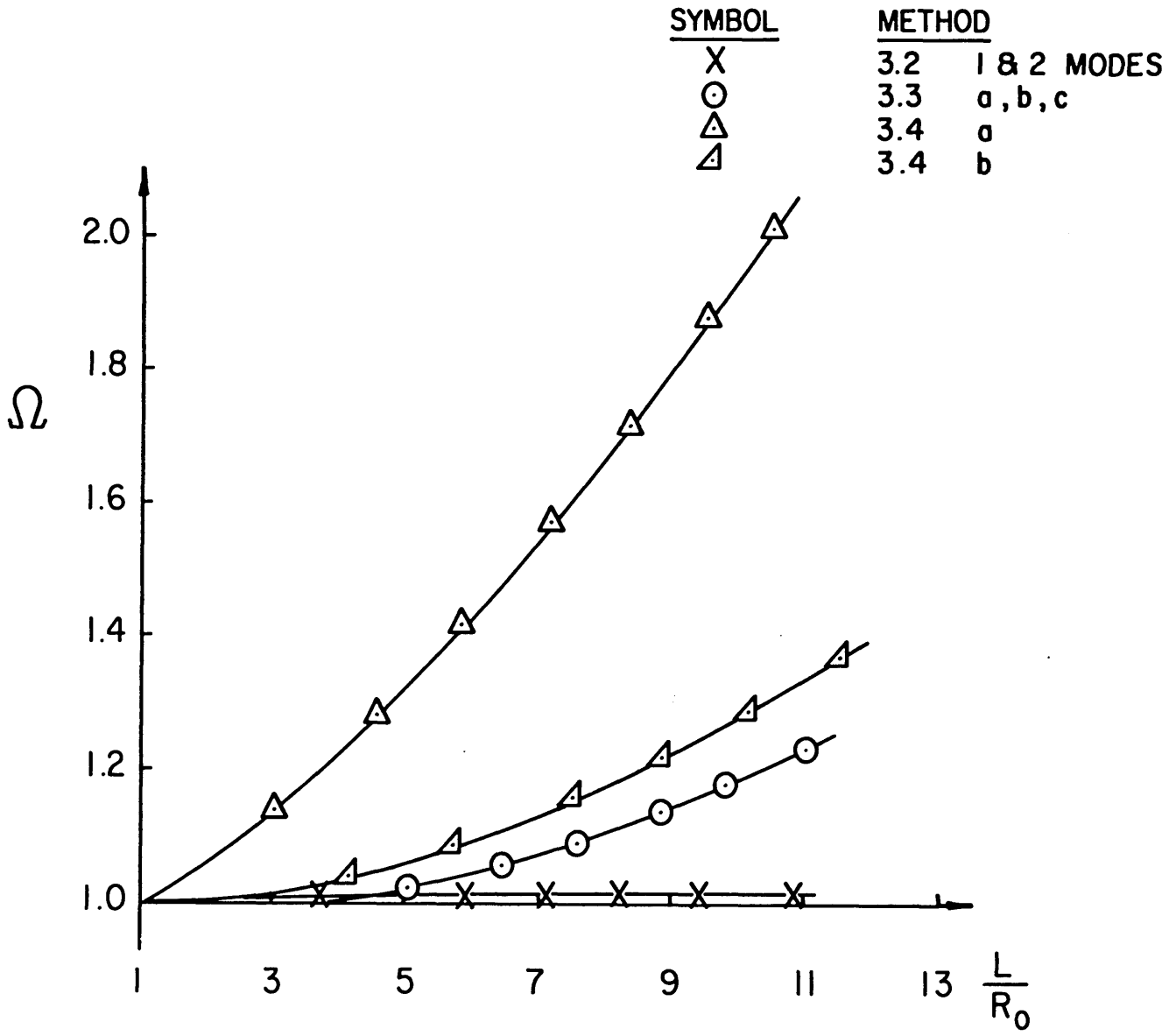

FIG. 3.4 COMPARISON OF FREQUENCY RATIOS BY DIFFERENT METHODS.

(a) $n = 4$, $h/R = 1/100$, $\alpha = 5°$

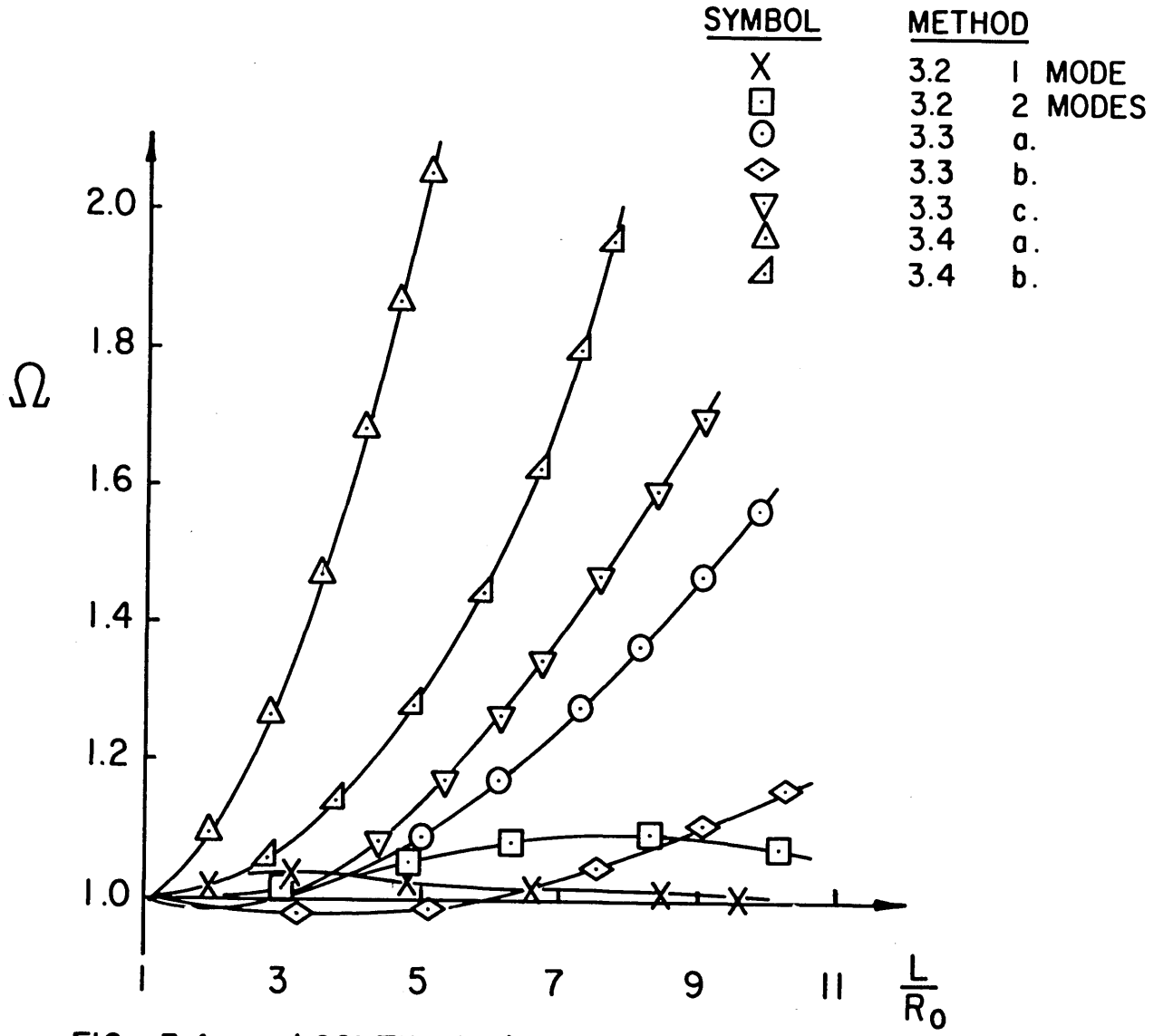

FIG. 3.4 (CONTINUED)

(b) $n = 4$, $h/R = 1/100$, $\alpha = 10°$

inder. Although the other methods indicate, for case (c), a trend which is opposite to the one predicted by the exact solution of Section 3.5, it will be shown that higher approximations reveal the correct trend, whereas Methods 3.2 will always converge to $\Omega = 1$. In addition, calculations have shown that this theory yields irregular results, i.e. the variation with α of the higher frequency is greater than that of the lower frequency, when two modes are used. On the basis of these facts, we are led to the conclusion that shallow-shell theory (at least as used here) cannot be generally applied to this problem.

Further inspection of the figures reveals that as the bending term predominates, the agreement between Methods 3.3 and 3.4 gets better. The reason for this is that under such conditions the w displacement plays a much more important role than the u and v displacements (or the stress function F which replaces them), and since Methods 3.3a, b, c and Method 3.4a use the same expression for w, the results should be similar. Furthermore, the good agreement between Methods 3.4a and 3.4b suggests that the simpler expression for w used in the latter, which satisfies the boundary condition $w = 0$, but not $M_r = 0$, may probably be used with confidence. As to be expected, the agreement gets poorer for larger α, for which the membrane effect gains in importance, and the different assumptions for u and v, or F, reveal themselves in the results. It therefore seems that the differences between these methods are important as far as the membrane terms are concerned.

It has now become evident that single mode expressions are not sufficient to predict the frequency behavior with confidence, and that higher approximations are therefore necessary. Thus it becomes a question of which of these methods is most suitable to such an extension. The relatively fair agreement within each group of methods suggests that the least compli-

cated method within each group should be used. We therefore limit ourselves to consideration of Methods 3.3a and 3.4b.

Each of these two methods has its advantages. For a fixed number of assumed modes N, Method 3.3a will always result in a determinant whose order is smaller by 2N. In addition, if an expression for w similar to Eq.(3-61c) is used instead of Eq.(3-26), the elements in the determinant will become much simpler, similar to those of Method 3.4b. On the other hand, Method 3.4b satisfies both geometrical boundary conditions, thus complying better with the requirements of the Rayleigh-Ritz method and insuring convergence. In addition, by retaining the tangential inertia terms, it is applicable to cases where $n < 2$, in contrast to Method 3.3a. It therefore seems that at the cost of some additional computational labor, use of Method 3.4b is preferable since it ensures convergent results and wider applicability.

The question of the particular method to be used thus been settled, we now turn our attention to some numerical results, the general evaluation of the method, discussion of the general problem and some conclusions.

3.7 Results and Discussion

Calculations were made using the method presented in Section 3.4b for various values of the parameters n, $\frac{h}{R_o}$, α and δ. The principal objectives of these calculations have been checking the convergence of the method and revealing the characteristic trends. In addition the results are to be compared with the exact solutions of Section 3.5 and with those of other investigations, whenever possible, so as to get an idea on their accuracy.

Since our main interest is in shells which depart but slightly from circular cylinders, the results are presented in the form of the frequency ratio Ω, which is, as already

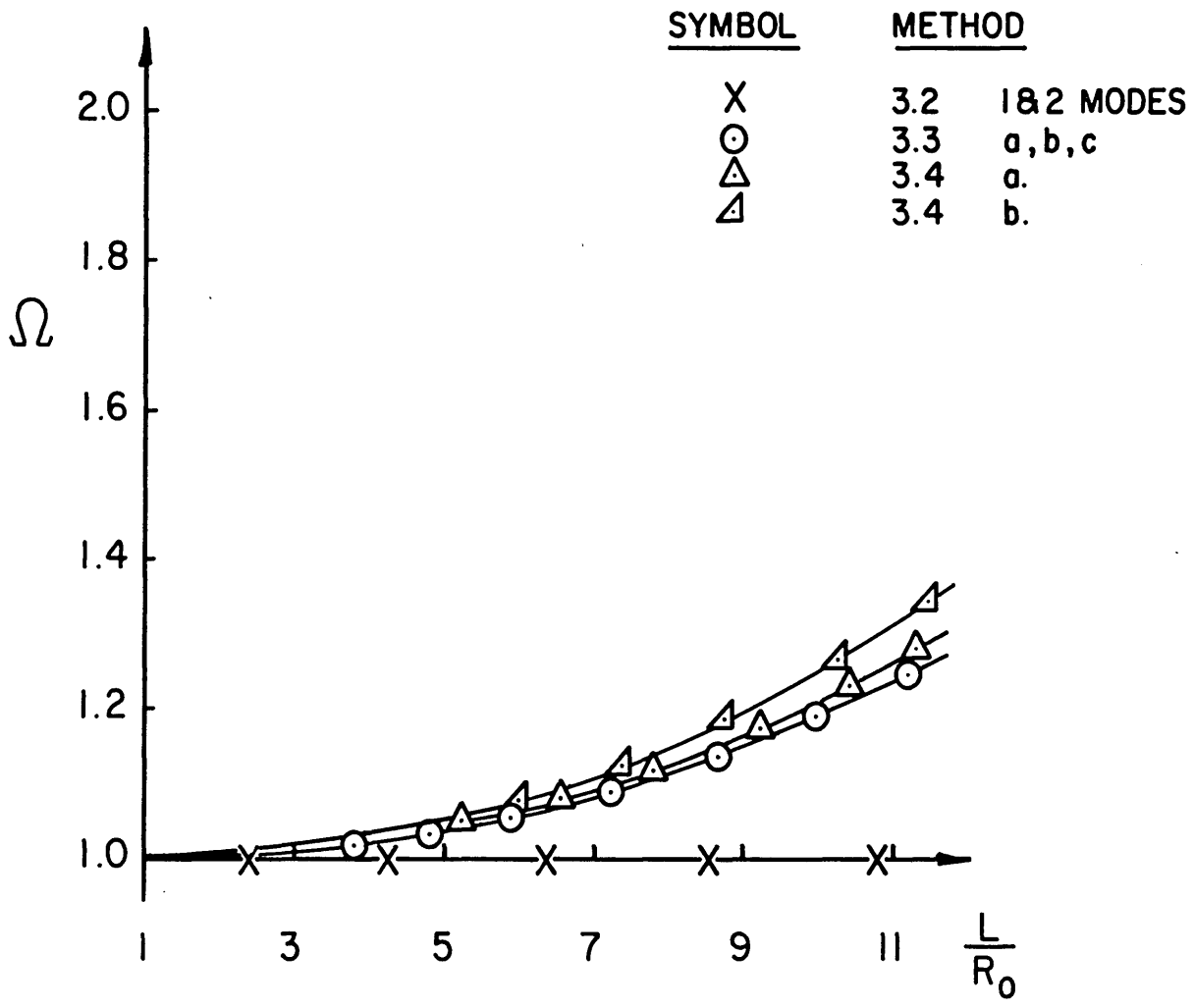

FIG. 3.5 COMPARISON OF FREQUENCY RATIOS BY DIFFERENT METHODS.

(a) $n = 6$, $h/R = 1/30$, $\alpha = 5°$

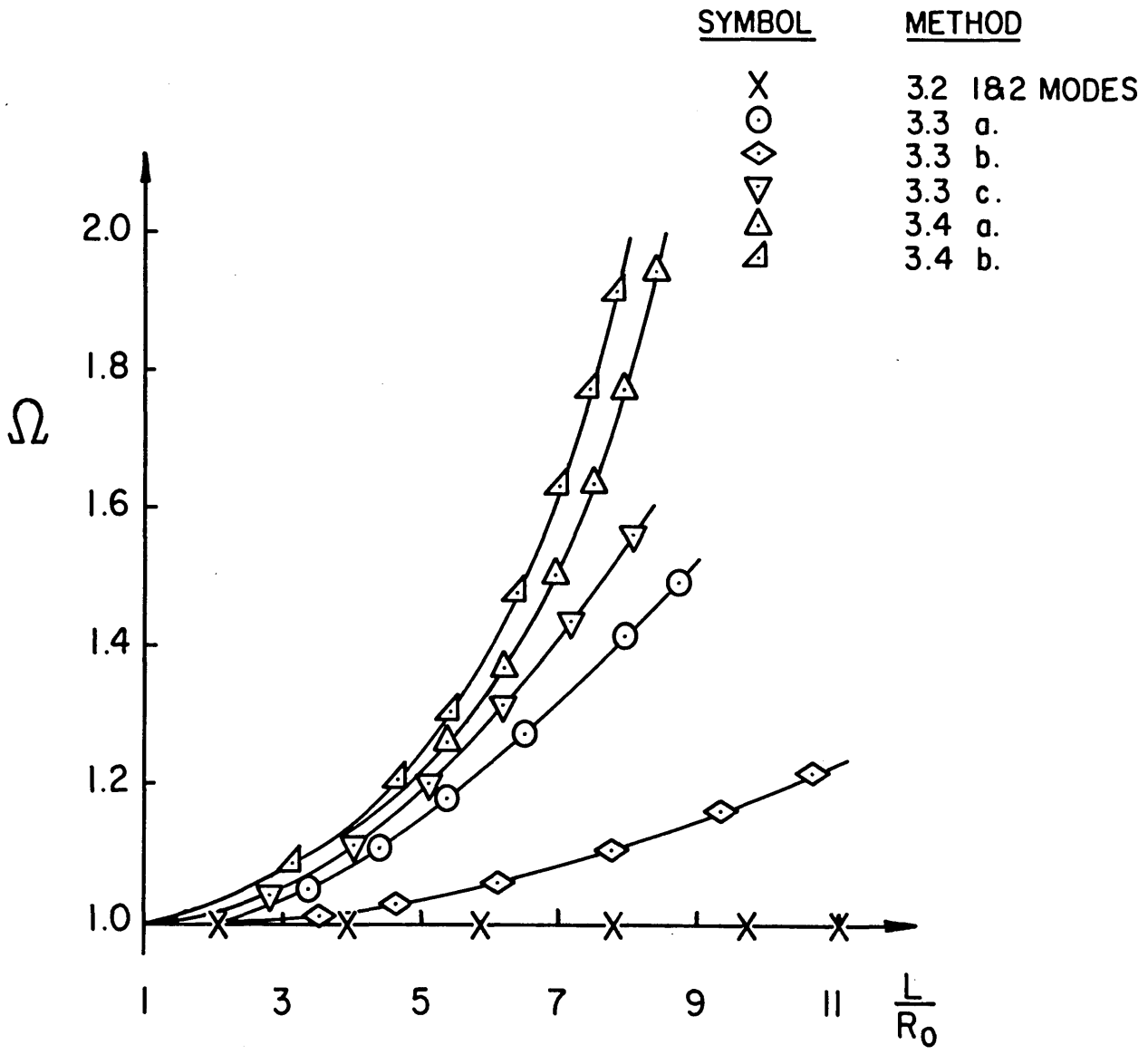

FIG. 3.5 (CONTINUED)

(b) $n = 6$, $h/R = 1/30$, $\alpha = 10°$

noted, the ratio of the cone's frequency to that of the corresponding cylinder with the same length-to-mean-radius ratio $\frac{L}{R_o}$ (unless otherwise specified). Both shells, of course, are of the same thickness ratio $\frac{h}{R_o}$, and the modes have the same number of circumferential waves n. The results, therefore, give the effect of taper (or "conicity") on the frequencies.

Fig. 3.6 shows these results as plotted vs. $\frac{L}{R_o}$ for n = 1 and $\alpha = 5^o$, 10^o, 15^o. Identical results were obtained for $\frac{h}{R_o} = 0, \frac{1}{100}, \frac{1}{30}$, which means that for this value of n bending effects are negligible and the shell acts essentially as a membrane. There is fairly good agreement between the 1 mode and 2 mode results for $\alpha = 5^o$, but the agreement get poorer as α and $\frac{L}{R_o}$ get larger. Comparison with the results of Herrmann and Mirsky [15] reveals a common trend but different values for the frequency ratio.

Fig. 3.7 is a plot of the results for n = 2, $\frac{h}{R_o} = \frac{1}{100}$ and $\alpha = 5^o$, 10^o, 15^o. In this case the results depend on the thickness ratio to some extent, i.e. the bending effect begins to appear. The observations to be made here are similar to those made in the previous case.

Fig. 3.8 is a plot of the 1 mode and 2 mode results for n = 3, $\alpha = 5^o$, 15^o and $\frac{h}{R_o} = 0^*, \frac{1}{100}$. It is evident that for $\alpha = 5^o$ the bending effect is significant even for the 1 mode solution, whereas for $\alpha = 15^o$ the 2 mode solution is needed to reveal this effect. The degree of agreement of the results seems to depend on the thickness ratio. For $\frac{h}{R_o} = 0$ the 1 mode and 2 mode solutions agree well, and a behavior similar to that of the previous two cases is displayed. For $\frac{h}{R_o} = \frac{1}{100}$, $\alpha = 5^o$, however, another phenomenon takes place. In this case the 2 mode result not only differs in value from the 1 mode result, but a different trend is revealed, namely, the frequency ratio reaches a peak and then

* $\frac{h}{R_o} = 0$ is of course a hypothetical case presented for illustration purposes only.

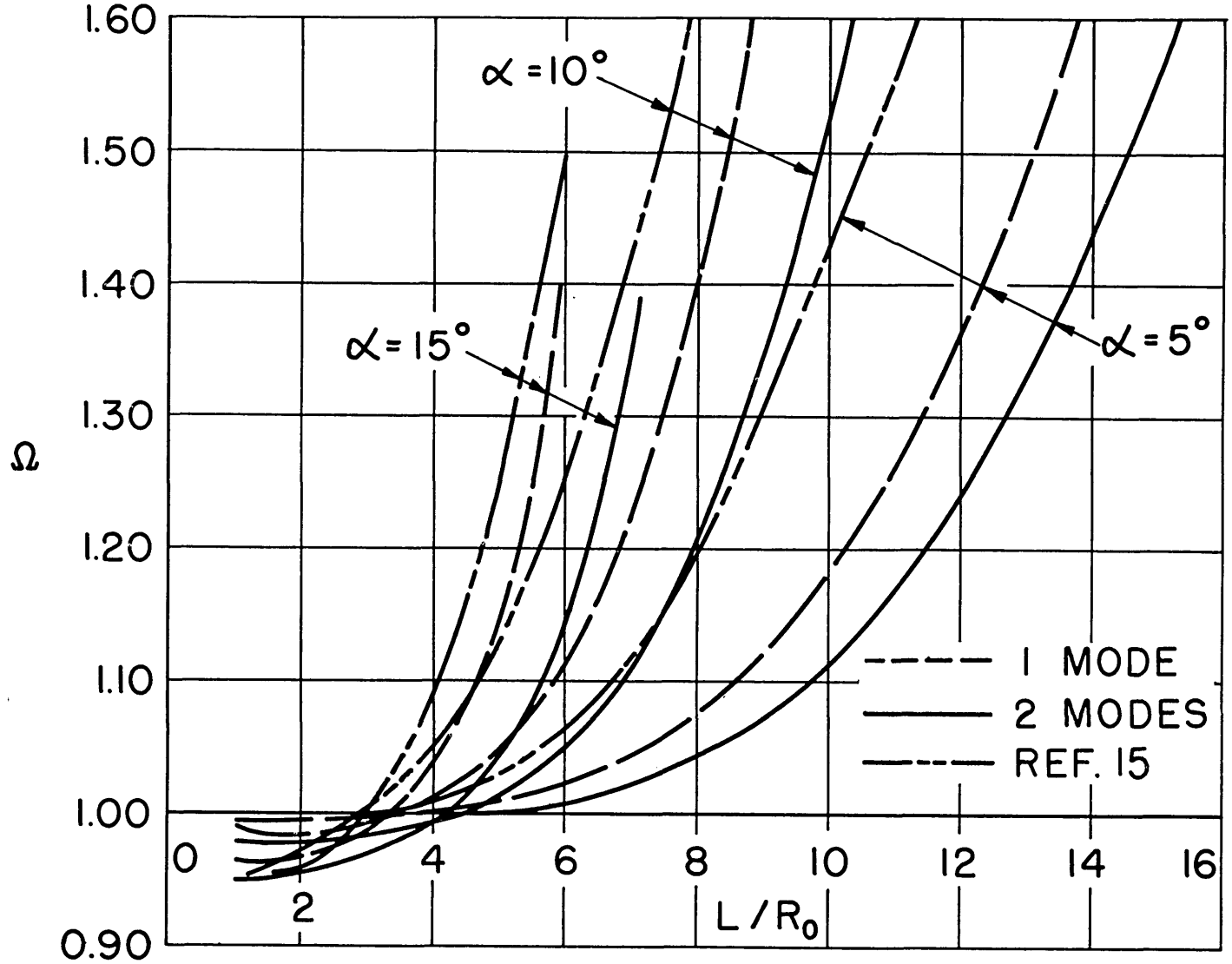

FIG. 3.6 FREQUENCY RATIO FOR n = 1

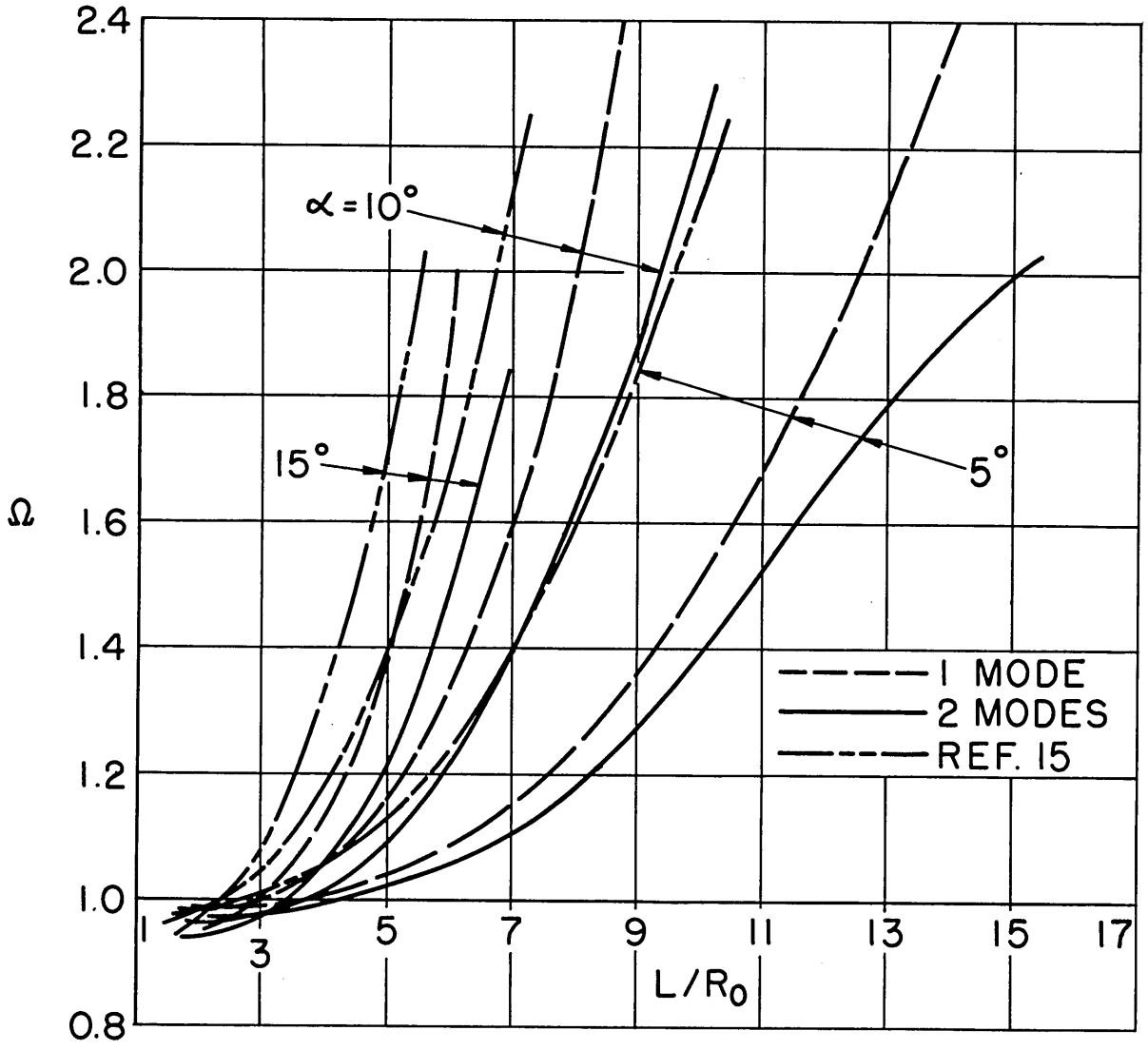

FIG. 3.7 FREQUENCY RATIO FOR $n = 2$, $\frac{h}{R_0} = \frac{1}{100}$

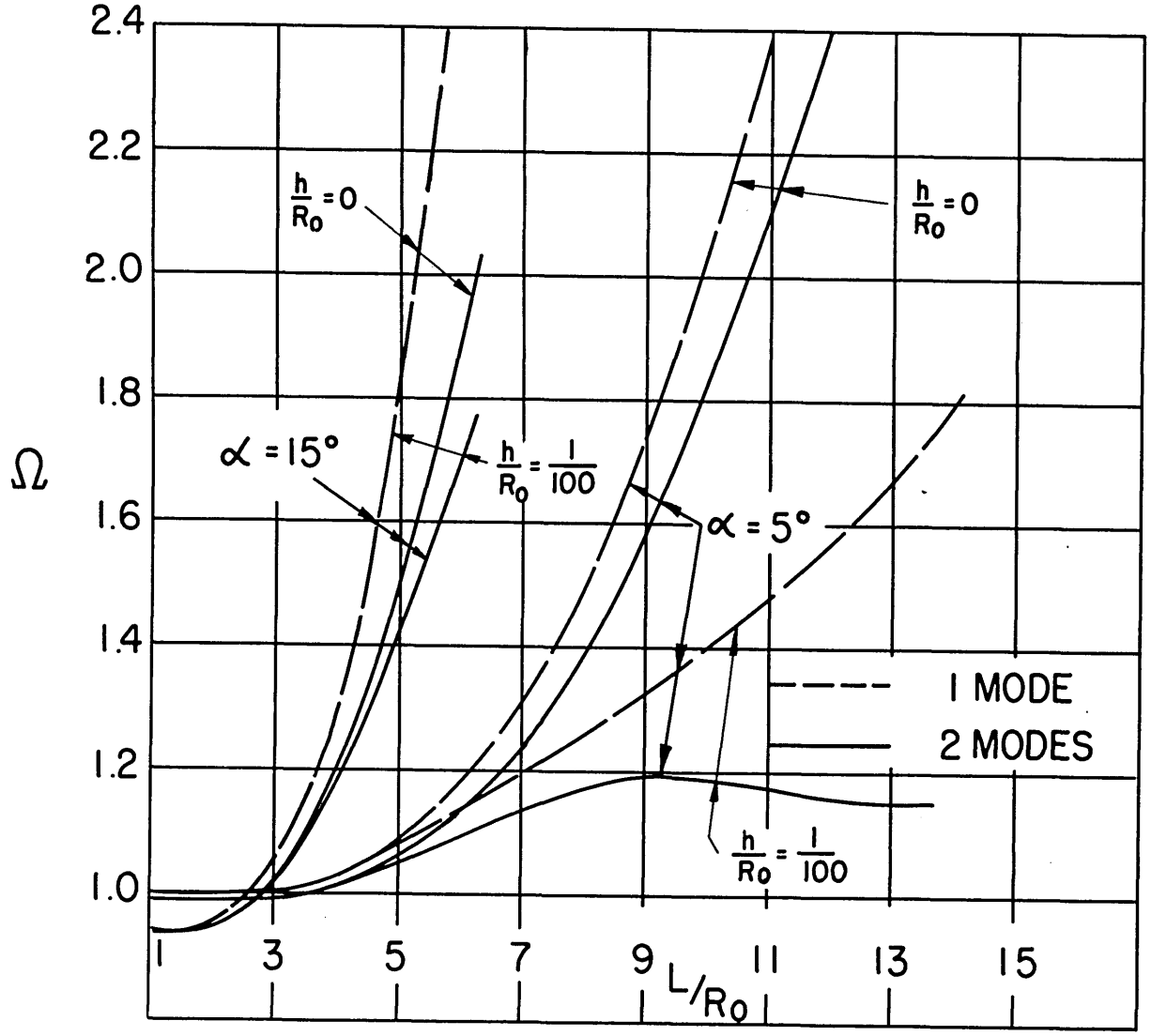

FIG. 3.8 FREQUENCY RATIO FOR n = 3

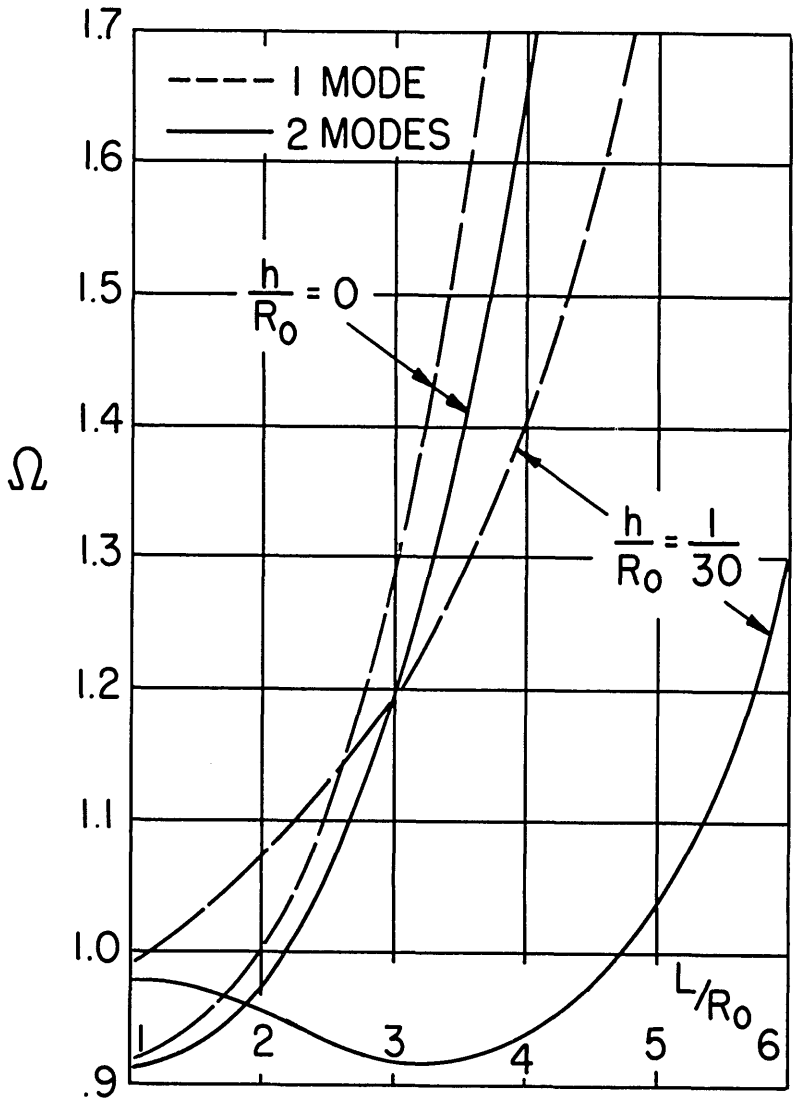

FIG. 3.9 FREQUENCY RATIO FOR
$n = 6$, $\alpha = 15°$

decreases. This decrease is due to the bending effect which now reaches a degree of importance comparable to the membrane effect. This behavior is true of $\alpha = 5^{o}$, the larger α still behaving very much like the membranes of n = 1, 2. Therefore, the contention made earlier that the membrane effect is more important for larger α is borne out.

Fig. 3.9 is a plot of the 1 mode and 2 mode results for n = 6, $\alpha = 15^{o}$, and two values of the thickness ratio. For $\frac{h}{R_o} = 0$ (which again is presented for illustration purposes only) the typical membrane behavior is repeated. For $\frac{h}{R_o} = \frac{1}{30}$, where the bending effect now predominates, the characteristic downward trend is clearly visible in the 2 mode result. The upturn at the higher $\frac{L}{R_o}$ will be explained presently.

The results shown in Figs. 3.6 through 3.9 suggest that the agreement between the 1 mode and 2 mode solutions is better in those cases where the membrane terms predominate. In such cases apparently a small number of assumed modes is needed for a satisfactory solution. Since the bending effect seems to converge more slowly, the number of assumed modes needed in cases where it is important will be larger.

The question of convergence in each case depends on the value of δ, the parameter which determines the degree of proximity of the shell to a complete cone. It is obvious that since this method, as well as all other methods employed here, fails when $\delta = 1$, the results are applicable to truncated cones only, and as δ approaches unity their accuracy gets poorer. This effect is responsible for the apparently wrong trend revealed in Fig. 3.9 at the higher $\frac{L}{R_o}$. This is better illustrated in Fig. 3.10 which shows the variation of Ω with δ for n = 6, $\frac{h}{R_o} = \frac{1}{30}$. It is seen that irrespective of the value of α, the 2 mode result breaks down for $\delta > .4$. It is an apparent certainty that when additional modes are used the range of applicability of δ will be wider. The

particular value of $\frac{L}{R_o}$ at which breakdown occurs depends on the semi-vertex angle α, since for given values of α and δ $\frac{L}{R_o}$ is fixed. For $\alpha = 15^o$, for example, $\delta = 1$ corresponds to $\frac{L}{R_o} = 7.46$. Fig. 3.10 also shows that for $\delta < .4$, Ω is higher for larger α. This is due to the membrane effect which tends to raise the frequency and is a further illustration of the fact that the importance of this effect increases with α.

Fig. 3.11 compares with results for $n = 6$, $\frac{h}{R_o} = \frac{1}{30}$ and $\alpha = 17.45^o$ with the exact solution of Section 3.5b. (In this case and also in Fig. 3.12, in order to facilitate the comparison, the cone is compared with a cylinder of equal ℓ/R_o, where ℓ is the slant height of the cone). The exact curve is definite proof that the effect of the bending terms is to decrease Ω, as mentioned above. The 2 mode solution is seen to follow this trend up to δ of about .4, following which it breaks down and starts to diverge. Since the exact solution takes no account of the membrane effect, which is relatively important for this value of α(this value was chosen to yield $\bar{n} = \frac{n}{\sin\alpha} = 20$, for which tables of Bessel functions are available), and since this effect tends to increase Ω, the true result probably lies in between the two curves. It therefore seems that the 2 mode solution yields fairly good results for low δ.

Fig. 3.12 compares the 1 mode and 2 mode solution for the torsional case with the exact solution of Section 3.5a.** The agreement between the 2 mode solution and the exact

---

** In this case, by comparing the cone with a cylinder of equal ℓ/R_o the result is made independent of α. This apparently is not true of the general case.

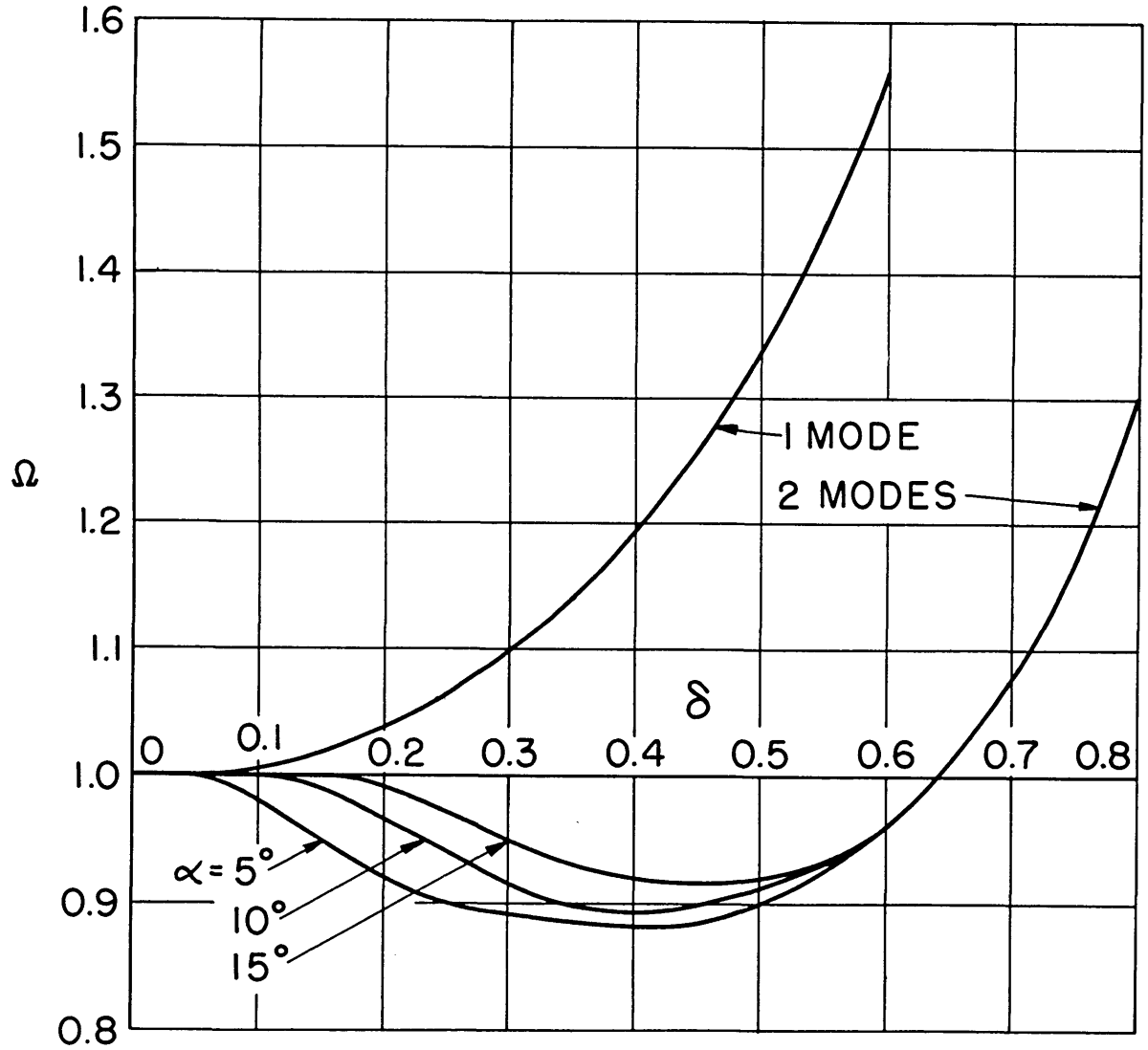

FIG. 3.10 EFFECT OF TAPER ON FREQUENCY FOR $n = 6$, $\frac{h}{R_0} = \frac{1}{30}$

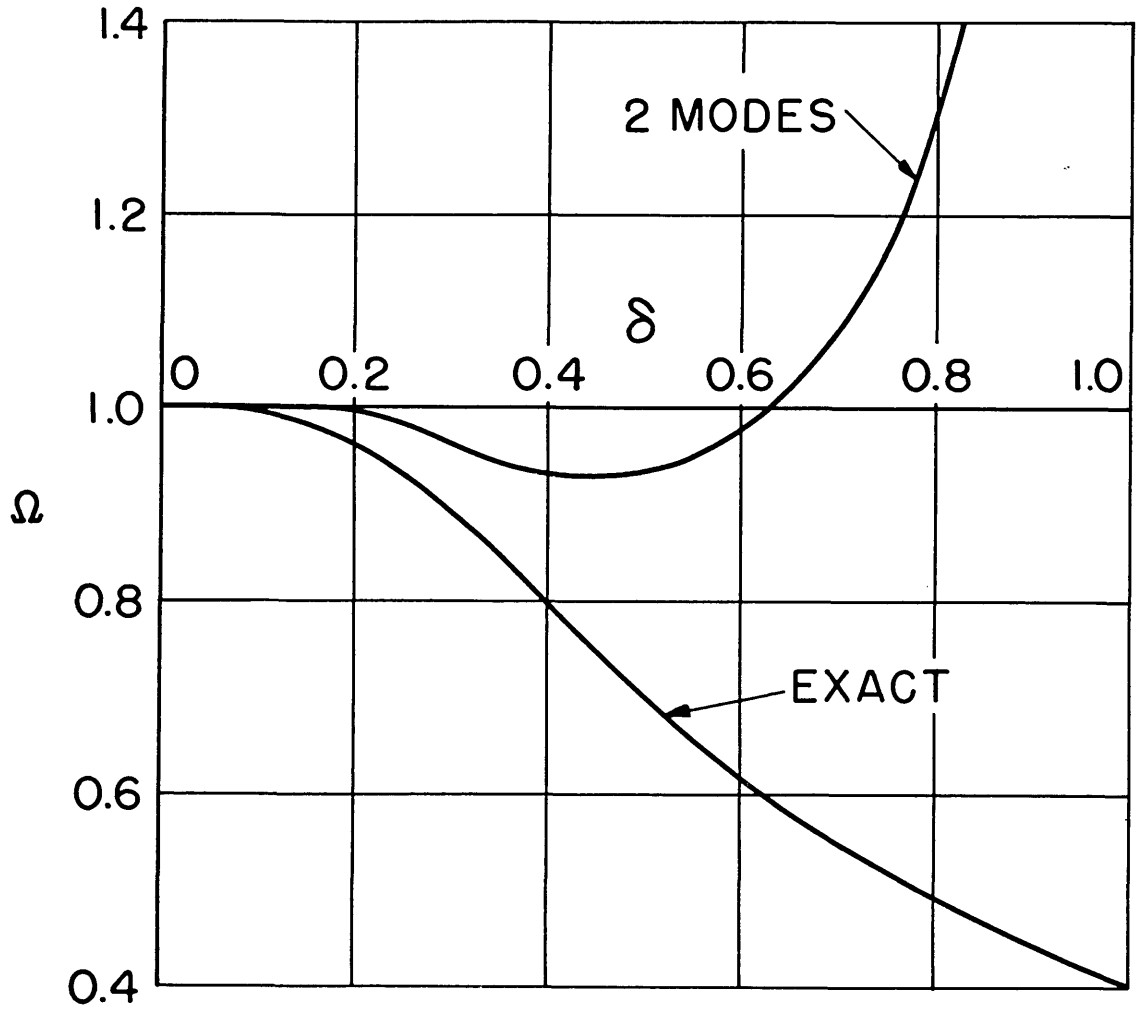

FIG. 3.11 EFFECT OF TAPER ON FREQUENCY. COMPARISON OF EXACT AND APPROXIMATE RESULTS FOR $n=6$, $\alpha = 17.45°$, $\frac{h}{R_0} = \frac{1}{30}$.

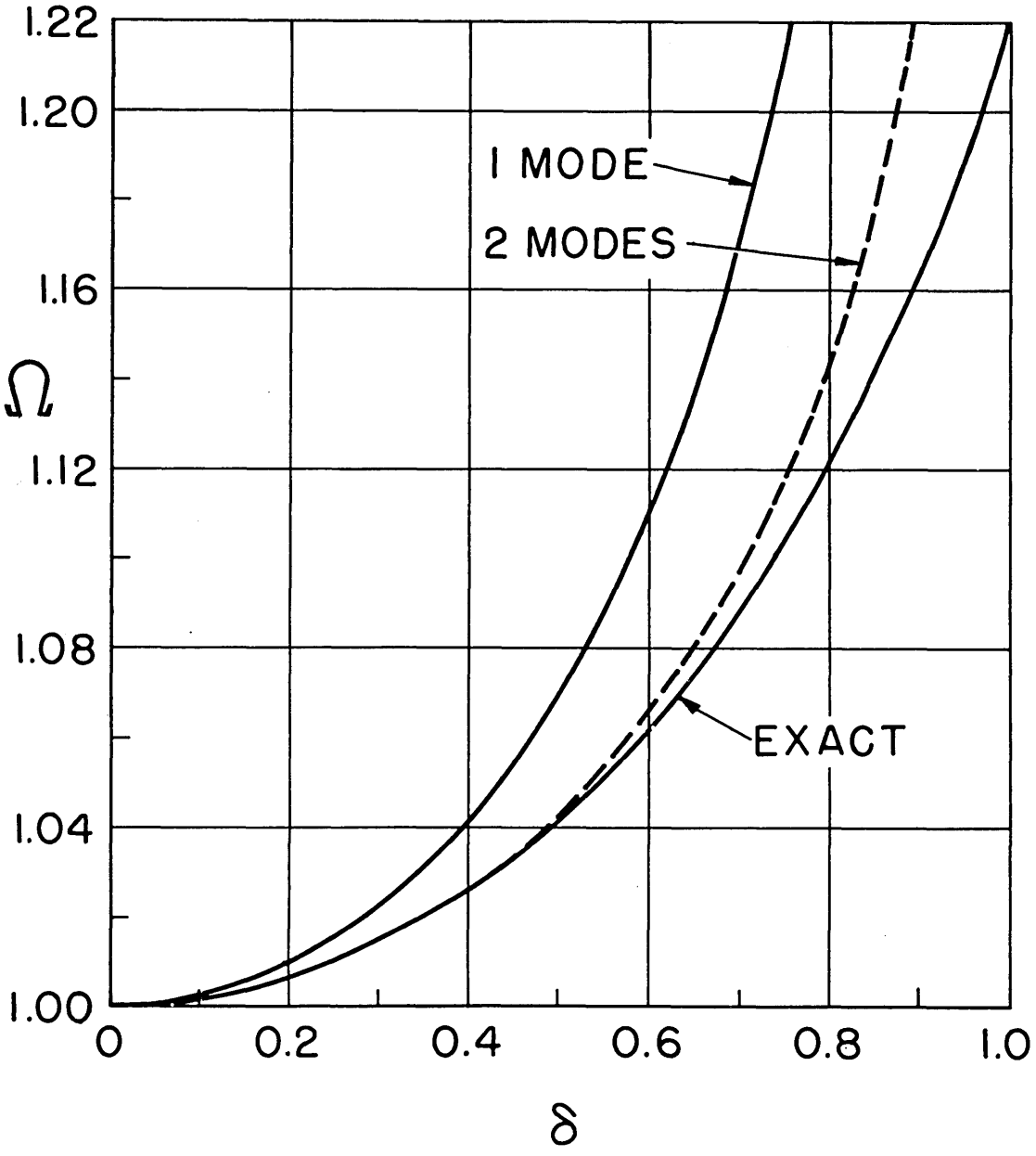

FIG. 3.12 EFFECT OF TAPER ON TORSIONAL FREQUENCY. COMPARISON OF EXACT AND APPROXIMATE RESULTS.

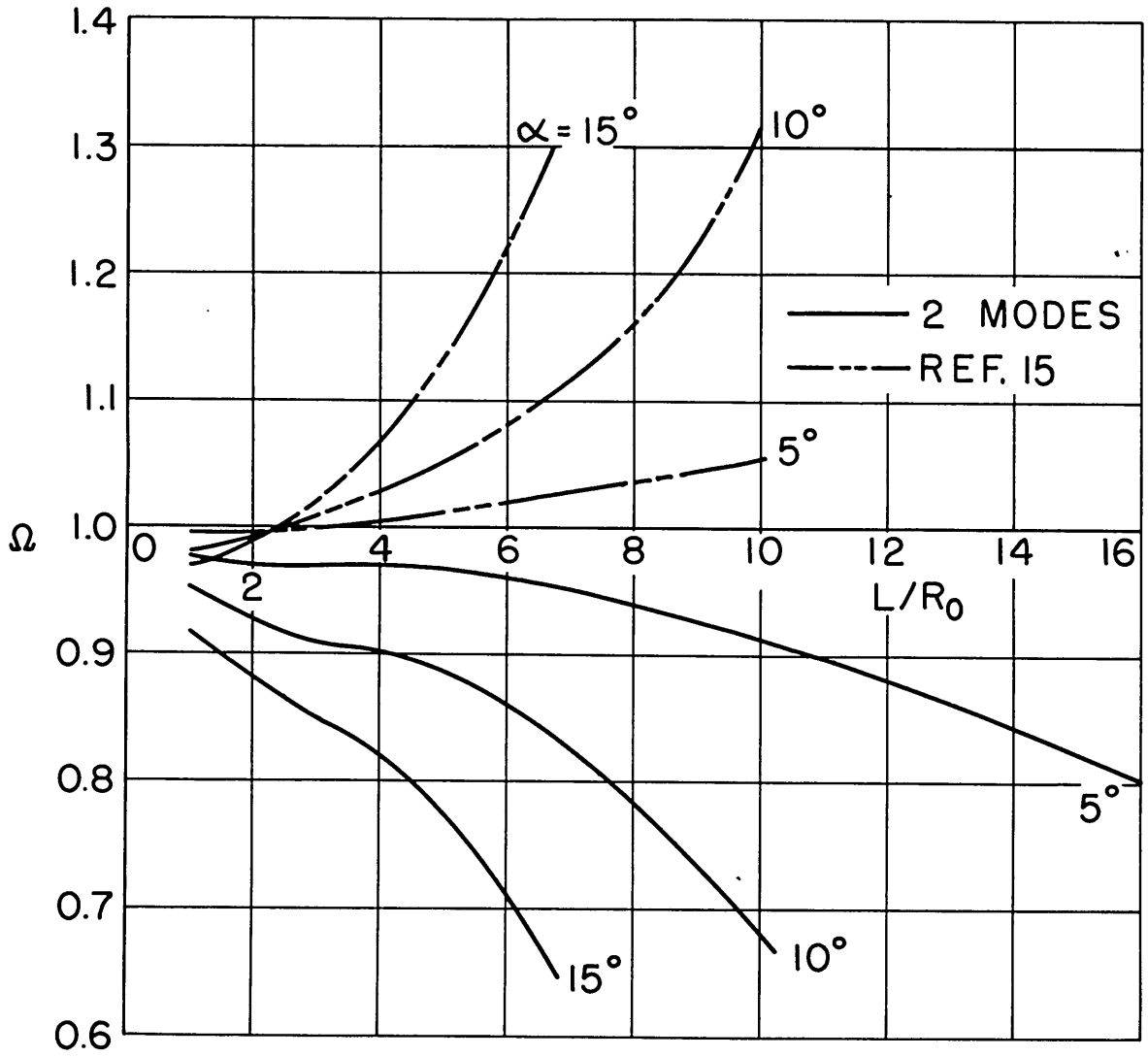

FIG. 3.13 LOWEST NON-TORSIONAL FREQUENCY RATIO FOR n = 0.

solution is quite satisfactory except for very high δ.

Fig. 3.13 presents the 2 mode solution for the lowest nontorsional axisymmetric (n = 0) case. Comparison with the results of Ref. [15] shows a completely different trend in the two solutions. This case, which is virtually independent of $\frac{h}{R_o}$, is interesting in that it indicates a decreasing Ω with $\frac{L}{R_o}$, which is in contrast with the usual membrane effect. However, higher approximations are required before this unusual effect can be definitely established.

The satisfactory agreement with the exact solutions, as shown in Figs. 3.11 and 3.12, indicates that the present method takes good account of both the membrane and the bending effects and therefore successfully accomplishes its purpose. Let us, then, recapitulate and point out its essential features.

The method employs the Rayleigh-Ritz approach, in which the strain energy is written in terms of the three displacement components. Due to the fact that the shell is a body of revolution, the displacements vary periodically around the circumference in the asymmetric case, and as the time variation is harmonic, the problem thus reduces to a one-dimensional dependence on the meridional variable r. Since the latitudinal metric and radius of curvature vary with r, the energy expression is an explicit function of r as well as the displacements u, v, w. As each of the three main terms in the expression, namely, membrane, flexure and inertia, involves different powers of r, the expression is not equidimensional, as are not the three differential equations of equilibrium derivable from it. This is the main source of difficulty in this problem.

By using the logarithmic coordinate transformation $\beta = \ln(r/r_o)$, most of this difficulty was removed since each of the three main terms became proportional to just one power of r(or e^{β}). This power is 0 for the membrane term, -2 for

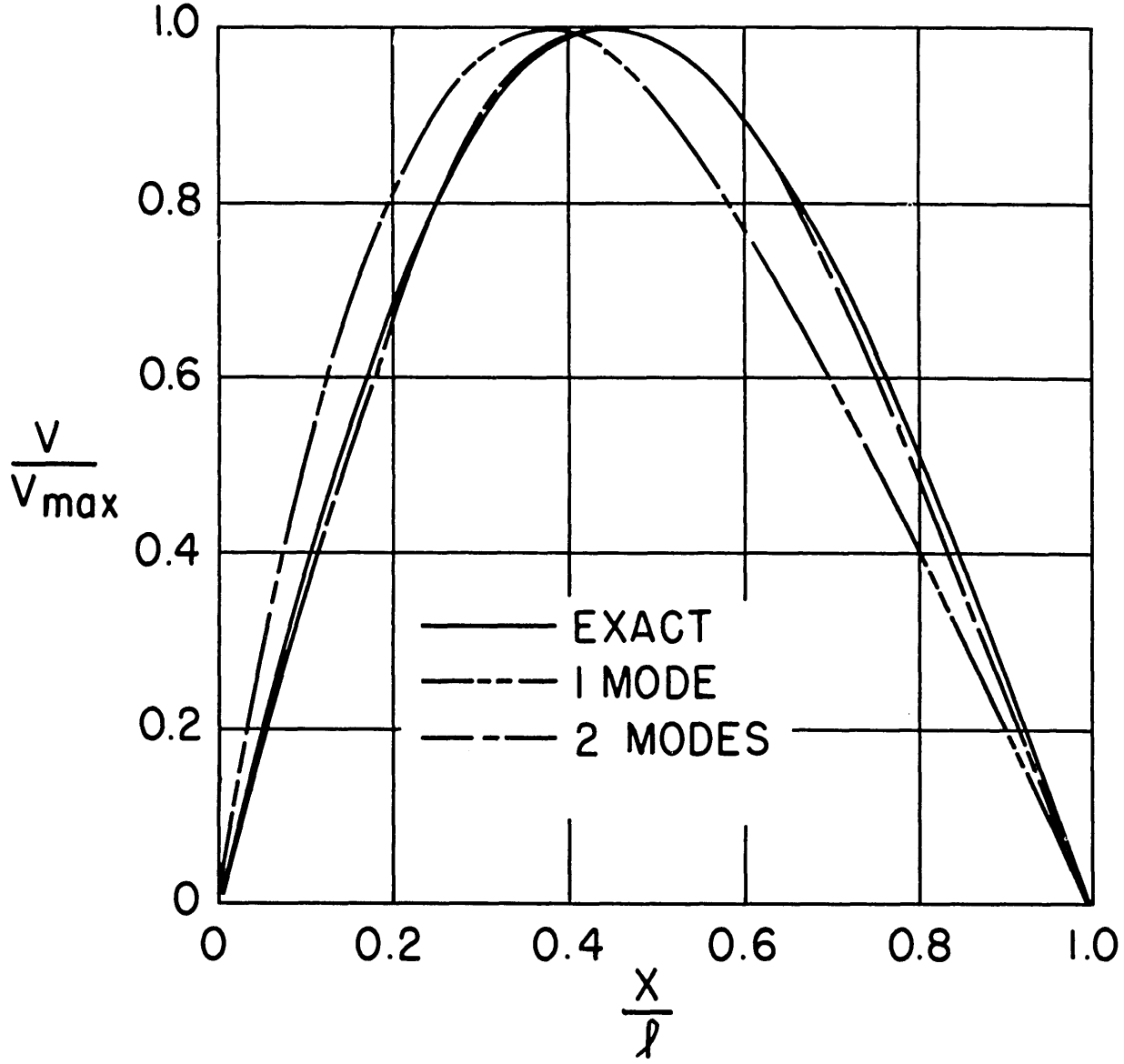

FIG. 3.14 COMPARISON OF TORSIONAL MODE SHAPES.

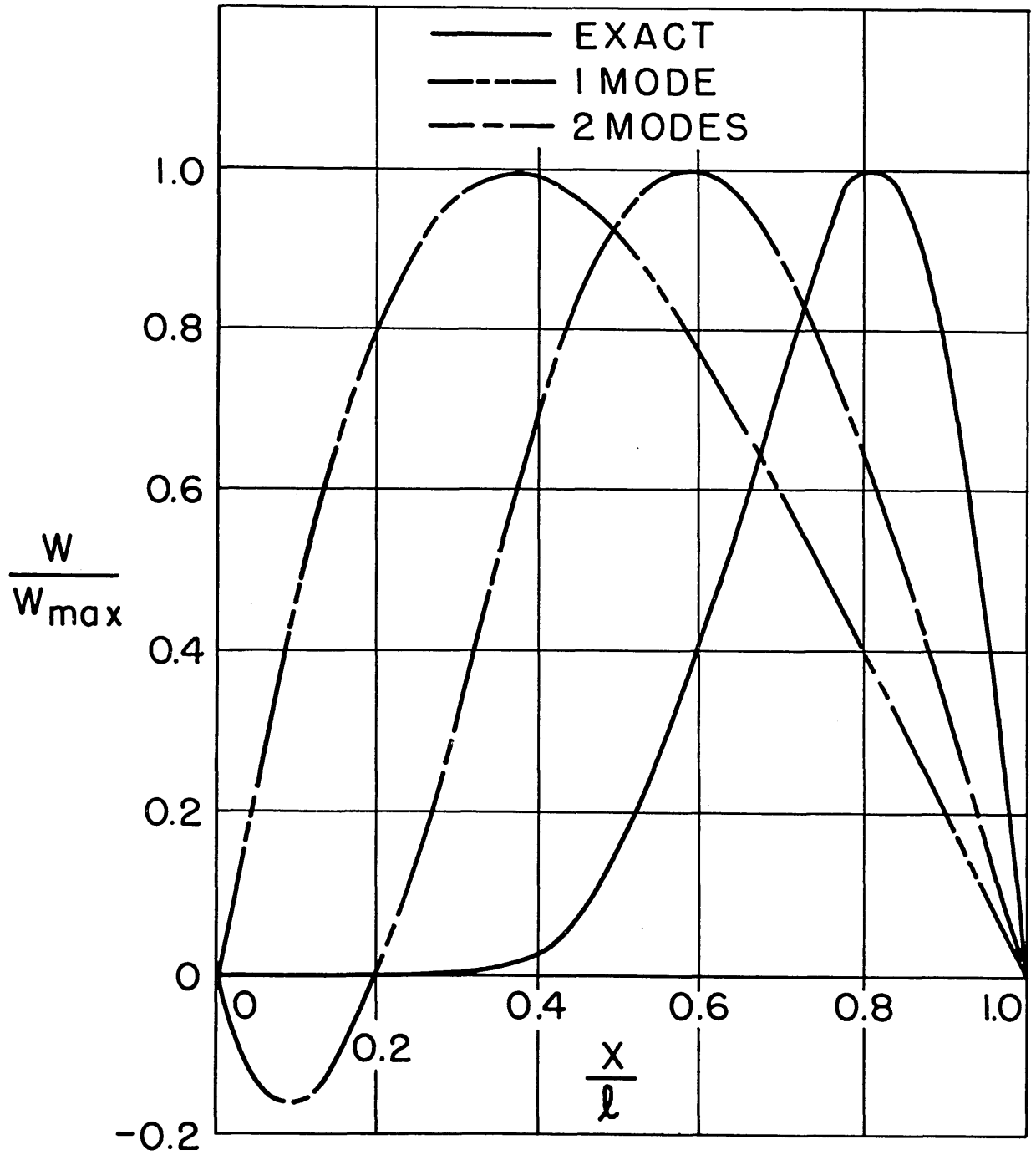

FIG. 3.15 COMPARISON OF MODE SHAPES FOR $n = 6$, $\alpha = 17.45°$, $\frac{h}{R_0} = \frac{1}{30}$.

the bending term and +2 for the inertia term. Assumption of trigonometric mode shapes (in the variable β), which satisfy the geometrical boundary conditions and which reduce to the cylindrical mode shapes as $\alpha \to 0$, then followed, and evaluation of the integrals thus became a fairly straightforward operation. The fact that the independent variable now did not appear explicitly in the membrane energy integral explains the simplicity of the membrane terms in the characteristic determinant, which resemble so closely the corresponding terms for the cylinder case. The bending terms in the determinant, however, involve δ explicitly. This is a direct consequence of the presence of $e^{-2\beta}$ in the flexure energy integral.

This essential difference between the two expressions provides a plausible explanation for the better convergence in the pure membrane cases. Fig. 3.14 shows a comparison between the exact and the approximate torsional mode shapes for $\delta = .5$. The excellent agreement between the exact and the two-mode results is clear. Fig. 3.15 shows a similar comparison for $n = 6$, $\alpha = 17.45^{o}$, $\delta = .5$. In this bending case, the agreement is seen to be much poorer. The exact solution suggests that in this case more appropriate assumed modes are ones weighed by r. This would remove the factor $e^{-2\beta}$ from the integral and, analogously to the membrane term in the present case, would most probably provide better convergence throughout the δ range. This approach may be used when the value of n is high, for which the bending effect is the most important. In the intermediate cases where both membrane and bending effects are of comparable importance, the present method, by virtue of the simplicity of the more numerous membrane terms in the determinant, is probably preferable. Of course, a combination of the two methods, by weighing the w displacement only, for example, is also possible, but it will result in somewhat more complex terms.

Some comments on the problem of obtaining higher approxi-

mations are in order.

The numerical problem consists of finding the smallest value of $\tilde{\omega}^2$ satisfying the matrix equation,

$$[A]\ \{q\} = \tilde{\omega}^2\ [C]\ \{q\} \tag{3-97}$$

where [A] is the matrix containing the membrane terms $a^{rs}_{u_i u_j}$ and bending terms $b^{rs}_{ww}\ C^2$, and [C] is the matrix of the inertia coefficients $c^{rs}_{u_i u_j}$. The standard matrix equation used for finding eigenvalues by iteration methods is,

$$[A^{-1}]\ [C]\ \{q\} = \frac{1}{\tilde{\omega}^2}\ [I]\ \{q\} \tag{3-98}$$

Since [A] is positive definite and [C] bears close resemblance to the unit matrix [I], no difficulties are expected and the iteration process should converge fairly rapidly onto the smallest $\tilde{\omega}^2$ even though $[[A^{-1}]\ [C]]$ is a non-symmetric matrix.

Equations (3-65) indicate that the coupling terms between even and odd modes (1 and 2 or 2 and 3) are proportional to $\sin\alpha$, whereas the coupling terms between even or odd modes (2 and 4 or 1 and 3) are proportional to $\sin^2\alpha$ and are therefore weaker. It therefore might be advantageous to add two modes at each successive approximation. The availability of high-speed digital computers would make this a fairly routine operation.

3.8 Conclusions

The conclusions which may be drawn from this study of the conical shell vibration problem are as follows:

(1) Unlike circular cylinders of constant radius, no simple and satisfactory formula for the frequencies exists for the case of tapered cylinders.

(2) The effect of taper on the frequencies of the circular

cylinder is greater for higher L/R_o and higher α.

(3) In general, the effect of taper on a circular cylinder is to increase its membrane frequencies and to decrease its bending frequencies. The general case contains a combination of these two effects and therefore the frequency may be higher, lower or the same, depending on the shell's geometry and the particular vibration mode of interest.

(4) The effect of taper on the mode shape of the w displacement in the bending case is to shift its peak towards the wider base and to strongly attenuate it in the narrow side of the shell. The effect in the membrane case is less conclusive, but seems to shift the displacement peak towards the narrow base.

(5) Use of the first approximation thin shell theory in this problem is of comparable accuracy to its use in the cylinder case, thus is satisfactory. On the other hand, use of shallow shell theory is not encouraged in this case due to its serious disadvantages.

(6) A satisfactory method has been developed which yields reliable frequency results for all cases (with simple support conditions). It is simple, easy to apply and may be used to any required degree of accuracy, limited by computational facilities only.

(7) A way of treating the cone problem has been shown which can be used to solve problems with other boundary conditions.

(8) The necessary structural ground work for the aeroelastic analysis of the conical shell has been laid down. It is therefore now possible to proceed with such an analysis.

As a concluding remark let us restate that the results

presented here should not be considered as final. Rather, they serve the double purpose of providing a first approximation to the actual results and of illustrating the simplicity and flexibility of the method developed here. The need for experimental verification of the final results should, of course, be stressed.

APPENDIX 3A

DEFINITION OF FUNCTIONS

$$a_1 = \frac{1}{b_3}\left\{\bar{\lambda}^2[1 + \mu(1-\mu)\Delta]b_1 - 4\mu(1-2\mu)\bar{\lambda}^4\Delta b_2\right\}$$

$$a_2 = \frac{1}{b_3}\left\{(1-2\mu)b_1 + 4\mu\bar{\lambda}^2[1 + \mu(1-\mu)\Delta]b_2\right\}$$

$$a_3 = -\frac{b_4 + b_5}{n - \sin\alpha}\, e^{-[n - (1+\mu)\sin\alpha]\frac{\pi}{\bar{\lambda}}}$$

$$a_4 = -\frac{b_4 - b_5}{n + \sin\alpha}$$

$$a_5 = \frac{b_4}{n + \sin\alpha}\, e^{-[n + (1-\mu)\sin\alpha]\frac{\pi}{\bar{\lambda}}}$$

$$a_6 = \frac{b_4}{n - \sin\alpha}$$

$$b_1 = [n^2 + \bar{\lambda}^2]^2 - 2\sin^2\alpha[(1+\mu^2)n^2 - (1-3\mu^2)\bar{\lambda}^2] + (1-\mu^2)^2\sin^4\alpha$$

$$b_2 = n^2 + \bar{\lambda}^2[1+(1-\mu^2)\Delta]$$

$$b_3 = b_1^2 + 16\mu^2\bar{\lambda}^4\Delta b_2^2$$

$$b_4 = 2(1+\mu)a_1 - \left\{n^2 + \bar{\lambda}^2[1-(1+\mu)^2\Delta]\right\}a_2$$

$$b_5 = \frac{2\sin\alpha}{n}\left\|2\mu a_1 + \left\{n^2 - \bar{\lambda}^2[1+(1-\mu^2)\Delta]\right\}a_2\right\|$$

$$b_6 = a_1 + (1+\mu)\sin^2\alpha a_2$$

$$b_7 = \bar{\lambda}^2 + [n-(1-\mu)\sin\alpha]^2$$

$$b_8 = \bar{\lambda}^2 + [n+(1-\mu)\sin\alpha]^2$$

$$b_9 = \bar{\lambda}^2 + [n-(1+\mu)\sin\alpha]^2$$

$$b_{10} = \bar{\lambda}^2 + [n+(1+\mu)\sin\alpha]^2$$

CHAPTER 4

THE GENERAL PANEL FLUTTER PROBLEM

4.1 Introduction

As defined by Bisplinghoff et al. [21] the term "Flutter" applies to the dynamic instability of an elastic body in an airstream. Among its many manifestations, e.g. wing flutter, stall flutter etc., is the phenomenon known as "Panel Flutter". This refers generally to the flutter of a thin plate, shell or membrane, one of whose surfaces is exposed to an airstream and the other to still air. Evidence that such a phenomenon occurs in practice has been amply shown in experiments (Refs.22,23,24,25). It is also blamed for some failures of the German V2 rocket during World War II [26].

Unlike the more familiar case of wing flutter, practical panel flutter occurs only in a supersonic stream. Its limited amplitude, due to structural nonlinearities, tends to make it more of a fatigue rather than a sudden failure-problem.

There have been numerous attempts in recent years to analyze this problem. The difficulties encountered by the various investigators and the number of diverse approaches were many. The lack of sufficient experimental data (due to some practical difficulties) needed to corroborate theoretical results throughout the range of the significant parameters, has also hindered obtaining a conclusive qualitative and quantitative understanding of what seems to be a many

faceted phenomenon.

The problems which were attacked may be classified in a number of ways. (1) According to structural characteristics: whether the panels are flat or curved, buckled or unbuckled, two dimensional or three dimensional, plate or membrane etc. (2) According to aerodynamic theory used: strip theory or surface theory, unsteady, quasi-steady or steady flow, exact linearized, first-order or piston theory etc. (3) According to method of solution: standing wave or traveling wave, assumed-modes vs. "exact" solution, differential equation or integral equation etc. It is obvious that there exist numerous combinations of these possibilities, all of which have not been exhausted as yet. The different approaches to the solution of any particular problem led on occasion to widely different conclusions, a fact that caused a mild controversy regarding the validity and applicability of some methods that were used. One of these discussions centered around the consequences of applying the familiar Rayleigh-Ritz method, which proved itself in the solution of self-adjoint problems such as the natural vibrations of elastic bodies, to the non-self-adjoint problems of flutter. Another concerned the applicability of traveling wave solutions to finite panels. Some recent work has shed more light on the problem, and the following is an attempt to bring it up-to-date and to give a plausible physical explanation of the phenomenon.

The problem which received widest attention, due to its relative simplicity, is the case when the panel is a simply-supported two- or three-dimensional flat plate. Miles [27], Shen [28], Nelson and Cunningham [29], Goland and Luke [30], Hedgepeth [31], Eisley [32], Luke and St. John [33], Movchan [34] and Houbolt [35], among others, have approached this problem by different methods and with varying assumptions. Out of the results of these studies, the following physical

picture of the behavior of flat panels emerges.

In vacuum (and neglecting structural damping) a bounded panel possesses an infinite number of natural modes whose shapes and frequencies depend on the nature of the edge supports. When excited, the panel may oscillate in any of these modes with a constant amplitude and in phase. In a flow, the panel is, of course, subjected to air pressures which change the characteristics of the vibratory system. The question is, what will be the flow's effect on the motion of the panel, i.e. will the modes and frequencies change? will the motion be in phase? will it be damped, neutral or divergent? Clearly, from the designer's viewpoint the most important questions concern the damping. Specifically, whether the flow tends to damp any excited mode, and whether for some flight condition the nature of the motion will become divergent with time. The first question is of course related to the fatigue problem, the second to the flutter problem.

The answers to these questions, at least for $M > 1.6$, may now be given with a fair degree of confidence. The initial effect of the flow is to introduce damping into the motion in each mode and to change its shape and frequency. The lowest aeroelastic mode always increases in frequency, whereas the behavior of the higher frequencies varies in each case. For pure membrane panels all frequencies increase with V, the damping remains positive throughout and no flutter condition appears. This was shown first by Ashley and Zartarian [36]. For cases where bending stiffness exists, the behavior is different. Here, as V increases the frequency of the second mode decreases accompanied by a change in shape and damping characteristics, until for some value of the flow speed which we define as the critical speed V_{cr}, the first two modes coalesce into one. As the flow speed continues to increase above V_{cr}, the two real modes change into two complex conjugate modes, the damping still being positive. These aeroelastic modes are different from the "standing wave" mode

shapes which existed prior to V_{cr}, in that their appearance is that of a pseudo-traveling-wave, since there is introduced a phase difference among points along the panel. Neither of the two original modes is "lost", as the complex modes may be thought of as being composed of two real modes, one with a real - the other with an imaginary-arbitrary amplitude. As V increases some more, the frequency, damping and shape of the complex modes continue to change until at the flutter speed the damping of one of them vanishes. For all speeds above $V_{flutter}$ the damping is negative and the motion in this mode is unstable. As V increases more and more, similar processes take place between different modes, but in practice, of course, the first V_{fl} is the significant one.

The explanation given above of the physical mechanism of flutter is made possible by the availability of piston theory which gives the aerodynamic loads for arbitrary motion. It has recently been argued by Pines [37] that this explanation may also be valid for the classical subsonic bending-torsion wing flutter. More recent investigations conducted at M.I.T. disclosed that in this case near-coalescence, rather than actual coalescence, takes place. This is due to the fundamental difference in the nature of the coupling terms between the two types of phenomena. However, in the case of shell flutter, the aerodynamic coupling is similar in nature to the panel flutter case. Therefore, it seems logical to assume the validity of this physical explanation in this case. This suggestion gains support from the recent work of Stepanov [38] on circular cylinders.

A most interesting and significant fact concerning the aerodynamic damping was uncovered when arbitrary-motion aerodynamics were used instead of harmonic-motion unsteady aerodynamics. Houbolt [35], Movchan [34] and also Pines [37] have shown that for practical values of the mass ratio use of static aerodynamics, first suggested by Hedgepeth [31], is perfectly

justified, since in such cases the damping is small and the difference between V_{cr} and V_{fl} is negligible. Flutter, therefore, can be considered to occur as soon as frequency coalescence takes place. Physically, the effect of neglecting the damping means that prior to flutter, the flow's effects are exhibited only as changes in the shapes and frequencies of the modes.

It should be noted that for certain cases, notably a cantilevered panel, static aeroelastic instability (divergence) occurs for speeds smaller than V_{fl}. This has been shown by Movchan [39]. The excellent agreement between piston theory, the static approximation and three-dimensional unsteady wing theory for, say, $M > 1.6$, suggests that these simple theories may be applied successfully at this range of Mach number for cases other than flat plates.

The extension of the analyses to the low supersonic range has been carried out by several of the authors mentioned above with varying degrees of success. The failure of the simplified aerodynamic theories in this range necessitates the use of the "exact" linear unsteady aerodynamic loading. The attempts to solve the resulting integro-differential equations have included use of Laplace transforms, approximations to the Bessel-function appearing in the aerodynamic terms or its numerical integration as part of a Galerkin procedure of solution. The problem has also been set up in terms of an integral equation by Fung [40] whose results for a plate agree well with those of Nelson and Cunningham [29] who used the Galerkin method.

The same problem has been approached from the point of view of it being a traveling wave phenomenon. Miles [41] and Jordan [26] for example, proceeded along this line. For a traveling-wave type of flutter, similar to a single degree of freedom flutter, and unlike the coupled mode flutter described above, the main feature is the loss of aerodynamic

damping. The process can be described as follows: At zero airspeed all wave lengths may be excited to yield undamped oscillatory motion (analogous to the natural modes for standing waves). As the airspeed increases the motion for all wave lengths is damped by the flow. As the flutter speed is approached, the damping in one or more wave lengths is reduced until at V_{fl} the damping vanishes for these wave lengths and the motion becomes unstable as V_{fl} is exceeded. The question as to which wave length is the most critical will depend on the panel's geometrical and structural properties. The plausibility of this description is shown by the fact that if no aerodynamic damping exists, then no eigen-solution can be obtained.

The question of the applicability of the results of a traveling-wave type analysis to a finite panel remains unanswered as yet, chiefly because of the difficulty of associating the critical wave lengths with the characteristic dimension of the panel. It has been shown [34] that in some cases this leads to erroneous conclusions.

The problem of the flutter of a buckled or curved panel has also attracted some attention. This is due primarily to the fact that in practice panels are not perfectly flat but have initial deformations due to imperfect fabrication and/or to thermal (or mechanical) buckling. Fung [40] and Eisley [23] for example, have looked into this problem. Experiments conducted by Eisley, and later by Mitchell [24] brought out the existence of two types of flutter--"small amplitude" (linear) and "large-amplitude" (presumably nonlinear). This fact prompted a large-deflection analysis whose results are in fair agreement with the experimental data. However, it seems that more conclusive experimental results must be obtained before this theory can be accepted.

The problem of thin shell flutter has also received some attention in recent years, as exemplified by the works

of Miles [42], Leonard and Hedgepeth [43], Stepanov [38] and Kopzon [44]. All of these analyses were confined to circular cylindrical shells (closed or supported along their generators), but the various approaches differed from one another in the aerodynamic expressions employed and in the methods of solution.

Both Miles and Leonard and Hedgepeth solved the problem employing the traveling wave concept, the former using plane wave aerodynamics, the latters-taking account of the curvature of the shell in their aerodynamic expressions. The results are practically identical, as far as the thickness required to prevent flutter is concerned. This is due to the fact that Miles' aerodynamic expressions very closely approximate Leonard and Hedgepth's more accurate expressions for a small number of circumferential nodes if the wave length is small relative to the radius.

Stepanov solved essentially the same problem employing piston theory, and his results compare favorably with those of Miles and Leonard and Hedgepeth. All of these results yield the highest value of the thickness-to-radius ratio for which at least one wave mode will flutter (a wave mode is determined by particular values of n, the number of circumferential waves and the longitudinal wave length). All results indicate that the lowest n's are the most critical. However, the question of which one of the two wave lengths associated with each n is more critical remains unsettled, though Miles concludes on the basis of his calculations of the damping present in each case that the shorter wave lengths are more critical. In this case his approximate aerodynamic expressions are acceptable.

All of these analyses are based on Donnell's shell equation, which, as is well known, is valid for $n \geqslant 2$ only. Since all results indicate that the low n's are the most critical, the question arises whether or not this equation is sufficiently accurate for the analysis. For the case of $n < 2$,

more refined shell equations are available, for example Flügge's equations, and in addition, tangential inertia effects become important, However, as the wave lengths become smaller relative to the radius, both of these effects diminish in importance. Since the critical wave lengths seem to be of the order of $(\frac{h}{R})^{\frac{1}{2}}$, it would seem that these effects are unimportant and the use of Donnell's equation is satisfactory. An analysis, presented in Appendix (4A), was carried out to investigate this point, and the results indicate that such is indeed the case.

The results mentioned above are applicable to infinitely long cylinders only. In a recent note, Holt [45] presented a method by which the aerodynamic forces on semi-infinite cylinders may be calculated. This was done by taking account of the boundary conditions at the leading edge of the cylinders. It is understood* that these results are soon going to be employed in flutter calculations.

In addition to the traveling wave solution, Stepanov [38] attacked the problem of the finite cylinder under various end-support conditions, utilizing piston theory. The approximate "medium-length-shell" theory was employed, thus reducing the order of the equation from eight to four and enabling the use of Movchan's method. The effect of this approximation is to neglect the longitudinal bending stiffness of the shell. Since the residual longitudinal stiffness is due solely to the membrane stresses and is inversely proportional to n^4, the result suggests that the flutter speed decreases monotonically with increasing n. This means that there always exists a particular n for which the shell will flutter at any given speed. Needless to say, this result is quite extraordinary. It is a direct consequence of the neglect of longitudinal

---

* Private communication

bending stiffness which increases with increasing n, thus "balancing" the effect of the membrane stiffness. It is therefore believed that use of the full eighth-order equation of Donnell's theory is necessary in order to determine the flutter conditions.

Kopzon [44] used an axial source distribution to obtain the aerodynamic loads on the cylinder, and employed the Laplace-transform method to solve the resulting integro-differential equation, similar to Goland and Luke's [30] approach in the case of the flat panel. No numerical results were presented. It is believed that Holt's expressions would prove to be more tractable than Kopzon's for actual calculations.

4.2 The Equation of Motion

We consider a thin panel, which may be a membrane, plate or shell of arbitrary geometry. In addition to air pressures induced by the supersonic flow about it, it may in general be subjected to other loads, such as thermal stresses, tension due to pressurization, acceleration loads etc.

Assuming (1) linearity (small deflections), (2) piston theory is applicable, (3) that the equation of motion of the panel can be written in terms of the transverse deflection w only (this may not always be strictly possible), then the governing equation will take the generalized form,

$$S(w) + L(w) + \rho h \frac{\partial^2 w}{\partial t^2} + \rho_a a\left(V \frac{\partial w}{\partial x} + \frac{\partial w}{\partial t}\right) = 0 \qquad (4\text{-}1)$$

where S(w) is the structural stiffness operator of the panel and L(w) is an operator embodying the effects of the various loadings such as those mentioned above. Both operators involve spatial derivatives of w only, and may also be considered independent of time, since the characteristic time

constants of the various coefficients appearing in these operators are usually much longer than those associated with the flutter problem with which we are concerned here. Any variation with time can therefore be taken care of by choosing the instantaneous values of the coefficients at the flutter conditions. For example, the value of E is taken at the flutter Mach number, or the value of the acceleration parameter is taken at the time when flutter speed is reached etc.

When Eq.(4-1) is properly nondimensionalized and a separable solution $w = \bar{w}e^{i\omega t}$ is assumed, we get,

$$\frac{1}{P}[S(\bar{w}) + L(\bar{w}) + \rho_a Va \frac{\partial \bar{w}}{\partial x}] = \lambda \bar{w} \qquad (4\text{-}2)$$

where,

P = Nondimensionalization factor,

$$[P] = FL^{-3} \qquad (4\text{-}3a)$$

$$\lambda = \frac{1}{P} (\rho h\omega^2 - i\rho_a a\omega) \qquad (4\text{-}3b)$$

λ plays the role of the eigenvalue. The problem is completely stated by Eq.(4-2) and an appropriate number of boundary conditions.

4.3 Adjoint Equations

The differential operator in Eq.(4-2),

$$S(\ ) + L(\ ) + \rho_a Va \frac{\partial(\ )}{\partial x} ,$$

is non-self-adjoint, due to the presence of the odd first derivative. [S( ) and/or L( ) may also be non-self-adjoint, though in most cases they are self-adjoint]. The behavior of the eigenvalues of equations such as this differs from that of self-adjoint equations, with which one is so familiar

from natural vibrations, buckling and other eigenvalue problems in mechanics. Whereas the eigenvalues of self-adjoint equations always exist and are always real, there is no existence theorem for the eigenvalues of non-self-adjoint equations, and furthermore, if they exist - they may be real or complex and there is as yet no way of telling when they will be real and when they will be complex. There is, however, a relationship between the eigenvalues of the differential operator and those of its adjoint operator. If the eigenvalues exist for the original equation - then their complex conjugates form the eigenvalues of the adjoint equation, and if they are real - then they are common to the two equations [46]. In fact, the solutions of the two adjoint equations form the bi-orthogonal system,

$$\int_{\ell} \phi_m (x)\, \tilde{\phi}_n (x)\, f(x)\, dx = 0 \qquad (4\text{-}4)$$

where $\phi_m(x)$ is a characteristic solution of the original equation,

$$M(\phi_m) = \lambda_m f(x)\, \phi_m \qquad (4\text{-}5)$$

for the eigenvalue λ_m, subject to the boundary conditions, and $\tilde{\phi}_n(x)$ is a characteristic solution of the adjoint equation,

$$\tilde{M}\,(\tilde{\phi}_n) = \lambda_n f(x)\, \tilde{\phi}_n \qquad (4\text{-}6)$$

for the eigenvalue λ_n, where $\lambda_m \neq \lambda_n$, subject to the adjoint boundary conditions. The adjoint boundary conditions (which are not necessarily the same as the boundary conditions of the original problem) may be obtained from Green's formula,

$$\int_{\ell} \tilde{\phi}\, M\,(\phi)\, dx - \int_{\ell} \phi\, \tilde{M}\,(\tilde{\phi})\, dx = Q\,(\phi, \tilde{\phi})\Big|_{\ell} = 0 \qquad (4\text{-}7)$$

where Q (ϕ, $\tilde{\phi}$) is a function known as the bilinear concomitant, using integration by parts and the original boundary conditions.

It can also be shown that the variational principle for a non-self-adjoint problem, whose Euler equations are the two adjoint differential equations, is given by,

$$\delta \int_{\ell} \tilde{\phi}(x) \, [M(\phi(x)) - \lambda f(x) \, \phi(x)] \, dx = 0 \qquad (4\text{-}8)$$

It is well-known that for the fimiliar self-adjoint problems, the variational integral which appears in Eq.(4-8) reduces to an energy expression, and its application in practice corresponds to minimum energy methods, foremost of which is the Rayleigh-Ritz method. Flax [47] suggested the concept of the "adjoint energy integral" and presented an approximate method of solution, analogous to the Rayleigh-Ritz method, utilizing two sets of assumed modes, one satisfying the original boundary conditions and the other - the adjoint boundary conditions. He has shown that for the problem he considered, divergence of swept wings, satisfactory results were obtained by application of this method. In addition, Wielandt [48] has shown that though no existence can be ascertained, an iteration process on non-self-adjoint differential or integral operators will converge to the lowest eigenvalue, if such an eigenvalue exists. This method has since been successfully applied in many problems.

The above seems to suggest that although mathematically a non-self-adjoint problem may not be as elegant as a self-adjoint problem, in practice approximate methods for its solution, whose validity may not have been rigorously established, may be used with a good chance for success.

Returning now to our original problem, we note that for this case, if both of the operators S( ) and L( ) are self adjoint, the physical meaning of the adjoint problem is that the flow has reversed its direction. Therefore, if the pro-

blem is invariant with respect to the flow direction, the eigenvalues of the two adjoint problems must be the same. Under such conditions, the solution of the adjoint problem (the mode shape) is the mirror image of its partner, which means that the symmetrical parts of the mode shapes are equal, and the antisymmetrical parts have opposite signs.

It may be observed in passing that the possibility of occurrence of flutter, and more generally, any self-excited dynamic instability, is associated with the presence of complex eigenvalues, which may occur only in a non-self-adjoint system. This, of course, is due to the fact that a self-adjoint system is conservative and thus cannot absorb the additional energy needed for instability to occur, since its energy is constant.

4.4 The Movchan-Houbolt Method

From the standpoint of the aeroelastician, the solution of Eq.(4-2) is interesting only insofar as it provides the flutter speed, and possibly also the rapidity with which flutter conditions are approached, namely the rate of loss of damping with speed.

The second question will not be dealt with here. However, the method to be described presently, which enables the determination of flutter conditions from the general solution, can also be used, in its general form, to deduce decay rates.

If we assume that Eq.(4-2) can be solved for the eigenvalue, either exactly or by some approximate method, then clearly this eigenvalue is a function of the flow speed as well as the properties of the panel and the fluid. Obviously, flutter conditions are reached whenever the eigenvalue is such as to cause the oscillatory panel motion to change from a convergent to a divergent behavior, i.e. when the complex frequency ω has a negative imaginary part.

Let,

$$\lambda = \lambda_R + i\,\lambda_I \qquad (4\text{-}9a)$$

$$\omega = \omega_R + i\,\omega_I \qquad (4\text{-}9b)$$

where λ_R, λ_I, ω_R, ω_I are real.

Substituting Eqs.(4-9) into Eq.(4-3b) and equating reals and imaginaries, we get,

$$\lambda_R = \frac{\rho h}{P}(\omega_R^2 - \omega_I^2) + \rho_a \frac{a}{P}\omega_I \qquad (4\text{-}10a)$$

$$\lambda_I = \frac{\omega_R}{P}(2\,\rho\,h\,\omega_I - \rho_a\,a) \qquad (4\text{-}10b)$$

Eliminating ω_R, we get,

$$\lambda_R = \frac{P\,\rho h\,\lambda_I^{\,2}}{(\rho_a a - 2\rho h\omega_I)^2} + \frac{1}{P}(\rho_a\,a\omega_I - \rho h\,\omega_I^2) \qquad (4\text{-}11)$$

It is clear that the parabola, of curvature $\frac{2P\,\rho\,h}{(\rho_a a)^2}$, passing through the origin in the complex λ plane corresponds to the case $\omega_I = 0$, the pure oscillatory motion case. This may be called the stability boundary. The stable ($\omega_I > 0$) and unstable ($\omega_I < 0$) regions lie below and above this boundary, respectively, as can be easily verified.

If, now, for any particular problem Eq.(4-2) is solved for λ, then this solution defines another relationship between λ_R and λ_I, say $\lambda_R = g(\lambda_I)$. Flutter conditions are therefore reached when the function g intersects the stability boundary. The part of g lying within the boundary corresponds to stable motion, the part outside the curve - to unstable motion.

The flutter speed, then, is obtained from the relation,

$$\frac{dg}{d\lambda_I} = \frac{2g}{\lambda_I} = \frac{2P\ \rho h}{(\rho_a a)^2}\lambda_I \qquad (4\text{-}12)$$

This method was first presented by Movchan [39] and later, independently, by Houbolt [35].

The function g can be obtained explicitly in a limited number of cases only. These include the traveling-wave case, where finiteness is the only boundary condition imposed on w, and the solution is simply given by $w = \bar{w}\, e^{i(\gamma x \pm \omega t)}$. Also for finite panels, when the order of the equation is low and a small number of boundary conditions must be satisfied so that λ can be solved for explicitly in terms of the system parameters.

As an example, the case of a membrane is illustrated.

For a membrane, Eq.(4-2) takes the form,

$$w'' - 2\,\bar{V}w' + (\lambda_R + i\lambda_I)\, w = 0 \qquad (4\text{-}13)$$

where,

$$w' = \frac{dw}{d(x/\ell)} = \frac{dw}{d\bar{x}} \qquad (4\text{-}14a)$$

$$\bar{V} = \frac{\rho_a a V \ell}{2T} \qquad (4\text{-}14b)$$

$$\ell = \text{non dimensionalization length.} \qquad (4\text{-}14c)$$

The proper choice for P in this case is T/ℓ^2, where T is the tension in the membrane.

For the unbounded membrane (where ℓ has no particular physical significance and it does not appear in the result) assume,

$$w = \bar{w} e^{i\bar{x}/L} \tag{4-15}$$

where L is the nondimensional wave length. Substituting Eq.(4-15) into Eq.(4-13), we get,

$$\lambda_R = \frac{1}{L^2} \tag{4-16a}$$

$$\lambda_I = \frac{2\bar{V}}{L} \tag{4-16b}$$

Eliminating L from Eqs.(4-16), we get,

$$\lambda_R = g(\lambda_I) = \frac{\lambda_I^2}{(2\bar{V})^2} \tag{4-17}$$

For this case Eq.(4-12) takes the form,

$$\frac{dg}{d\lambda_I} = \frac{2T}{\ell^2} \frac{\rho h}{(\rho_a a)^2} \lambda_I \tag{4-18}$$

Substituting for g from Eq.(4-17) into Eq.(4-18) we get the flutter criterion,

$$V_{fl} = \sqrt{\frac{T}{\rho h}} = a_m = \text{Speed of sound in membrane} \tag{4-19}$$

It can be seen that in this case the flutter mode is arbitrary, since all wave lengths L may flutter as soon as V reaches the wave propagation speed of the membrane. (Note that this result differs from Miles' result [42] $V_{fl} = a + a_m$, due to our employment of piston theory.)

For bounded membrane (where ℓ is the panel length) we have in addition to Eq.(4-13), the boundary conditions,

$$w = 0 \qquad \text{at} \quad \bar{x} = 0,\ 1 \tag{4-20}$$

Assuming an exponential solution,

$$w = \bar{w} e^{p\bar{x}} \tag{4-21}$$

and substituting it into Eq.(4-13), we get the general solution,

$$w = e^{\bar{V}\bar{x}} \left[C_1 \sin \sqrt{\lambda - \bar{V}^2}\ \bar{x} + C_2 \cos \sqrt{\lambda - \bar{V}^2}\ \bar{x}\right] \tag{4-22}$$

Substituting Eq.(4-22) into Eqs.(4-20), we get,

$$C_2 = 0 \tag{4-23a}$$

$$\lambda = \lambda_R + i\lambda_I = (m\pi)^2 + \bar{V}^2 \tag{4-23b}$$

Since the right-hand side of Eq.(4-23b) is always real, $\lambda_I = 0$. Substituting in Eqs.(4-10), we get,

$$\omega_I = \frac{\rho_a a}{2\rho h} \tag{4-24a}$$

$$\omega_R = \frac{m\pi}{\ell} \sqrt{\frac{T}{\rho h}}\ \sqrt{1 + \left(\frac{\rho_a a V \ell}{2m\pi T}\right)^2} \tag{4-24b}$$

(the other possibility, $\omega_R = 0$ in Eq.(4-10b), need not be considered, since λ_R is positive).

The solution is therefore given by,

$$w = e^{\bar{V}\bar{x}} \sum_m \bar{w}_m \sin m\pi\bar{x}\ e^{im\omega_o \sqrt{1 + \left(\frac{\bar{V}}{m\pi}\right)^2}\ t}\ e^{-\frac{a}{2\mu\ell} t} \tag{4-25}$$

where,

$$\omega_o = \frac{\pi}{\ell}\sqrt{\frac{T}{\rho h}} = \text{fundamental "in vacua" frequency} \quad (4\text{-}26a)$$

$$\mu = \frac{\rho h}{\rho_a \ell} = \text{mass ratio} \quad (4\text{-}26b)$$

It is seen that the motion is always damped and no flutter can occur. The effect of V is to distort the mode shapes and to stiffen the panel by a factor depending on each mode, while retaining the real characteristic of the motion, i.e. no phase shift is introduced.

The identical conclusions, of course, were obtained by Ashley and Zartarian [36], who employed a different method.

The two examples given above illustrate cases where the function $g(\lambda_I)$ can be obtained explicitly. These, to be sure, are the exceptions rather than the rule, because when the order of the characteristic equation is higher than two, as it is for plates and shells, no such explicit expressions are possible. In such cases either a numerical procedure or some approximate method must be used.

Despite the difficulty in obtaining an explicit expression for g in these cases, some deductions can be made concerning the qualitative behavior of λ with V, for panel flutter. The eigenvalues λ are continuous functions of the speed V forming an infinite number of branches. At first all λ's are real. As V increases, successive branch pairs of the real λ's meet and become complex conjugates. In general, for a higher V, they may become real again and the process may repeat itself many times. This process may take place among any branch pair, and in addition the real branches may, for some cases, assume such negative values as to cause the motion corresponding to these branches to be unoscillatory and unstable, $\omega_R = 0$, $\omega_I < 0$, i.e a "divergence" motion.

Obviously, for practical purposes one is interested in the lowest speed V causing an unstable motion. For all cases where the panel is supported at both ends divergence does not occur, and the flutter condition sets in soon after the first coalescence of a pair of branches occurs, i.e. when λ_I is very small. This is due to the fact that the curvature of the stability boundary is very large. Indeed the equation of this boundary can be written in the form,

$$\lambda_I = \frac{a}{a_m} \frac{1}{\mu} \sqrt{\lambda_R} \qquad (4\text{-}27)$$

where a_m is the speed of sound in the panel.

Equation (4-27) indicates that at flutter the magnitude of λ_I is much smaller than λ_R. This explains the reason for the flutter speed being very close to V_{cr}, the speed at which the first complex λ appears. This fact immediately suggests the simplification possible in the aerodynamic expression, namely, the neglect of the damping term, resulting in the steady approximation,

$$\Delta p(x) = -\rho_a a V \frac{\partial w}{\partial x} \qquad (4\text{-}28)$$

Eq.(4-3b) is now replaced by,

$$\lambda = \frac{\rho h}{P} \omega^2 \qquad (4\text{-}29)$$

From Eq.(4-29) it is immediately seen that under this approximation flutter occurs as soon as λ becomes complex. The validity of this approximation is limited to cases where $\mu > 10$, say, which include, however, most practical configurations.

It should be emphasized that this approximation is absolutely inapplicable to the unbounded panel problem, since

in this case no mode coalescence occurs and damping is of the essence. In addition, if the interest is in the actual damping in each mode at $V < V_{cr}$, this approximation is not valid either.

As may be seen from the membrane example presented above, the aeroelastic modes undergo a change in shape as a result of the air loads. For $V > V_{cr}$ the change in shape is accompanied by a phase change as well. This, of course, follows from the fact that a solution to an equation possessing complex coefficients must be complex. The degree of success of an assumed mode approach would therefore depend, among other things, on how well these modes approximate the true aeroelastic mode at or near flutter. Since the true flutter mode is always complex, the coefficients of the assumed modes will also be complex. The results of previous analyses of panel flutter, as well as classical bending-torsion flutter, indicate that the Galerkin method using "in vacua" mode shapes may be successfully used. A fuller discussion of the use and interpretation of the results of this method will be made in the next chapter.

APPENDIX 4A

EFFECTS OF FLÜGGE'S THEORY AND TANGENTIAL INERTIA ON FLUTTER OF INFINITE CYLINDERS

Flügge's shell equations, as are given by Eqs.(5-28) in the next chapter, reduce in the case of axisymmetrical deformations to the form,

$$\frac{\partial^2 u}{\partial \xi^2} + \nu\frac{\partial w}{\partial \xi} - C^2\frac{\partial^3 w}{\partial \xi^3} + \frac{R^2(1-\nu^2)}{Eh}X = 0 \qquad (4A\text{-}1a)$$

$$\left(\frac{1-\nu}{2}\right)(1+3C^2)\frac{\partial^2 v}{\partial \xi^2} + \frac{R^2(1-\nu^2)}{Eh}\Theta = 0 \qquad (4A\text{-}1b)$$

$$\nu\frac{\partial u}{\partial \xi} + w + C^2\left[\frac{\partial^4 w}{\partial \xi^4} + w - \frac{\partial^3 u}{\partial \xi^3}\right] + \frac{R^2(1-\nu^2)}{Eh}Z = 0 \qquad (4A\text{-}1c)$$

In this case it is seen that the torsional deformation is uncoupled from the axial and radial deformations.

By proper differentiation, the variable u may be eliminated from Eqs.(4A-1), resulting in a single equation,

$$(1-C^2)\frac{\partial^5 w}{\partial \xi^5} + 2\nu\frac{\partial^3 w}{\partial \xi^3} + \frac{\partial w}{\partial \xi} + \frac{1}{C_*^2}\frac{\partial w}{\partial \xi} - \frac{R^2}{EhC_*^2}\left[\frac{\partial Z}{\partial \xi} + C^2\frac{\partial^2 X}{\partial \xi^2} - \nu X\right] = 0 \qquad (4A\text{-}2)$$

The effect of the additional terms of Flügge's theory is investigated first. Accordingly, the longitudinal inertia

is neglected, X=0. In addition, the coefficient of the first term is approximated by 1.

Using piston theory, the equation of motion reads,

$$\frac{\partial^4 w}{\partial \xi^4} + 2\nu\frac{\partial^2 w}{\partial \xi^2} + w + \frac{1}{C_*^2}w + \frac{\rho_a aVR}{EhC_*^2}\frac{\partial w}{\partial \xi} + \frac{\rho R^2}{EC_*^2}\frac{\partial^2 w}{\partial t^2} + \frac{\rho_a aR^2}{EhC_*^2}\frac{\partial w}{\partial t} = 0 \quad (4A\text{-}3)$$

Let,

$$w = \bar{w}e^{i(\omega t - k\xi)} \quad (4A\text{-}4)$$

Substituting Eq.(4A-4) into Eq.(4A-3) and equating real and imaginary parts, we get,

$$\omega = \frac{V}{R}k \quad (4A\text{-}5)$$

and,

$$k^4 - 2[\nu + \frac{\rho V^2}{2EC_*^2}]k^2 + [1+\frac{1}{C_*^2}] = 0 \quad (4A\text{-}6)$$

The analogous equation for Donnell's theory is,

$$k^4 - 2[\frac{\rho V^2}{2E\ C_*^2}]k^2 + \frac{1}{C_*^2} = 0 \quad (4A\text{-}7)$$

Equation (4A-6) yields the flutter criterion,

$$\frac{\rho V_f^2}{2E} = C_*[\sqrt{1+C_*^2} - \nu C_*^2] \quad (4A\text{-}8)$$

Or, written in the more conventional way,the thickness to prevent flutter is given by,

$$\frac{h}{R} = \sqrt{3(1-\nu^2)}\ \left(\frac{a}{a_m}\right)^2 M^2\left\{1 + \left[\nu\left(\frac{a}{a_m}\right)^2 \frac{M^2}{2} - \frac{1}{16}\left(\frac{a}{a_m}\right)^4 M^4 + ..\right]\right\} \quad (4A\text{-}9)$$

where the terms in brackets are due to the inclusion of Flügge's terms. It is seen that these terms are quite small and have negligible effect on the results based on Donnell's equation. For example, for an aluminum cylinder at sea-level, Eq.(4A-9) becomes,

$$\frac{h}{R} = .77\left(\frac{M}{10}\right)^2\left[1 + .07\left(\frac{M}{10}\right)^2 - .014\left(\frac{M}{10}\right)^4 + ...\right] \quad (4A\text{-}10)$$

Next, the tangential inertia effect is investigated. Accordingly, Flügge's additional terms are dropped, and X is taken as,

$$X = \rho h \frac{\partial^2 u}{\partial t^2} \quad (4A\text{-}11)$$

Upon substitution of Eq.(4A-11) into Eq.(4A-1a) and assuming in addition to Eq.(4A-4) the form,

$$u = \bar{u}e^{i(\omega t - k\xi)} \quad (4A\text{-}12)$$

the same procedure as before would yield the equation,

$$k^4 - \frac{\rho V^2}{EC_*^2} k^2 + \frac{1}{C_*^2}\left[1 - \nu^2 \frac{\frac{\rho V^2}{E}}{1 - \frac{\rho V^2}{E}(1-\nu^2)}\right] = 0 \quad (4A\text{-}13)$$

which yields the thickness to prevent flutter as,

$$\frac{h}{R} = \sqrt{3(1-\nu^2)}\ \left(\frac{a}{a_m}\right)^2 M^2\left[1 + \nu^2\left(\frac{a}{a_m}\right)^2 \frac{M^2}{2} + ...\right] \quad (4A\text{-}14)$$

It is seen that as in the previous case, the effect is quite small. Therefore it is concluded that the two effects together have a negligible influence on the result obtained by using Donnell's equation.

CHAPTER 5

CYLINDRICAL SHELL FLUTTER

5.1 Aerodynamic Theory

Before the results of the preceding chapter are applied to the case of a thin cylindrical shell, it is worthwhile to review the various results for the aerodynamic loads acting on such a body in the speed range of interest, namely, $M > 1.6$.

In a system of cylindrical coordinates, with the flow directed along the positive x axis, the potential equation for steady supersonic flow is,

$$\beta^2 \frac{\partial^2 \phi}{\partial x^2} - \frac{\partial^2 \phi}{\partial r^2} - \frac{1}{r} \frac{\partial \phi}{\partial r} - \frac{1}{r^2} \frac{\partial^2 \phi}{\partial \theta^2} = 0 \qquad (5\text{-}1)$$

where $\beta^2 = M^2 - 1$

The boundary conditions are,
On the body (r=R),

$$\frac{\partial \phi}{\partial r} (x,R,\theta) = V \frac{\partial w}{\partial x} (x,R,\theta) \qquad (5\text{-}2)$$

The outgoing radiation condition,

$$\phi = \phi (x-\beta r, \theta) \quad \text{for large } r \qquad (5\text{-}3)$$

At the undisturbed stream,

$$\phi \longrightarrow 0 \qquad \text{as} \qquad r \longrightarrow \infty \tag{5-4}$$

Solutions periodic in θ are admissible. Therefore let,

$$\phi(x,r,\theta) = \bar{\phi}(x,r) \cos n\theta \tag{5-5a}$$

$$w(x,\theta) = \bar{w}(x) \cos n\theta \tag{5-5b}$$

Substituting in Eqs.(5-1) through (5-3) we get,

$$\beta^2 \bar{\phi}_{xx} - \bar{\phi}_{rr} - \frac{1}{r} \bar{\phi}_r + \frac{n^2}{r^2} \bar{\phi} = 0 \tag{5-6}$$

$$\bar{\phi}_r \Big|_{r = R} = V \bar{w}_x \tag{5-7}$$

$$\bar{\phi} = \bar{\phi}(x - \beta r) \Big|_{r \gg R} \tag{5-8}$$

Applying Laplace transformation to Eq.(5-6), we take,

$$L\left\{\phi(x,r)\right\} = \tilde{\phi}(p,r) \tag{5-9a}$$

$$L\left\{\bar{w}(x)\right\} = \tilde{w}(p) \tag{5-9b}$$

Eq.(5-6) becomes,

$$\tilde{\phi}_{rr} + \frac{1}{r} \tilde{\phi}_r - (\beta^2 p^2 + \frac{n^2}{r^2}) \tilde{\phi} = 0 \tag{5-10}$$

The general solution is,

$$\tilde{\phi}(p,r) = C_1(p)\ I_n(\beta pr) + C_2(p)\ K_n(\beta pr) \qquad (5\text{-}11)$$

where I_n and K_n are the modified Bessel functions of the first and second kind, respectively, of order n.

Applying Eq.(5-4) we get,

$$C_1(p) = 0 \qquad (5\text{-}12)$$

Applying Eq.(5-7), we get,

$$\tilde{\phi}(p,r) = - V[p\tilde{w}(p) - \tilde{w}(0)]\ \tilde{\psi}_n(p,r) \qquad (5\text{-}13)$$

where,

$$\tilde{\psi}_n(p,r) = - \frac{K_n(\beta pr)}{\beta p K_n'(\beta pR)} \qquad (5\text{-}14)$$

Therefore, the velocity potential is given by,

$$\phi(x,r,\theta) = - V \int_0^x \bar{w}_x(x_1)\ \psi_n(x-x_1,\ r)\ dx_1 \cos n\theta \qquad (5\text{-}15)$$

where $\psi_n(x,r)$ is the inverse transform of $\tilde{\psi}_n(p,r)$, and is given by,

$$\psi_n(x,r) = \frac{1}{2\pi i} \int_{-i\infty}^{i\infty} \tilde{\psi}_n(p,r)\ e^{px} dp \qquad (5\text{-}16)$$

As Nielsen [49] pointed out, the functions $\psi_n(x,r)$ may be considered as the impulse-response functions to a unit impulse

in the downwash $V\frac{\partial w}{\partial x}$. Therefore, for a sinusoidal $\bar{w}_x$, the function $\tilde{\psi}_n(p,r)$ may be considered as the transfer function of the system.

If we now assume the periodic form for $\bar{w}$,

$$\bar{w}(x) = \bar{w}e^{-i\sigma x} \tag{5-17}$$

we have, by virtue of Eqs.(5-13) and (5-14),

$$\bar{\phi}(x,r) = \frac{V}{\beta}\bar{w}e^{-i\sigma x}\frac{K_n(-i\sigma\beta r)}{K_n'(-i\sigma\beta R)} \tag{5-18}$$

But,

$$K_n(-is) = \frac{\pi}{2} i^{n+1} H_n^{(1)}(s) \tag{5-19a}$$

$$K_n'(-is) = \frac{\pi}{2} i^{n+2} H_n^{(1)'}(s) \tag{5-19b}$$

where $H_n^{(1)}$ is the Hankel function of the first kind, of order n. Thus the velocity potential is given, for this case, by,

$$\phi(x,r,\theta) = -\frac{iV}{\beta}\frac{H_n^{(1)}(\sigma\beta r)}{H_n^{(1)'}(\sigma\beta R)}\bar{w}e^{-i\sigma x}\cos n\theta \tag{5-20}$$

Since the asymptotic behavior of $H_n^{(1)}(\sigma\beta r)$ is proportional to $e^{i\sigma\beta r}$, Eq.(5-3) is satisfied. The two solutions, Eqs.(5-15) and (5-20) differ in that the former is applicable at any value of x, whereas the latter is strictly applicable for large x. [Eq.(5-20) can be obtained formally by letting x be large in Eq.(5-15)]. The two expressions are

analogous, respectively, to the complete time solution and to the steady state solution of a spring-mass-dash-pot system subjected to sinusoidal load.

The physical meaning of the assumption of Eq.(5-17) is that the cylinder deflections are waves extending to infinity along the axis in both directions, i.e. the cylinder is infinitely long. Therefore Eq.(5-20) is applicable to the unbounded cylinder problem. On the other hand the solution given by Eq.(5-15) is applicable to a semi-infinite cylinder extending from $x = 0$ to $x = +\infty$. Even this solution, however, is not strictly applicable for the case of a finite cylinder, since it fails to take account of the conditions at the finite boundary.

The aerodynamic loads corresponding to the two cases are given by,

Infinite cylinder,

$$\Delta p(x,\theta) = \frac{\rho_a V^2 \sigma}{\beta} \frac{H_n^{(1)}(\sigma\beta R)}{H_n^{(1)'}(\sigma\beta R)} \bar{w} e^{-i\sigma x} \cos n\theta \qquad (5\text{-}21)$$

Semi-infinite cylinder,

$$\Delta p(x,\theta) = \frac{\rho_a V^2}{\beta} \frac{\partial}{\partial x} \left\{ \int_0^x \bar{w}_x(x_1) \left[\frac{1}{2\pi i} \int_{-i\infty}^{i\infty} - \frac{K_n(\beta p R)}{p K_n'(\beta p R)} e^{p(x-x_1)} dp \right] dx_1 \right\} \cos n\theta \qquad (5\text{-}22)$$

For comparison purposes we note the following two simplified expressions,

Hayes' [50] approximation,

$$\Delta p(x,\theta) = -\frac{\rho_a V^2}{\beta}\frac{\partial \bar{w}(x)}{\partial x}\cos n\theta \qquad (5\text{-}23)$$

Static piston theory,

$$\Delta p(x,\theta) = -\rho_a a V \frac{\partial \bar{w}(x)}{\partial x}\cos n\theta \qquad (5\text{-}24)$$

The expressions given by Eqs.(5-21) and (5-22) do not apply, of course, to the unsteady problem. Since their use is limited to the traveling wave type of flutter for which aerodynamic damping plays a decisive role, they must be modified by including the unsteady terms in the potential equation. Rather than go through the derivation, we note here the result for the first case, obtained by Leonard and Hedgepeth [43],

$$\Delta p(x,\theta,t) = +\rho_a\left(V-\frac{\omega}{\sigma}\right)^2 \sigma \bar{w} e^{-i\sigma x}\cos n\theta\, e^{i\omega t}\,\overline{\Delta p} \qquad (5\text{-}25)$$

where,

$$\overline{\Delta p} = \begin{cases} \dfrac{K_n\left(\sigma R\sqrt{1-[M-k]^2}\right)}{\sqrt{1-[M-k]^2}\,K_n'\left(\sigma R\sqrt{1-[M-k]^2}\right)}, & |M-k|<1 \\ \dfrac{H_n^{(j)}\left(\sigma R\sqrt{[M-k]^2-1}\right)}{\sqrt{[M-k]^2-1}\,H_n^{(j)\prime}\left(\sigma R\sqrt{[M-k]^2-1}\right)}, & |M-k|>1, \quad j=\begin{cases}1 & M>k\\ 2 & M<k\end{cases} \end{cases} \qquad (5\text{-}26)$$

where,

$$k = \frac{\omega}{\sigma a} = \text{reduced frequency} \qquad (5\text{-}27)$$

It seems clear from these results that, similar to the flat panel case, use of piston theory would simplify the flutter analysis considerably. In addition Eqs.(5-23) or (5-24) may be applied to the finite cylinder case for any deflection shape.

The cost in accuracy of applying these approximate expressions is probably small, as shown by the good agreement between the results of the traveling wave analysis of Stepanov [38], based on piston theory, and that of Leonard and Hedgepeth [43] based on Eq.(5-25). In the ensuing analysis, therefore, aerodynamic piston theory, as given by Eq.(5-24) will be employed.

5.2 Structural Theory

It is well-known that unlike beam and plate theories, for which the structural operators are well defined and universally accepted, the situation in shell theory, including thin cylindrical shells, is not so clear cut.

Ever since Love presented his shell bending theory [51] (where he refers to yet earlier work) there have been numerous attempts to improve upon it on the one hand and to simplify it on the other. The various refinements and approximations resulted in a variety of forms for the governing equations.

The theory presented in Chapter 2 may be considered as the first approximation to shells of finite thickness beyond membrane theory. It bears close resemblance to shallow shell theory, and as was illustrated earlier, by a proper definition of the coordinates the two theories yield identical results in the case of cylindrical shells.

Some of the more familiar of the more exact theories are those due to Flügge [16], Vlasov [52] (shells of 'medium thickness') and Timoshenko [53]. For cylindrical shells the equations of equilibrium in terms of the displacements may be

written in the general form,

$$L_1^{(0)}(u,v,w) + C^2 L_1^{(1)}(u,v,w) + \frac{1-\nu^2}{Eh} X = 0 \qquad (5\text{-}28a)$$

$$L_2^{(0)}(u,v,w) + C^2 L_2^{(1)}(u,v,w) + \frac{1-\nu^2}{Eh} \Theta = 0 \qquad (5\text{-}28b)$$

$$L_3^{(0)}(u,v,w) + C^2 L_3^{(1)}(u,v,w) + \frac{1-\nu^2}{Eh} Z = 0 \qquad (5\text{-}28c)$$

where the functions $L_i^{(0)}(u,v,w)$ are common to all forms and the functions $L_i^{(1)}(u,v,w)$ represent the different terms included in each theory. The functions $L_i^{(0)}$ are given by,

$$L_1^{(0)} = \frac{\partial^2 u}{\partial x^2} + \frac{1-\nu}{2R^2}\frac{\partial^2 u}{\partial \theta^2} + \frac{1+\nu}{2R}\frac{\partial^2 v}{\partial x \partial \theta} + \frac{\nu}{R}\frac{\partial w}{\partial x} \qquad (5\text{-}29a)$$

$$L_2^{(0)} = \frac{1+\nu}{2R}\frac{\partial^2 u}{\partial x \partial \theta} + \frac{1}{R^2}\frac{\partial^2 v}{\partial \theta^2} + \frac{1-\nu}{2}\frac{\partial^2 v}{\partial x^2} + \frac{1}{R^2}\frac{\partial w}{\partial \theta} \qquad (5\text{-}29b)$$

$$L_3^{(0)} = \frac{\nu}{R}\frac{\partial u}{\partial x} + \frac{1}{R^2}\frac{\partial v}{\partial \theta} + \frac{w}{R^2} + \frac{C^2}{R^2}\nabla^4[w] \qquad (5\text{-}29c)$$

where the operator ∇^4 is given in this case by,

$$\nabla^4 w = R^4 \frac{\partial^4 w}{\partial x^4} + 2R^2 \frac{\partial^4 w}{\partial x^2 \partial \theta^2} + \frac{\partial^4 w}{\partial \theta^4} \qquad (5\text{-}30)$$

In the first approximation, all $L_i^{(1)}$'s are zero. In the three other forms they are given in Table 5.1.

TABLE 5.1

	TIMOSHENKO	VLASOV	FLÜGGE
			same as Vlasov, plus these added terms
$L_1^{(1)}$	—	$\frac{1-\nu}{2R}\frac{\partial^3 w}{\partial x \partial \theta^2} - R\frac{\partial^3 w}{\partial x^3}$	$\frac{1-\nu}{2R^2}\frac{\partial^2 u}{\partial \theta^2}$
$L_2^{(1)}$	$-\frac{\partial^3 w}{\partial x^2 \partial \theta} - \frac{1}{R^2}\frac{\partial^3 w}{\partial \theta^3} + (1-\nu)\frac{\partial^2 v}{\partial x^2} + \frac{1}{R^2}\frac{\partial^2 v}{\partial \theta^2}$	$-\frac{3-\nu}{2}\frac{\partial^3 w}{\partial x^2 \partial \theta}$	$\frac{3}{2}(1-\nu)\frac{\partial^2 v}{\partial x^2}$
$L_3^{(1)}$	$-(2-\nu)\frac{\partial^3 v}{\partial x^2 \partial \theta} - \frac{\partial^3 v}{R^2 \partial \theta^3}$	$\frac{2}{R^2}\frac{\partial^2 w}{\partial \theta^2} + \frac{w}{R^2} - R\frac{\partial^3 u}{\partial x^3} + \frac{1-\nu}{2R}\frac{\partial^3 u}{\partial x \partial \theta^2} - \frac{3-\nu}{2}\frac{\partial^3 v}{\partial x^2 \partial \theta}$	—

It is clear that since the additional terms are proportional to the small quantity C^2, their magnitude is small and in most cases they may therefore be neglected. In certain problems, however, they may be important, as, for example, in the calculation of stresses in the edge region of the shell.

In the free vibration problem, the forces X, Θ, Z, represent the inertia loads. If the tangential inertia is neglected, then these equations may be reduced in each case to a simple eighth-order equation in the function ϕ. These may be written as,

$$L_4^{(0)}(\phi) + C_*^2 L_4^{(1)}(\phi) + \frac{\rho R^2}{E}\frac{\partial^2 \phi}{\partial t^2} = 0 \qquad (5\text{-}31)$$

The common term $L_4^{(0)}(\phi)$ is given by,

$$L_4^{(0)}(\phi) = R^4 \frac{\partial^4 \phi}{\partial x^4} + C_*^2 \nabla^8 \phi \tag{5-32}$$

and the additional term $L_4^{(1)}(\phi)$, for Vlasov's theory, is given by,

$$L_{4\ \text{Vlasov}}^{(1)}(\phi) = (2\nabla^2+1)\nabla^4\phi - 2(1-\nu)\ R^2 \frac{\partial^2}{\partial x^2}\left(R^4\frac{\partial^4\phi}{\partial x^4} - \frac{\partial^4\phi}{\partial \theta^4}\right) \tag{5-33}$$

and for Flügge's theory, by,

$$L_{4\ \text{Flugge}}^{(1)}(\phi) = L_{4\ \text{Vlasov}}^{(1)}(\phi) + R^2 \frac{\partial^2}{\partial x^2}\left[2(1-\nu)\frac{\partial^2\phi}{\partial\theta^2} - R^2\frac{\partial^2\phi}{\partial x^2}\right] \tag{5-34}$$

For the first approximation, $L_4^{(1)}(\phi) = 0$, and the equation reads,

$$R^4 \frac{\partial^4 \phi}{\partial x^4} + C_*^2 \nabla^8 \phi + \frac{\rho R^2}{E}\frac{\partial^2}{\partial t^2}(\nabla^4\phi) = 0 \tag{5-35}$$

The relationship between the displacements u,v,w, and the function ϕ vary in each case. For $L_4^{(1)}(\phi) = 0$, they are given by,

$$w = \nabla^4 \phi \tag{5-36a}$$

$$u = R \frac{\partial}{\partial x}\left(\frac{\partial^2\phi}{\partial\theta^2} - \nu R^2 \frac{\partial^2\phi}{\partial x^2}\right) \tag{5-36b}$$

$$v = -\frac{\partial}{\partial \theta}\left(\frac{\partial^2 \phi}{\partial \theta^2} + (2+\nu)\, R^2 \frac{\partial^2 \phi}{\partial x^2}\right) \qquad (5\text{-}36c)$$

The frequencies obtained using Eq.(5-35) compare quite favorably with those obtained by using the more exact theories and including tangential inertia, for $n > 2$. As mentioned earlier Eq.(5-35) may also be obtained by using shallow-shell theory, provided the variable y is defined as $y = R\,\theta$, therefore the idential frequency results are obtained.

All the theories mentioned above fail when the axial wave length of the vibration mode is small compared with the cylinder radius, since transverse shear deformation and rotational inertia effects, which are not included in these theories, become important in this case.

Another theory, due to Goldenveiser [54] is of interest. This is the so called "medium shell" theory which yields the following form for the equilibrium equation,

$$R^4 \frac{\partial^4 \phi}{\partial x^4} + C_*^2 \left(\frac{\partial^2}{\partial \theta^2} + 1\right)^2 \frac{\partial^4 \phi}{\partial \theta^4} + \frac{\rho R^2}{E} \frac{\partial^2}{\partial t^2}\left(\frac{\partial^4 \phi}{\partial \theta^4}\right) = 0 \qquad (5\text{-}37)$$

Comparison of Eqs.(5-35) and (5-37) shows that the latter neglects axial bending stiffness, as was pointed out in Chapter 4 in connection with Stepanov's results.

On the basis of comparison, it seems that the first approximation, Eq.(5-35) may be used with confidence in the ensuing development provided its limitations are borne in mind.

5.3 Exact Solutions

Now that the structural and aerodynamic operators have been determined, the formulation of the flutter problem can be undertaken.

A thin cylindrical shell, of constant thickness h, radius R and length ℓ, and "simply supported" along its edges, is immersed in a supersonic airstream passing over its outside surface, while the fluid within it remains at rest. The cylinder configuration and the coordinate system used are illustrated in Fig. 5.1.

Using Eqs.(5-24) and (5-35) and including aerodynamic damping, the equation of motion reads,

$$R^4\frac{\partial^4\phi}{\partial x^4} + C_*^2\nabla^8 w + \frac{\rho_a a R^2}{Eh}\left(V\frac{\partial}{\partial x} + \frac{\partial}{\partial t}\right)(\nabla^4\phi) + \frac{\rho R^2}{E}\frac{\partial^2}{\partial t^2}(\nabla^4\phi) = 0 \quad (5\text{-}38)$$

For a "simply supported" cylinder the moment, axial force, radial and circumferential displacements vanish at the edges. Since the equation is written in terms of the function ϕ, all these quantities must be expressed in terms of ϕ. The boundary conditions would then read,

At x = 0, ,

$$w = \nabla^4\,\phi = 0 \quad (5\text{-}39a)$$

$$v = -\frac{\partial}{\partial\theta}\left[\frac{\partial^2\phi}{\partial\theta^2} + (2+\nu)\,R^2\,\frac{\partial^2\phi}{\partial x^2}\right] = 0 \quad (5\text{-}39b)$$

$$N_x = EhR\,\frac{\partial^4\phi}{\partial x^2\partial\theta^2} = 0 \quad (5\text{-}39c)$$

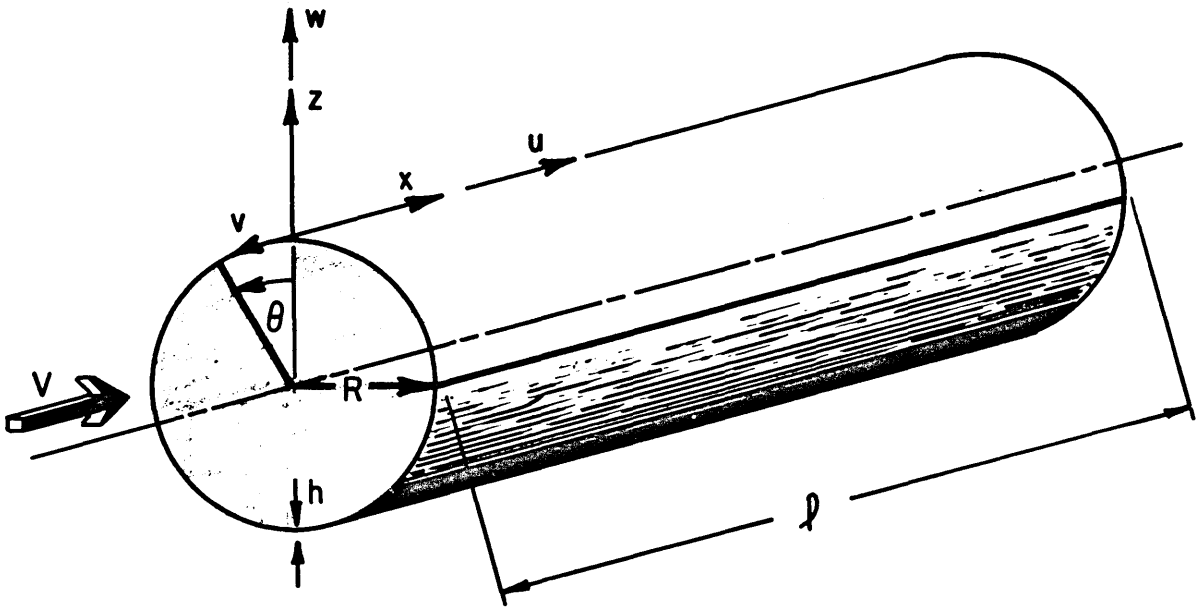

FIG. 5.1 CYLINDER COORDINATE SYSTEM

$$M_x = Eh\ C_*^2\ (R^2 \frac{\partial^2}{\partial x^2} + \nu \frac{\partial^2}{\partial \theta^2})(\nabla^4 \phi) = 0 \qquad (5\text{-}39d)$$

Eq.(5-38) is now nondimensionalized and by assuming a solution of the form,

$$\phi = \bar{\phi}\ (\xi)\ \cos\ n\theta\ e^{i\omega t} \qquad (5\text{-}40)$$

the following ordinary differential equation is obtained,

$$\frac{d^4\bar{\phi}}{d\xi^4} + C_*^2\ \nabla^8\bar{\phi} + \tilde{V}\ \frac{d}{d\xi}\ (\nabla^4\bar{\phi}) - \lambda\ \nabla^4\bar{\phi} = 0 \qquad (5\text{-}41)$$

where,

$$\xi = \frac{x}{R} \qquad (5\text{-}42a)$$

$$\tilde{V} = \frac{\rho_a aVR}{Eh} \qquad (5\text{-}42b)$$

$$\lambda = \frac{\rho R^2}{E}\ (\omega^2 - \frac{\rho_a a}{\rho h}\ i\omega) \qquad (5\text{-}42c)$$

and where,

$$\nabla^2\ \bar{\phi} = \frac{d^2\bar{\phi}}{d\xi^2} - n^2\ \bar{\phi} \qquad (5\text{-}43)$$

Using Eqs.(5-42) and (5-43), the boundary conditions given by Eqs.(5-39) simplify into,

$$\bar{\phi} = \frac{d^2\phi}{d\xi^2} = \frac{d^4\phi}{d\xi^4} = \frac{d^6\phi}{d\xi^6} = 0 \quad \text{at} \quad \xi = 0,\ \ell/R \tag{5-44}$$

Eqs.(5-41) and (5-44) define the flutter problem, where λ is the eigenvalue and $\tilde{V}$ is the velocity parameter. Eq.(5-41) is obviously a special case of the general equation, Eq.(4-2), where $S(\phi)$ is given by Eq.(5-32), $L(\phi) = 0$, and $P = \frac{Eh}{\kappa^2}$. The general solution of Eq.(5-41) is given by,

$$\bar{\phi}(\xi) = \sum_{i=1}^{8} c_i e^{p_i \xi} \tag{5-45}$$

Substitution of Eq.(5-45) into Eqs.(5-44) would result in an 8 x 8 characteristic determinant whose elements involve the eight roots p_i. It seems obvious that a solution of this determinant which would yield an explicit expression for λ in terms of ℓ/R, n, C_*^2 and V is impossible. Moreover, even a numerical solution for given values of these parameters seems to be quite impractical since the roots cannot be expressed in terms of λ or another set of convenient variables. It must therefore be concluded that an exact solution of this problem should be ruled out.

It will now be shown that by employing the approximate "middle shell" theory, the problem reduces to that of an equivalent flat plate and an exact solution is therefore possible.

Using Eq.(5-37) we get the equation of motion,

$$\frac{1}{n^4}\frac{d^4\bar{\phi}}{d\xi^4} + \tilde{V}\frac{d\bar{\phi}}{d\xi} - [\lambda - C_*^2 (n^2-1)^2]\,\bar{\phi} = 0 \tag{5-46}$$

and the boundary conditions,

$$\overline{\phi} = \frac{d^2\overline{\phi}}{d\xi^2} = 0 \quad \text{at} \quad \xi = 0,\ \ell/R \tag{5-47}$$

Equations (5-46) and (5-47) represent the problem treated by Stepanov [38]. Their form is identical to the flat plate problem treated by Hedgepeth [31], Movchan [34] and Houbolt [35], whose solutions may be applied to this problem. A cursory examination is sufficient to reveal that a paradoxical situation exists, namely, that the flutter velocity parameter decreases monotonically with an increasing n and therefore the cylinder will flutter at any speed.

The reason for this behavior is, of course, the fact that the "middle shell" theory admits no axial bending stiffness. If included, this stiffness would balance the membrane effect by introducing terms which increase with n, and thus tend to offset the trend. "Middle shell" theory may yield fairly good approximate flutter speeds at low n, where the axial bending effect is small for thin shells. However, it seems that it fails to reveal the true behavior for higher n and therefore it is inadequate in predicting the minimum flutter speed of the cylinder.

On the basis of this argument it seems necessary to go back to Eq.(5-41), and since a practical exact solution cannot be obtained, approximate methods of solution must be resorted to.

5.4 Use of Galerkin's Method

As mentioned earlier, assumed mode methods have been successfully used in the non-self-adjoint problem of flutter despite the lack of rigor in their applicability. The present problem, therefore, will also be treated using this

approximate method. The particular method to be used is the Galerkin process using "in vacua" natural modes.

In view of the fact that aerodynamic damping was shown to have a small effect on the flutter speed, it will be neglected in the analysis.

Under this assumption, Eq.(5-41), the equation of motion, reads,

$$\frac{d^4\bar{\phi}}{d\xi^4} + C_*^2 \nabla^8\bar{\phi} + \tilde{V} \frac{d}{d\xi} (\nabla^4\bar{\phi}) - \bar{\omega}^2 \nabla^4\bar{\phi} = 0 \qquad (5\text{-}48)$$

where,

$$\bar{\omega}^2 = \frac{\rho R^2}{E} \omega^2 \qquad (5\text{-}49)$$

Since the aerodynamic loads are axially symmetric, there is no coupling among the various circumferential modes. Therefore n may be taken as a parameter and we assume,

$$\bar{\phi}(\xi) = \sum_m \bar{\phi}_m \sin \frac{m\pi x}{\ell} = \sum_m \bar{\phi}_m \sin m\lambda\xi \qquad (5\text{-}50)$$

where conventionally,

$$\lambda = \frac{\pi R}{\ell} \qquad (5\text{-}51)$$

Substituting Eq.(5-50) into Eq.(5-48) and integrating along the cylinder's axis, we get,

$$(\bar{\omega}_o^{(m)})^2 - \bar{\omega}^2)\bar{\phi}_m - \sum_{\substack{\bar{m} \\ \text{Odd}^*}}^{m+\bar{m}} \bar{\phi}_{\bar{m}} \left(\frac{n^2+\bar{m}^2\lambda^2}{n^2+m^2\lambda^2}\right)^2 \frac{4m\bar{m}}{\bar{m}^2-m^2} \frac{\lambda\tilde{V}}{\pi} = 0 \quad m=1,2\ldots (5\text{-}52)$$

---

* See footnote on page 52.

where,

$$\bar{\omega}_o^{(m)^2} = \frac{(m\lambda)^4}{[n^2+(m\lambda)^2]^2} + C_*^2[n^2+(m\lambda)^2]^2 \qquad (5\text{-}53)$$

$\bar{\omega}_o^{(m)}$ are the "in vacua" natural frequencies of the cylinder.

It can be seen that symmetrically located off-diagonal elements in the determinant of Eq.(5-52) differ by their sign and by a mutually reciprocal factor. In the expansion of the determinant these elements will always appear in such a way that the product of the reciprocal factors will be unity. Therefore these factors which depend on n and λ may be dropped.

By extracting from $\bar{\omega}_o^{(m)^2}$ the portion which does not vary with m and dividing Eq.(5-52) by λ^4, we obtain the final set of equations,

$$[\Omega_m^2 - \bar{\Omega}^2]\bar{\phi}_m - \sum_{\substack{\bar{m} \\ \text{Odd}}}^{m+\bar{m}} \bar{\phi}_{\bar{m}} \frac{4m\bar{m}}{\bar{m}^2-m^2} \bar{V} = 0 \qquad m=1,2, \quad (5\text{-}54)$$

where,

$$\Omega_m^2 = m^4\left[\frac{1}{[n^2+(m\lambda)^2]^2} + C_*^2\right] + m^2 \frac{2n^2}{\lambda^2} C_*^2 \qquad (5\text{-}55a)$$

$$\bar{\Omega}^2 = \frac{1}{\lambda^4}\left[\bar{\omega}^2 - C_*^2 n^4\right] \qquad (5\text{-}55b)$$

$$\bar{V} = \frac{1}{\pi^4}\left(\frac{\rho a}{E}\right)\left(\frac{R}{h}\right)\left(\frac{\ell}{R}\right)^3 V \qquad (5\text{-}55c)$$

The set of Eqs.(5-54) is of the same form and has the same coupling terms as the corresponding set for the plate and the membrane problems. This immediately suggests that the solutions will behave in a similar manner. Here, however, care should be exercised.

Past experience has shown that for plates, or plate-membranes, Galerkin solutions using a fairly small number of modes converge upon the exact V_{fl} and $\bar{\Omega}_{fl}$. For pure membranes, however, this method yields values for V_{fl} and $\bar{\Omega}_{fl}$ which are completely spurious, since the exact solution was shown to yield no finite flutter speed. Since a cylinder contains the features of both of these cases, the question is raised concerning the success of the method for this case.

A close examination of these problems has revealed the following, which is offered as an explanation of the reasons for the different behavior of this method in each case and also as a guide to the future use of the Galerkin method in similar problems.

The exact solution of the membrane problem, as given by Eq.(4-25), is illustrated in Fig. 5.2, which is a plot of the frequencies of the aeroelastic modes as a function of the velocity parameter. Fig. 5.3 illustrates the same results as obtained by Galerkin's method employing different numbers of modes. It is evident from this figure that in this case the assumed mode approach tends always to cause the highest two modes to coalesce yielding an apparent finite flutter speed, in contrast to the exact solution. However, the important thing is that the more modes are included in the analysis the better is the approximation to the exact behavior of the low modes, although the results for the higher modes are in error. This is quite significant, since it is reasonable to assume that flutter involves two of the lowest modes (though not necessarily the absolutely lowest mode, perhaps, as shown for a panel on many supports by Leonard and

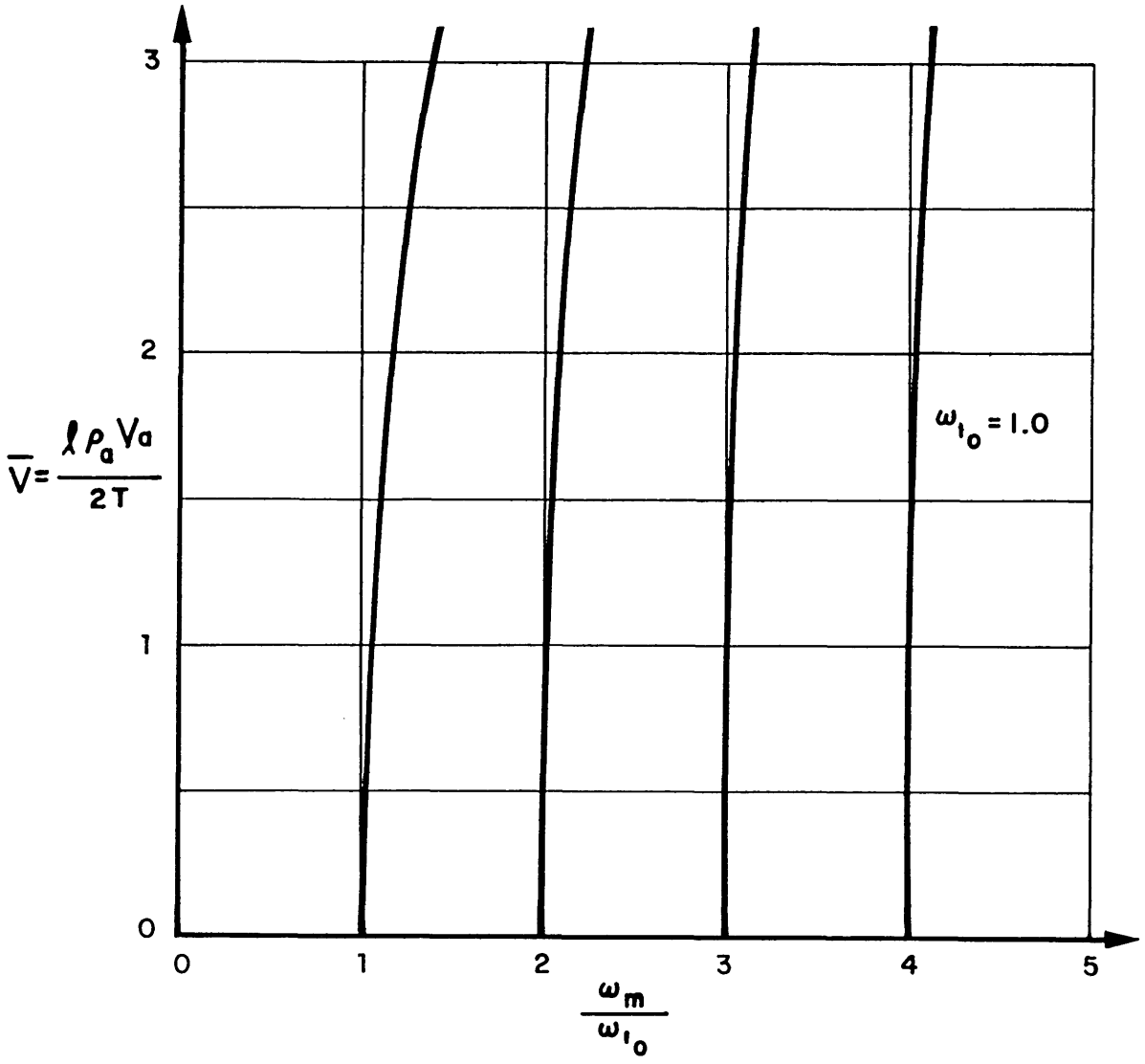

FIG. 5.2 EFFECT OF AIR FLOW ON MEMBRANE FREQUENCIES – EXACT

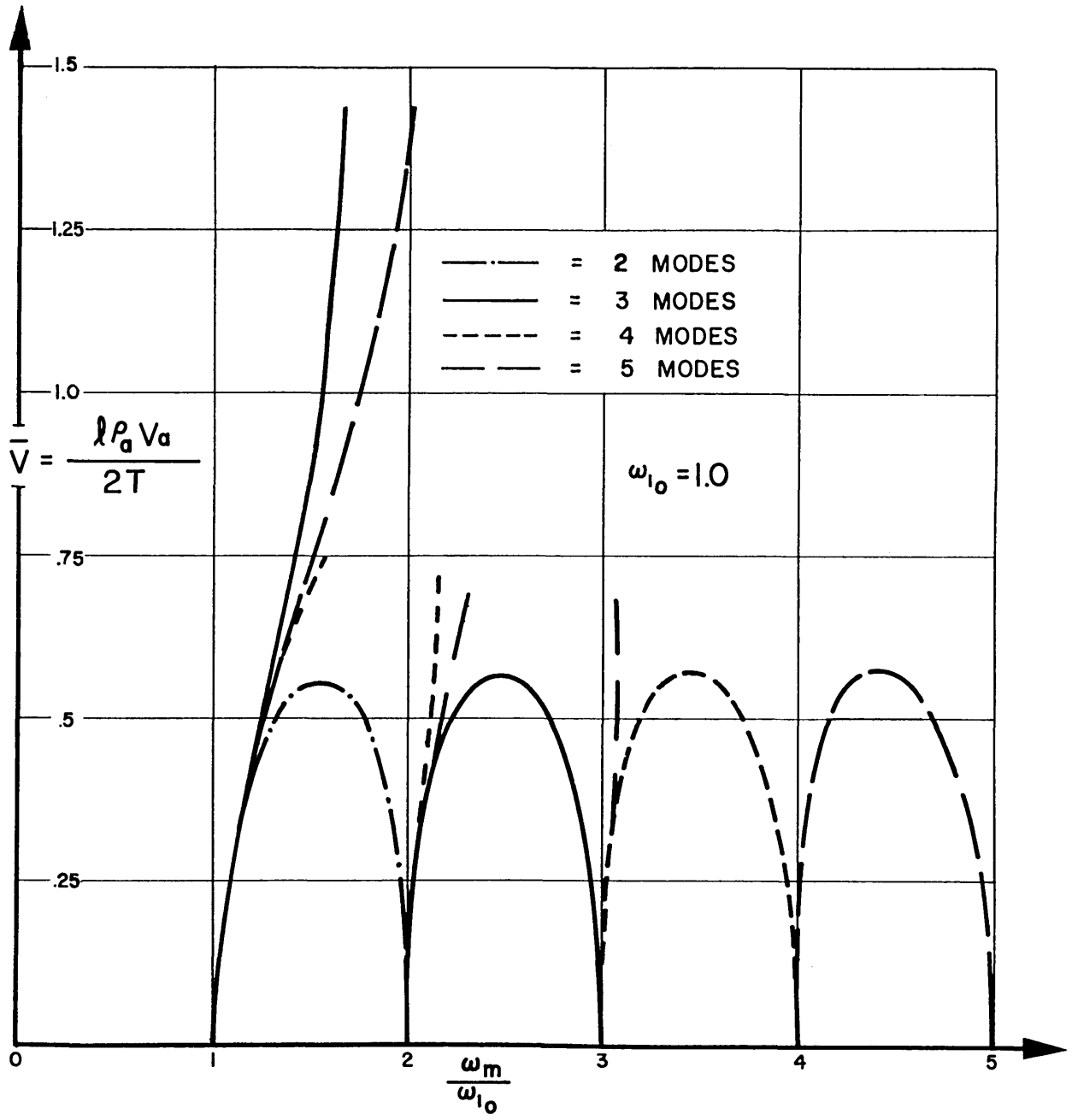

FIG. 5.3 EFFECT OF AIR FLOW ON MEMBRANE FREQUENCIES – GALERKIN METHOD

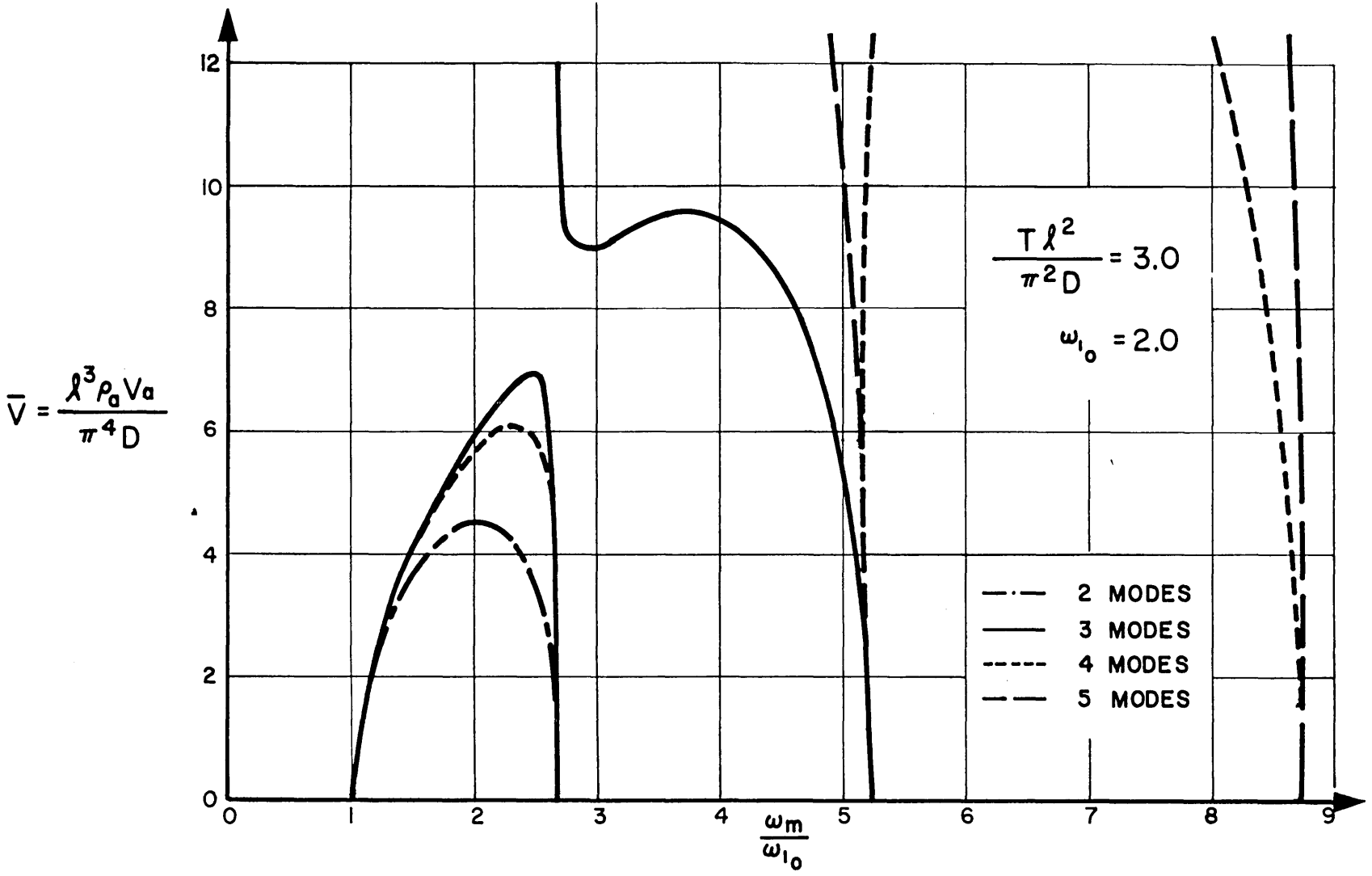

FIG. 5.4 EFFECT OF AIR FLOW ON FREQUENCIES OF PLATE IN TENSION

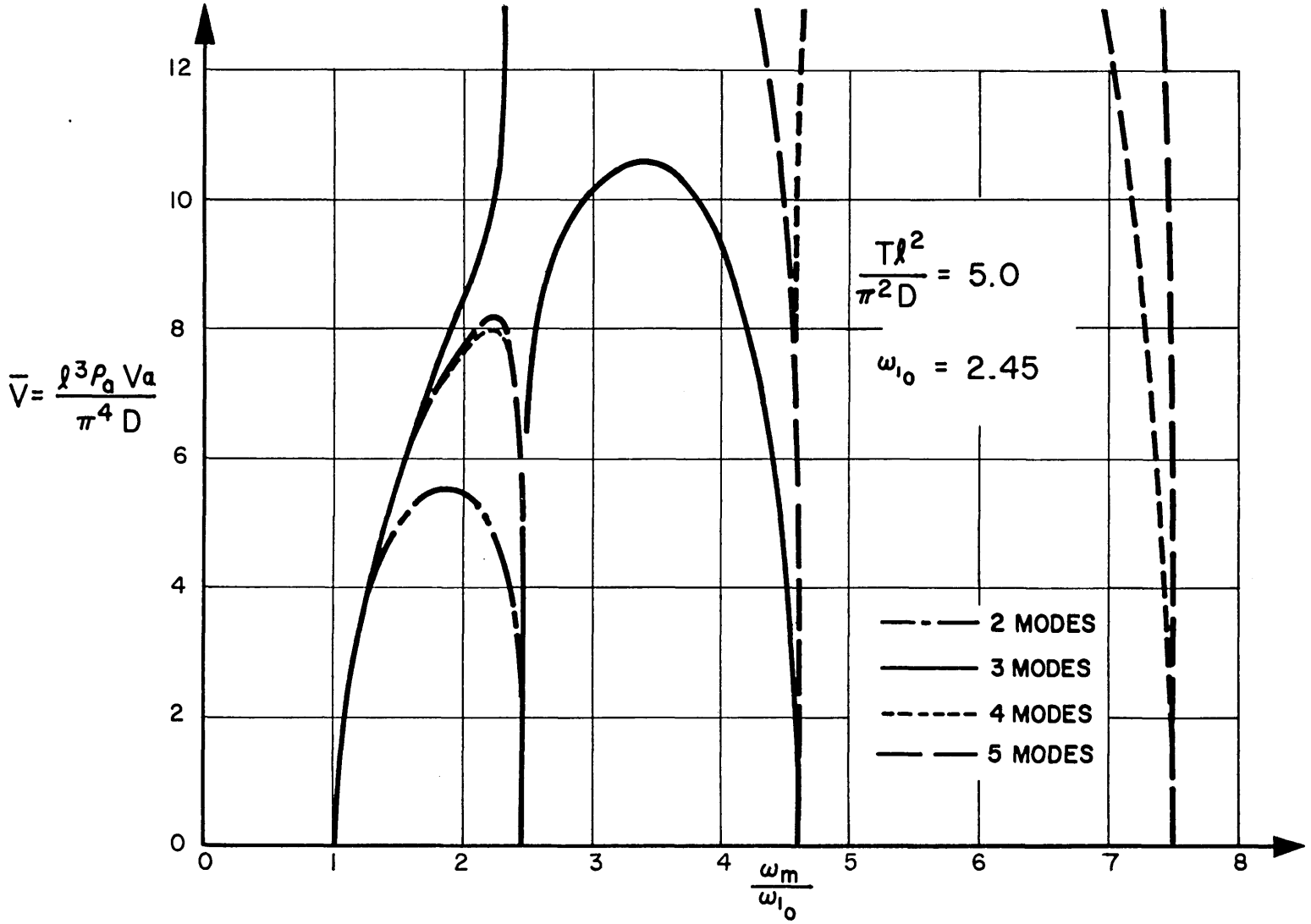

FIG. 5.5 EFFECT OF AIR FLOW ON FREQUENCIES OF PLATE IN TENSION

Hedgepeth [55]). Therefore, if the attention is restricted to the lowest modes only, an analysis which uses a not unreasonable number of modes will give a good approximation to the true flutter behavior.

Figs. 5.4 and 5.5 illustrate the comparison between Galerkin results for different number of modes for a plate in tension for two different values of the tensile force. It is seen that in one case the true flutter which involves the lowest two modes is well approximated by a three-mode analysis. In the other case, however, convergence is poorer, and a three-mode analysis shows the false coalescing of the 2nd and 3rd branches, similar to the pure membrane case. A four-mode analysis, however, gives already a good approximation to the exact result. Here again, the Galerkin method exhibits its characteristic of approximating well the low mode behavior while being in error for the higher modes. The question of just how many modes are required before convergence is obtained is directly related to the initial frequency distribution of the modes. The more separated the frequencies are - the smaller the number of required modes. Since usually the complete picture of the frequency vs. velocity behavior is not at hand, but rather the (true or apparent) flutter speeds and frequencies are obtained from the analysis, convergence must be shown by both speed and frequency before one is assured of the result.

In summary, the proper interpretation of Galerkin results is that for a sufficient number of assumed modes, fairly reliable information on the low-mode behavior is obtained while results for the higher modes are doubtful. A way of determining the degree of reliability is to compare results obtained by a successive increase in the number of modes employed.

These conclusions may be utilized for the case of the cylinder, for which obtaining an exact solution was shown to be impractical. Fig. 5.6 shows the distribution of the Ω_m 's,

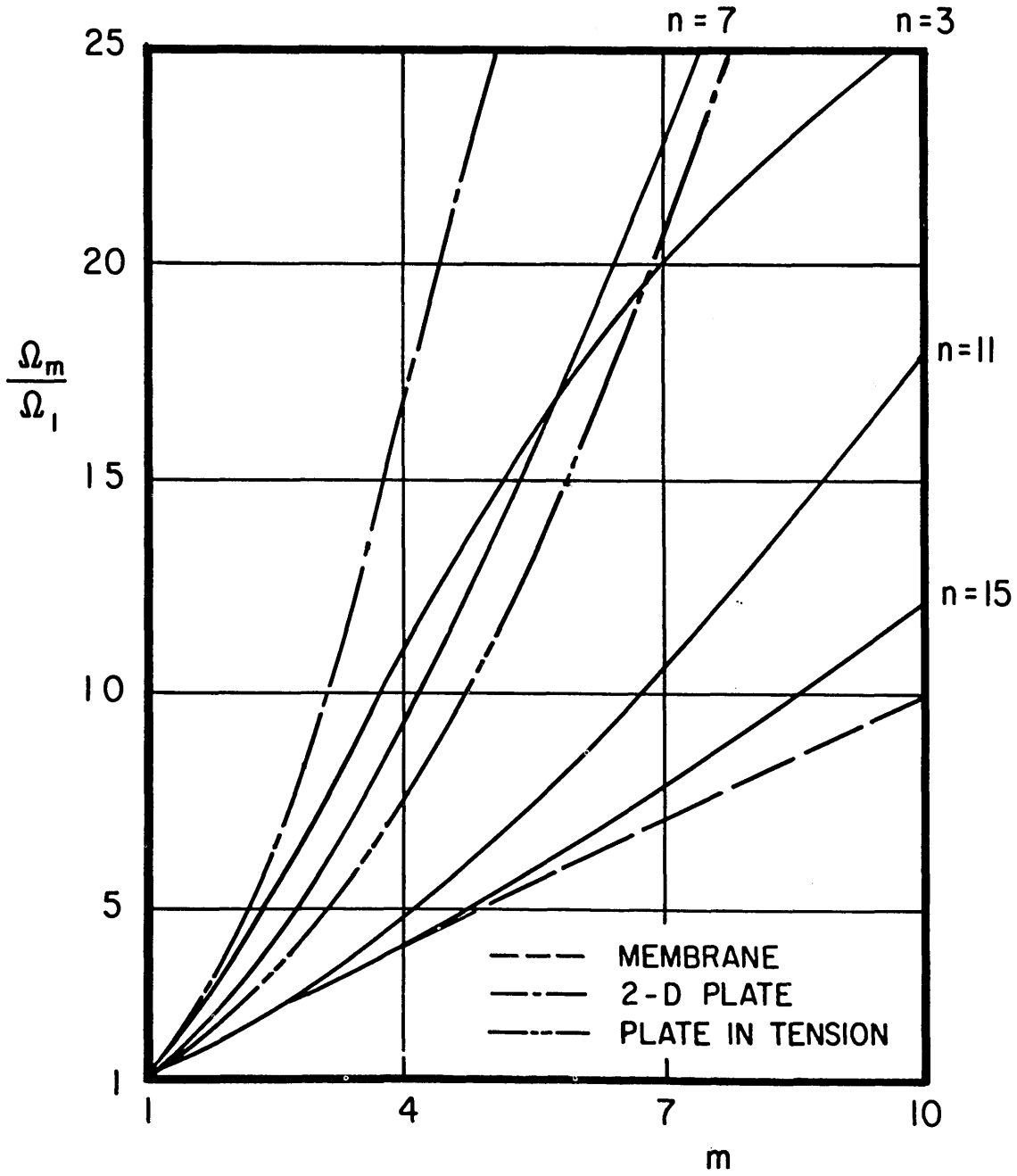

FIG. 5.6 VARIATION OF CYLINDER FREQUENCIES WITH MODE NUMBERS m AND n.

$$\frac{\ell}{R} = 6 \,, \quad \frac{h}{R} = \frac{1}{200}$$

which is seen to be bounded by the ordinal sequence, 1,2,3,4.. of membranes and the quadratic sequence 1,4,9,16...of two-dimensional plates, its shape being strongly dependent on the parameters $\frac{h}{R}$, ℓ/R and n. This characteristic of the cylinder's frequency sequence precludes us from predicting with certainty whether its flutter behavior will resemble that of a plate or that of a membrane, but it is fairly certain that for a given cylinder geometry this behavior will depend on n. Since the integer value of n is arbitrary, the variation of flutter speed with n must be investigated and the minimum V_{fl} so obtained will then be the true flutter speed of the cylinder.

An indication of the approximate value of n which will yield the minimum flutter speed is provided by the results of a two mode Galerkin solution. By writing Eq.(5-54) for m = 1,2, an explicit expression for the flutter speed is obtained as,

$$\bar{V}_{fl} = \frac{3}{16} (\Omega_2^2 - \Omega_1^2) \qquad (5\text{-}56)$$

We now seek the value of n which will minimize Eq.(5-56). By substituting Eq.(5-55a) into Eq.(5-56) and assuming that $n^2 \gg 4\lambda^2$ we obtain,

$$\frac{\partial \bar{V}_{fl}}{\partial n} = 0 = -\frac{60}{n^5} + \frac{12n}{\lambda^2} C_*^2 \qquad (5\text{-}57)$$

Solving for n, we obtain,

$$n^6 \Big|_{\bar{V}_{fl}=\min} = \frac{5\lambda^2}{C_*^2} \qquad (5\text{-}58)$$

For a cylinder of given geometry, the values of λ^2 and C_*^2 are fixed, and Eq.(5-58) gives the n for minimum flutter speed, based on a two-mode analysis. The existence of such

a value of n proves that the flutter speed does not decrease monotonically with n, as indicated in Ref. [38], but rather it reaches a minimum, following which it increases with n. This behavior, which is due to the second term on the right-hand-side of Eq.(5-57) is precisely the result of including the axial bending stiffness of the shell in the equation of motion.

The n for minimum frequency of the cylinder, to the same degree of approximation employed above, is given as,

$$n^6 \left| \bar{\omega}_o(1)_{=\min} \right. = \frac{\lambda^3}{C_*^{3/2}} \qquad (5\text{-}59)$$

By comparing Eqs.(5-58) and (5-59) it is found that in general they are not the same, indicating that unlike plate-membranes, for a cylinder flutter does not necessarily involve the modes of lowest natural frequency.

These conclusions are based on the two-mode result. Since such results are only approximate, the degree of approximation depending on the rate of convergence in each case, it is expected that the actual integer value of n for the flutter mode would be given to an accuracy of ± 1 by Eq.(5-58). This equation, therefore, serves the useful purpose of limiting the range of n for which the flutter calculations must be performed.

Since there is little advance indication of the convergence rate of the method for each case, solutions must be obtained using different numbers of modes. Comparison of the results for successively higher number of modes used will then reveal the true flutter behavior for each case.

5.5 Results and Conclusions

In order that the flutter behavior of cylinders will

be determined with a good degree of certainty, it was decided to utilize up to eight modes in the solution of each case. The complexity and the large volume of the calculations necessitated the use of the large-scale electronic digital computer, IBM model 704, available through the facilities of the M.I.T. Computation Center.

Since it was important to track down the behavior of each mode as a function of the velocity parameter, in order to determine the modes which coalesce at flutter, all the eigenvalues of the characteristic determinant had to be obtained for each $\bar{V}$. The best method of obtaining this result is a direct expansion of the determinant and factorization of the characteristic polynomial. By dividing Eq.(5-54) by $\bar{V}$, all the off-diagonal terms become constants, the dependence on $\bar{V}$, n, $\frac{h}{R}$ and $\frac{\ell}{R}$ is limited to the main-diagonal terms and the amount of calculations is thus reduced. Since computation time was at a premium, it was decided that rather then go through calculations for different values of the geometrical parameters $\frac{h}{R}$ and ℓ/R and limited values of n in the vicinity of the value given by Eq.(5-58), it would be wiser to fix the geometrical properties of the cylinder and to go through a wide range of n, so that the behavior of the flutter speed as a function of n may be illustrated.

The values chosen for the geometrical parameters were $\frac{h}{R} = \frac{1}{200}$ and $\frac{\ell}{R} = 6$. The steps involved in the calculations were as follows:

(1) Select n = 2

(2) Choose the number of modes M and calculate the Ω_m's.

(3) Assume $\bar{V}_o = \frac{3}{16}(\Omega_2^2 - \Omega_1^2)$ and calculate the main-diagonal terms of the determinant.

(4) Expand the determinant and factor the resulting polynomial to obtain the M eigenvalues Ω^2.

(5) Calculate $\Delta\bar{\Omega}^2$, the smallest difference between successive eigenvalues.

(6) Calculate the next value for $\bar{V}$ by using the formula,

$$\bar{V}_1 = \bar{V}_o[1 + \frac{1}{2}(\frac{\Delta\bar{\Omega}^2}{\Omega_2^2 - \Omega_1^2})^2] \qquad (5\text{-}60)$$

and repeat steps 4 and 5.

(7) Repeat step 6 until the difference between successive $\bar{V}$ for which all the eigenvalues are real, is less than 1 $^o/_o$.

(8) If for any $\bar{V}$ some eigenvalues are complex, choose another $\bar{V}$ half-way between it and the previous $\bar{V}$ and repeat until all the eigenvalues are real again. Repeat step 7.

(9) Increase M and repeat steps 3-8. Repeat until M = 8.

(10) Increase n by 1 and repeat steps 2-9. Repeat until n = 14.

The results of these calculations are shown in Table 5.2 in which are tabulated for each n and for each M (number of modes used) the flutter speed and frequency, i.e. the value of $\bar{V}$ at which two real branches coalesce and the corresponding value of $\bar{\Omega}^2$.

It is seen from the results that for $3 \leq n \leq 9$ convergence is reached in both speed and frequency for M = 6, the results for six and eight modes being practically identical. For these values of n a 4 mode solution yields results which are accurate to within 5 $^o/_o$. For n = 10, the difference between the six and eight mode results is less than 4 $^o/_o$, but for n = 11, 12 convergence, though definitely existing, is poorer, and M must be increased beyond 8 in order to determine the exact $\bar{V}$ and $\bar{\Omega}^2$ in these cases. In all cases coalescence occured between the lowest two branches. Fig. 5.7 shows the

TABLE 5.2

FLUTTER SPEEDS AND FREQUENCIES FOR CYLINDRICAL SHELL

$\frac{h}{R} = \frac{1}{200}$ $\quad \frac{\ell}{R} = 6$

n	M	$\bar{V}$ ($\times 10^{-3}$)	$\bar{\Omega}^2$ ($\times 10^{-2}$)	n	M	$\bar{V}$ ($\times 10^{-3}$)	$\bar{\Omega}^2$ ($\times 10^{-2}$)
3	4	36.8	11.8	8	4	1.77	.653
	6	37.6	12.2		6	1.83	.673
	8	38.0	12.3		8	1.83	.675
4	4	12.7	4.01	9	4	1.76	.685
	6	13.1	4.13		6	1.87	.732
	8	13.1	4.14		8	1.88	.738
5	4	5.61	1.78	10	4	1.90	.774
	6	5.68	1.81		6	2.15	.892
	8	5.69	1.81		8	2.22	.925
6	4	3.10	1.01	11	4	2.10	.880
	6	3.14	1.03		6	2.53	1.10
	8	3.15	1.04		8	2.70	1.18
7	4	2.11	.729	12	4	2.07	.937
	6	2.14	.745		6	2.94	1.30
	8	2.14	.750		8	3.26	1.42

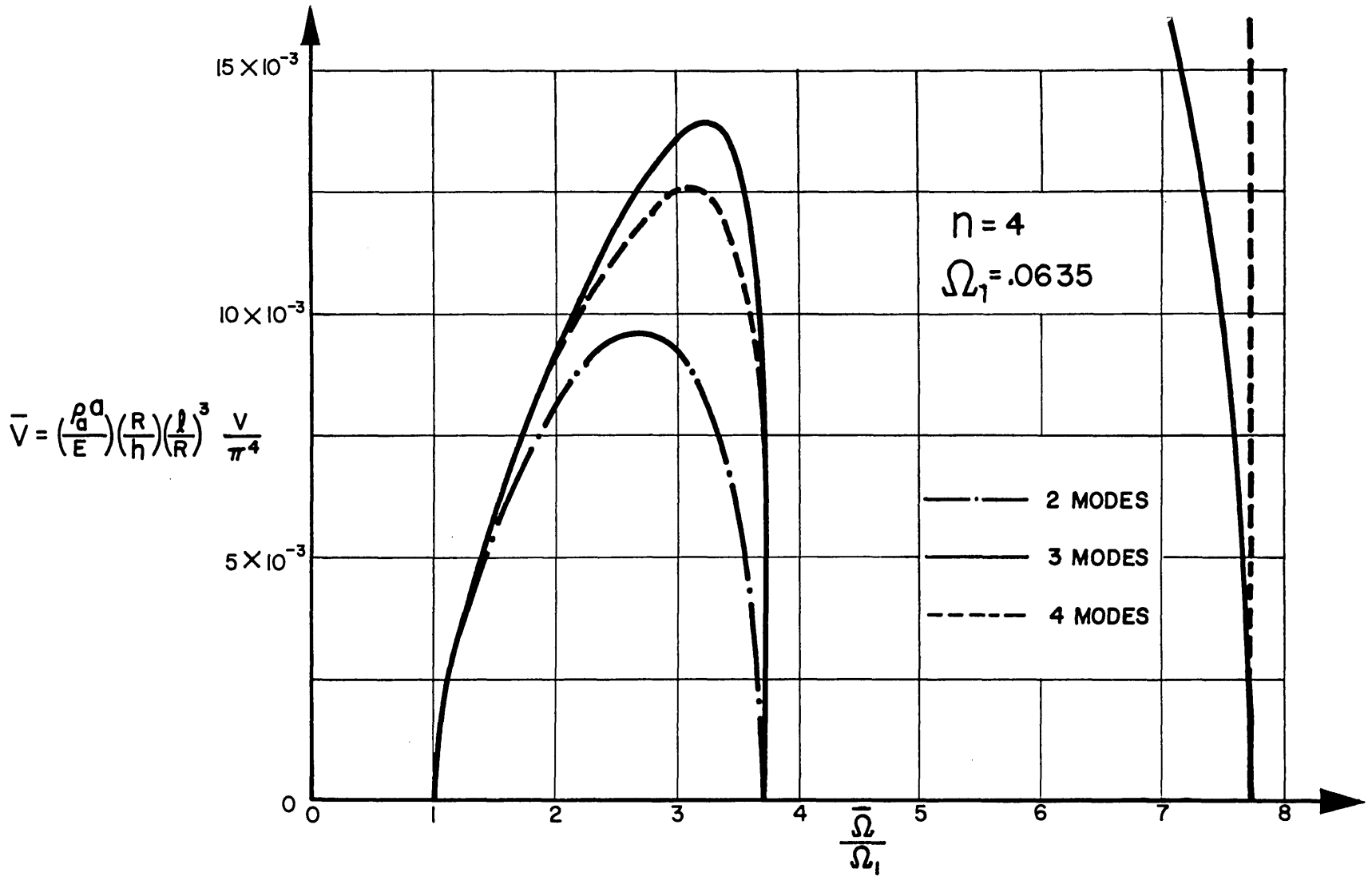

FIG. 5.7 EFFECT OF AIRFLOW ON FREQUENCIES OF CYLINDER $\frac{\ell}{R} = 6$ $\frac{h}{R} = \frac{1}{200}$

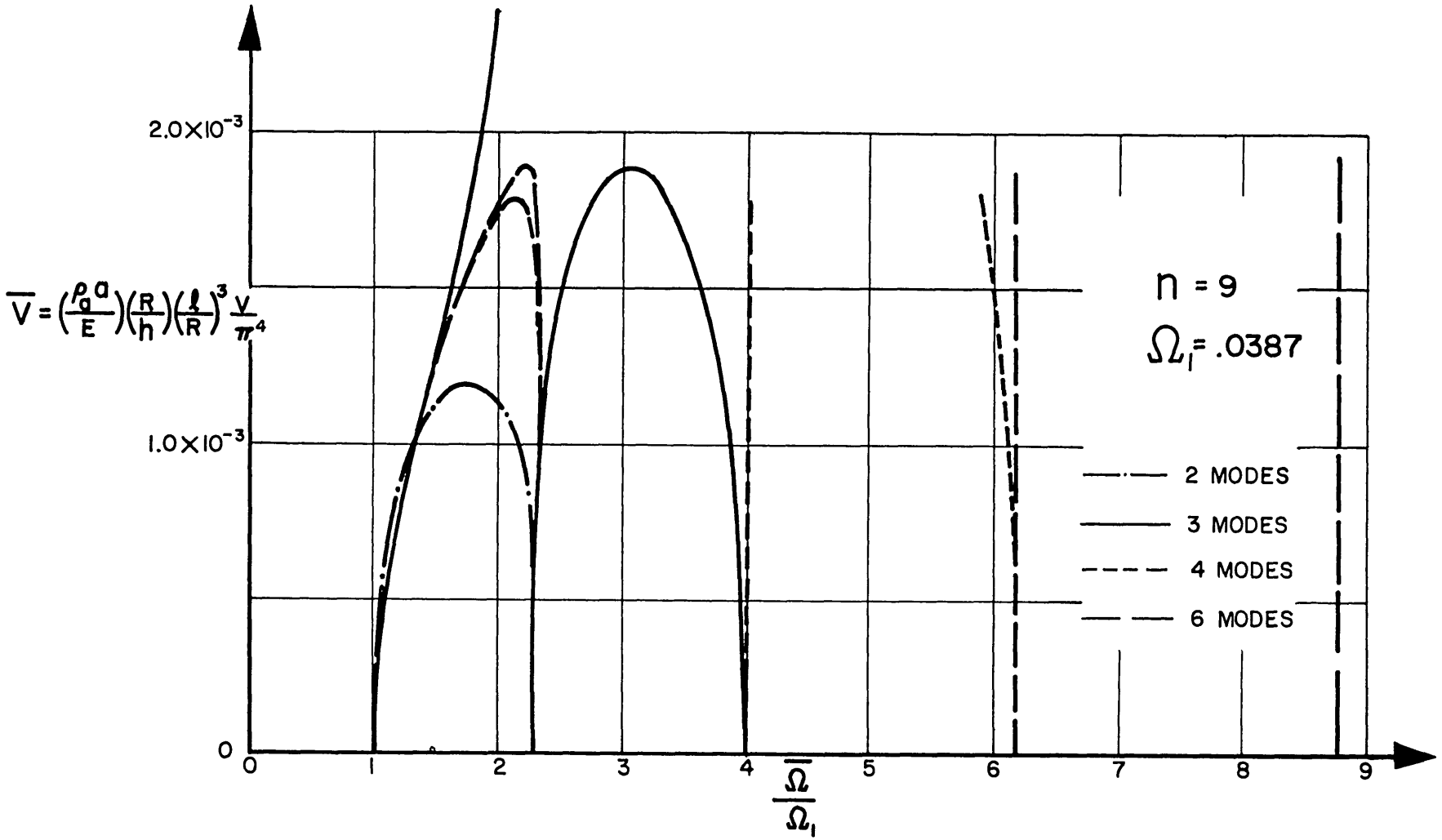

FIG. 5.8 EFFECT OF AIRFLOW ON FREQUENCIES OF CYLINDER $\frac{\ell}{R} = 6$ $\frac{h}{R} = \frac{1}{200}$

variation of frequencies with $\bar{V}$ for n = 4. A behavior very similar to that of Fig. 5.4 is seen. Fig. 5.8 shows the variation of frequencies with V for n = 9. In this case the behavior is similar to that of Fig. 5.5. Calculations were also made for n = 2, 13 and 14. For these cases initial coalescence always involved the highest two branches, similar to the membrane behavior shown in Fig. 5.3. This is due to the fact that for these cases the natural frequency distribution is very close to that of a membrane. Since the computer program was designed to stop at $\bar{V}$ for which the initial complex eigenvalues appeared, the true flutter speed for these cases, as indicated by the coalescence of the lowest two modes, was not obtained. However, $\bar{V}$ for n = 2 is certain to be higher than for n = 3 and $\bar{V}$ for n = 13 and 14 is certain to be higher than for n = 12.

The results of the calculations, as shown by Table 5.2, prove conclusively that the flutter speed reaches a minimum, which in this case occurs at n = 8. It is seen that the order of magnitude of the minimum flutter speed is considerably smaller than the $\bar{V}_{f1}$ for the low n's. As n increases more and more beyond n_{f1}, the frequency distribution becomes closer to that of a membrane and therefore the flutter speeds tend to infinity in the limit.

Application of Eq.(5-58) would indicate flutter to occur for n = 9. It is seen from Table 5.2 that the difference in $\bar{V}_{f1}$ between n = 8 and n = 9 is indeed quite small. This shows the usefulness of Eq.(5-58) in providing a good estimate of n_{f1}. For this case the lowest natural frequency as calculated by Eq.(5-59) occurs for n = 4, and the lowest Ω_1 occurs for n = 7. The flutter speeds for n = 4 and 7 are seen to be higher than the minimum $\bar{V}_{f1}$. It is therefore seen that the flutter mode does not involve the modes with lowest $\bar{\omega}_o$ or Ω. However, it is seen that although for n = 8, Ω_1, and Ω_2 are higher than those for n = 4 or 7 the flutter frequency

for n = 8 is the minimum of all n's. Thus the flutter mode is formed by the coalescence of two aeroelastic modes having the lowest frequency at $\bar{V}_{f1}$. Both flutter speed and frequency, therefore, reach a minimum for the same value of n.

The calculations were conducted for those values of n for which Donnell's equation is valid. For n = 0,1, however, this equation is not valid and use must be made of a set of simultaneous equations involving the tangential displacement components. In some cases, as was shown in Appendix 4A, they may be reduced to a single equation. Although no explicit expressions exist for the natural frequencies in these cases, an assumed mode approach may be utilized in the solution of these cases as well. It remains to be seen how the flutter speeds associated with these modes compare with those obtained here.

On the basis of the development and the results of this chapter, the following conclusions may be drawn concerning cylindrical shell flutter:

(1) The phenomenon of cylindrical shell flutter is similar to the panel flutter phenomenon.

(2) In contrast with the panel flutter case, and due to the particular frequency distribution of cylindrical shells, the flutter speed varies with n, the mode number in the transverse direction to the flow, in such a way that a minimum exists for a particular value of n.

(3) 'Medium Shell' theory, due to its neglect of axial bending stiffness, fails to predict the minimum flutter speed of the shell.

(4) For the case analyzed numerically, a 4 mode Galerkin analysis yields results accurate to within 5 $^{o}/_{o}$. In general, the convergence of the results depends on the initial frequency distribution of the shell.

(5) The value of n_{fl} is not identical with n for lowest natural frequency, but is closely related to the proximity of its lowest modes. A criterion developed on the basis of a two-mode analysis yields a good estimate of n_{fl}. The value of n_{fl} decreases for thicker and longer shells of given radius.

(6) Both flutter speed and frequency are at their minimum for n_{fl}.

(7) The Galerkin method of analysis of cylindrical shell flutter was shown to yield reliable results. It is now possible to perform the extensive calculations needed to reveal the dependence of the flutter speed on the geometrical parameters of the shell.

CHAPTER 6

CONICAL SHELL FLUTTER

6.1 Introduction

The study of the conical shell free vibration problem presented in Chapter 3 and the study of the cylindrical shell flutter problem presented in Chapter 5 have both indicated that the only feasible way to tackle the flutter problem of the conical shell is by approximate means. The question, then, is which approximate method is best suited for this purpose?

From the results of the free vibration study the conclusion was drawn that formulation of the problem in terms of the three displacement components and use of the Rayleigh-Ritz energy approach yielded the best results for that case. On the other hand, the study of the cylindrical shell flutter problem has indicated that use of Galerkin's method in conjunction with a single eighth-order differential equation proved to be the most convenient method for that problem. This study has shown that the flutter mode results from coupling of two longitudinal modes, and that due to the frequency distribution of the shell, a number of longitudinal "in vacua" assumed modes must be used before convergence is reached.

This behavior of the shell is most probably true of tapered cylinders as well. The difference in this case is that an assumed mode approach is required even to obtain the "in vacua" modes. It is immediately seen, then, that the total

number of assumed modes needed for convergence in this case will be greater than in the cylindrical case.

This consideration rules out the method which utilizes the three displacement functions, since its application would result in a prohibitively large order for the characteristic determinant. Since flutter involves modes with relatively high n, the neglect of tangential inertia inherent in the single-equation formulation is probably of little importance.

The use of aerodynamic piston theory in the case of the cylindrical shell was found to be quite satisfactory. Since the shells of interest in this problem have a small semi-vertex angle, use of this simple theory is justified in this case, at least as a first approximation.

6.2 Flutter Equations

As shown in Chapter 3, the single eighth-order equation in the displacement w is obtained by eliminating the stress function F from the equilibrium and compatibility equations written in terms of w and F.

When the aerodynamic term, neglecting damping, is included, Eqs.(3-16) become,

$$\nabla^4 F - Eh \frac{\cot\alpha}{r} w_{rr} = 0 \qquad (6\text{-}1a)$$

$$D\nabla^4 w + \frac{\cot\alpha}{r} F_{rr} + \rho h\ddot{w} + \rho_a a V w_r = 0 \qquad (6\text{-}1b)$$

Using the identity of Eq.(3-17) we eliminate F in Eqs.(6-1) and obtain,

$$r^2\nabla^4[r^3(D\nabla^4 w + \rho h\ddot{w} + \rho_a aVw_r)] + Eh\cot^2\alpha[r^3 w_{rr}]_{rr} = 0 \quad (6\text{-}2)$$

Using the transformation given by Eq.(3-19) and the expression for w given by Eq.(3-22a), Eq.(6-2) becomes,

$$(1-\delta)^2\cos^2\alpha e^{-\beta}[\bar{w}'^{v} - \bar{w}''] + e^{-2\beta}\bar{\nabla}^4[\sin^4\alpha C_*^2 e^{-\beta}\bar{\nabla}^4\bar{w}$$

$$-(1-\delta)^4\bar{\omega}^2 e^{3\beta}\bar{w} + (1-\delta)^3\sin\alpha\tilde{V}e^{2\beta}\bar{w}'] = 0 \quad (6\text{-}3)$$

where,

$$\bar{\nabla}^4\bar{w} = \bar{w}'^{v} - 4\bar{w}''' + (4-2\bar{n}^2)\bar{w}'' + 4\bar{n}^2\bar{w}' + (\bar{n}^4 - 4\bar{n}^2)\bar{w} \quad (6\text{-}4a)$$

$$\bar{w}' = \frac{d\bar{w}}{d\beta} \quad (6\text{-}4b)$$

$$\tilde{V} = \frac{\rho_a aVR_o}{Eh} \quad (6\text{-}4c)$$

and where C_*^2 and $\bar{\omega}^2$ are defined by Eqs.(3-10).

Inspection of Eq.(6-3) reveals that each one of the four terms: bending, membrane, inertia, and aerodynamic, is multiplied by a different power of e^{β}. This is the same situation, of course, which existed in the free vibration problem, except for the presence of the aerodynamic term in this case. Since we are interested in modes with high n, i.e. those modes where the bending effect predominates, the results of Chapter 3 indicate that a proper choice for assumed modes in this case is,

$$\bar{w}(\beta) = e^{\beta} \sum_m \bar{w}_m \sin\frac{m\pi}{\beta_1}\beta \quad (6\text{-}5)$$

These modes satisfy two geometrical boundary conditions only, namely, the vanishing of w at the ends ($\beta = 0, \beta_1$). This means that the accuracy of this method is somewhat inferior to the one using all three displacement components. However, if δ is small, this drawback is outweighed by the advantage of this method with regard to the order of the characteristic determinant.

Using Galerkin's method, we substitute Eq.(6-5) into Eq.(6-3), then multiply by $e^{\beta}\sin\frac{m\pi}{\beta_1}\beta$ and integrate along the shell to obtain,

$$\left\| C_*^2[n^2+m^2\bar{\lambda}^2][n^2+\bar{\lambda}^2(m^2-4\Delta)] + \frac{\cos^2\alpha}{f(\delta)} \frac{m^4\bar{\lambda}^4}{(n^2+m^2\bar{\lambda}^2)^2} \frac{m^2-\Delta}{m^2+\Delta} \right.$$

$$\left. -\bar{\omega}^2 \frac{1+\delta^2}{f(\delta)} \frac{m^2}{m^2+4\Delta} - \tilde{V} \frac{\bar{\lambda}}{\pi} \delta\left(1+\frac{\delta^2}{3}\right) \frac{n^2-15m^2\bar{\lambda}^2}{n^2+m^2\bar{\lambda}^2} \frac{m^2}{m^2+2.25\Delta} \right\| \bar{w}_m$$

$$+ \frac{\bar{\lambda}^4\cos^2\alpha}{(n^2+m^2\bar{\lambda}^2)^2} \sum_{\bar{m}} \frac{[2\bar{m}^2m^2-\Delta(\bar{m}^2+m^2)]8m\bar{m}\bar{w}_{\bar{m}}}{(\bar{m}^2-m^2)^2+8\Delta(\bar{m}^2+m^2)+16\Delta^2} \begin{cases} \frac{\Delta}{f(\delta)}; & \text{even}^* \\ -\frac{\Delta^{\frac{1}{2}}}{\pi}(1+\delta^2); & \text{odd} \end{cases}$$

$$- \sum_{\bar{m}} \frac{n^2+\bar{m}^2\bar{\lambda}^2}{n^2+m^2\bar{\lambda}^2} \frac{32\bar{\omega}^2m\bar{m}\bar{w}_{\bar{m}}}{(\bar{m}^2-m^2)^2+32\Delta(\bar{m}^2+m^2)+256\Delta^2} \begin{cases} \frac{2\Delta}{f(\delta)}(1+\delta^2) ; & \text{even} \\ -\frac{\Delta^{\frac{1}{2}}}{\pi}(1+6\delta^2+\delta^4); & \text{odd} \end{cases} \tag{6-6}$$

$$+ \sum_{\bar{m}} \left\| \frac{(\bar{m}^2-m^2-3\Delta) + 24\Delta\bar{\lambda}^2\frac{\bar{m}^2+m^2}{n^2+\bar{m}^2\bar{\lambda}^2}}{(\bar{m}^2-m^2)^2 + 18\Delta(\bar{m}^2+m^2) + 81\Delta^2} \right\|$$

$$\left\| \left(\frac{n^2+\bar{m}^2\bar{\lambda}^2}{n^2+m^2\bar{\lambda}^2}\right)^2 4\bar{\lambda}\tilde{V}m\bar{m}\bar{w}_{\bar{m}} \right\| \begin{cases} \delta(3+\delta^2); & \text{even} \\ -(1+3\delta^2); & \text{odd} \end{cases} = 0; m=1,2,..$$

---

* See footnote on page 52.

In obtaining this set of equations, certain terms which are negligible for $n > 4$ and $\delta < .4$ have been dropped. It can be easily verified that as $\alpha \rightarrow 0$, the set of equations (6-6) reduces to the set (5-52) derived for the cylinder.

It is noted that due to the fact that the assumed modes used in this case are not the true "in vacua" modes, the determinant contains inertia, as well as aerodynamic, coupling terms. This fact makes this problem somewhat different from the cylinder problem in which the off-diagonal elements were aerodynamic terms only. The computational aspect of the present problem is thus further complicated, in addition to the increased difficulty due to the larger number of modes used in this case.

In the panel flutter problem we are looking for the condition where two successive longitudinal modes coalesce for a given n. For $n > 4$, the major part of the stiffness comes from circumferential bending. Therefore, in order to be able to detect the flutter condition accurately, it is necessary to extract from the stiffness the part which does not vary with m, similar to the step taken in the case of the cylinder when we changed from Eqs.(5-52) to (5-54). This step requires the approximation $\frac{m^2}{m^2 + 4\Delta} \simeq 1$, which gets better as m increases. Defining, for this case,

$$\bar{V} = \frac{\tilde{V}}{\bar{\lambda}^3 \pi} = \frac{1}{\pi^4} \left(\frac{\rho a}{E}\right)\left(\frac{R_o}{h}\right)\left(\frac{\ell}{R_o}\right)^3 [f(\delta)]^3 V \qquad (6\text{-}7a)$$

$$\bar{\Omega}^2 = \frac{1}{\bar{\lambda}^4} \left[\bar{\omega}^2 - C_*^2 n^4 \frac{f(\delta)}{1+\delta^2}\right] \qquad (6\text{-}7b)$$

Eqs.(6-6) can be written in matrix form,

$$[D^{(1)}] + \bar{V}[D^{(2)}] - \bar{\Omega}^2[D^{(3)}] = 0 \qquad (6\text{-}8)$$

where the elements of the matrices are given by,

$$d_{mm}^{(1)} = 2C_*^2\frac{2n^2}{\bar{\lambda}^2}(m^2-2\Delta) + C_*^2m^2(m^2-4\Delta) + \frac{\cos^2\alpha}{f(\delta)}\frac{m^4}{(n^2+m^2\bar{\lambda}^{-2})^2}\frac{m^2-\Delta}{m^2+\Delta} \quad (6\text{-}9a)$$

$$d_{mm}^{(\underline{1})} = \frac{8m\bar{m}\cos^2\alpha}{(n^2+m^2\bar{\lambda}^{-2})^2}\frac{2m^2\bar{m}^2 - \Delta(\bar{m}^2+m^2)}{(\bar{m}^2-m^2)^2+8\Delta(\bar{m}^2+m^2)+16\Delta^2}\begin{cases}\frac{\Delta}{f(\delta)}\ ; & \text{even}\\ -\frac{\Delta^{\frac{1}{2}}}{\pi}(1+\delta^2)\ ; & \text{odd}\end{cases}$$

$$-\frac{n^2+\bar{m}^2\bar{\lambda}^{-2}2C_*^2n^4f(\delta)}{n^2+m^2\bar{\lambda}^{-2}(1+\delta^2)\bar{\lambda}^4}\frac{32m\bar{m}}{(\bar{m}^2-m^2)^2+32\Delta(\bar{m}^2+m^2)+256\Delta^2}\begin{cases}\frac{2\Delta}{f(\delta)}(1+\delta^2); & \text{even}\\ -\frac{\Delta^{\frac{1}{2}}}{\pi}(1+6\delta^2+\delta^4)\ ;\text{odd}\end{cases} \quad (6\text{-}9b)$$

$$d_{mm}^{(2)} = -\delta\left(1+\frac{\delta^2}{3}\right)\frac{n^2-15m^2\bar{\lambda}^{-2}}{n^2+m^2\bar{\lambda}^{-2}}\frac{m^2}{m^2+2.25\Delta} \quad (6\text{-}9c)$$

$$d_{mm}^{(\underline{2})} = 4m\bar{m}\left[\frac{n^2+m^2\bar{\lambda}^{-2}}{n^2+m^2\bar{\lambda}^{-2}}\right]^2\frac{\bar{m}^2-m^2-3\Delta+24\Delta\bar{\lambda}^{-2}\frac{m^2+\bar{m}^2}{n^2+\bar{m}^2\bar{\lambda}^{-2}}}{(\bar{m}^2-m^2)^2+18\Delta(\bar{m}^2+m^2)+81\Delta^2}\begin{cases}\delta(3+\delta^2)\ ;\text{even}\\ -(1+3\delta^2)\ ;\text{odd}\end{cases} \quad (6\text{-}9d)$$

$$d_{mm}^{(3)} = \frac{1+\delta^2}{f(\delta)} \quad (6\text{-}9e)$$

$$d_{mm}^{(\underline{3})} = \frac{n^2+\bar{m}^2\bar{\lambda}^2}{n^2+m^2\bar{\lambda}^{-2}}\frac{32m\bar{m}}{(\bar{m}^2-m^2)^2+32\Delta(\bar{m}^2+m^2)+256\Delta^2}\begin{cases}\frac{2\Delta}{f(\delta)}(1+\delta^2); & \text{even}\\ -\frac{\Delta^{\frac{1}{2}}}{\pi}(1+6\delta^2+\delta^4)\ ;\text{odd}\end{cases} \quad (6\text{-}9f)$$

The solution of the problem requires the determination of the value of $\bar{V}_{fl}$ which will cause coalescence between the lowest eigenvalues $\bar{\Omega}^2$ of the determinant,

$$\left|\ [D^{(1)}] + \bar{V}[D^{(2)}] - \bar{\Omega}^2[D^{(3)}]\ \right| = 0 \quad (6\text{-}10)$$

Due to the fact the most iteration methods fail when the two lowest eigenvalues are equal or nearly equal, the most suitable numerical method in this case is the direct expansion of the determinant and factorization of the result-

ing characteristic polynomial in $\bar{\Omega}^2$. These steps are similar to those taken in the case of the cylinder. In this case, however, the numerical calculation procedure is more involved than in the case of the cylinder, due to the fact that $[D^{(3)}]$ is not a unit matrix, i.e. inertia coupling exists. This situation is similar to the one encountered in Section 3.7, in connection with the calculation of the frequencies of free vibration of the conical shell.

The flutter behavior of conical shells is expected to be similar to that of cylinders, inasmuch as a similar physical process takes place, i.e. a coalescence of modes at the flutter speed. This means that for the conical shell, as for the cylindrical shell, the minimum flutter speed will be associated with a particular value of n, all other values of n resulting in higher flutter speeds. Due to the fact that in this case no explicit expressions are available for the natural frequencies, one is unable to obtain an estimate of n_{fl}, based on a two-mode analysis, as was the case for the cylinder.

The results of the free vibration study of Chapter 3 have indicated that the bending effect of taper, which becomes more important with increasing values of n, tends to lower the fundamental frequency for each n, the higher frequencies being less affected. On the other hand, the membrane effect of taper is to increase the fundamental frequency, this effect being most pronounced for the lower n's. These effects would tend to raise the flutter speed for the higher n's by increasing the difference between Ω_1^2 and Ω_2^2, and to lower the flutter speeds for the lower n's, by reducing this difference. The net effect would then be to lower n_{fl} and to increase $\bar{V}_{fl}$. No quantitative estimate, however, can be made of these effects and numerical results must be relied upon.

6.3 Results and Conclusions

The numerical calculation procedure employed in this

case essentially follows the one used in Chapter 5, as far as the methods employed to obtain the flutter speed and frequency from the characteristic equation are concerned. However, due to the existence of inertia coupling in this case, some preliminary matrix inversion and multiplication is required in order to obtain the final characteristic determinant. Since these operations must be performed for each value of $\bar{V}$ and since the order of the matrices is fairly high, it may be seen immediately that the computation times in this case are going to be much greater than those in the case of the cylinder. This fact coupled with the fact that computation time on the IBM 704 computer was at a premium, has influenced the decision regarding the range of n and the number of modes used.

In view of the time limitation, it was felt that primary consideration should be given to obtaining data which would reveal the major trend in the flutter characteristics of the shell, and that accuracy would be of secondary importance. It was therefore decided to perform the calculations using four expansion modes only, rather than to investigate the convergence of the results by using a different number of modes. The results of the previous chapter have indicated that a four mode analysis gave a $5^{o}/o$ accuracy. In view of the fact that the assumed modes in this case are not the true natural vibration modes, it is estimated that the accuracy of such an analysis in this case is not better than $15 - 20^{o}/o$. This, however, is probably sufficient to achieve the primary objective of the calculations, namely, to reveal the major trend of the results. Regarding n, it was decided to carry the calculations to the point where a minimum flutter speed is indicated, rather than to canvass the entire range of n covered in the previous case. In addition, in order to enable one to determine the effect of taper on the flutter of the shell, the same values for the geometrical parameters that were used in the study of the cylinder were used in this case, a single

value for the semi-vertex angle being taken.

Calculations, then, were performed using the following values for the parameters: $\frac{h}{R_o} = \frac{1}{200}$, $\frac{\ell}{R_o} = 6$, $\alpha = 5^o$. The results of the calculations are shown in Table 6.1.

TABLE 6.1

FLUTTER SPEEDS AND FREQUENCIES FOR CONICAL SHELL USING A FOUR MODE ANALYSIS

$$\frac{h}{R_o} = \frac{1}{200} \quad \frac{\ell}{R_o} = 6 \quad \alpha = 5^o$$

n	$\bar{V}$ $(x10^{-3})$	$\bar{\Omega}^2$ $(x10^{-2})$
3	44.2	12.8
4	15.2	4.29
5	8.38	2.33
6	8.15	2.15
7	8.68	1.58

The results show that similar to the case of the cylinder, a minimum exists in the flutter speed. In this case, the minimum occurs for n = 6. Due to the inaccuracy inherent in the results, this value of n_{fl} should not be taken as final, since the results for the neighboring n's differ by less than the assumed margin of confidence. The same argument applies to the values of the flutter speed and especially the frequency. However, it is believed that the results of

Table 6.1 serve their main purpose of revealing the trend of the flutter behavior of the conical shell. Comparison with the results for the cylinder can probably be made on a qualitative basis only. Although the results show that the flutter speeds for the cone are much higher than those for the cylinder, the actual difference is probably not as large as the results seem to indicate. The reason is that the natural frequency distribution of the conical shell, which is the major factor affecting the flutter speed, which will be given much more accurately by an analysis using a higher number of modes is not very different from that of the cylinder, for the given value of α. Therefore it seems reasonable to expect that more accurate analyses, i.e. analyses using a larger number of modes, will tend to cause coalescence to occur at a value of $\bar{V}$ closer to that of the cylinder than the result of a four-mode analysis.

Comparison of the results shows that the value of n_{fl} for the cone is 6, whereas that for the cylinder is 8. Though the actual value of n_{fl} for this case is questionable, as stated earlier, it seems safe to conclude that the effect of taper is to reduce the value of n_{fl}. Thus the qualitative prediction of the effect of taper is borne out by the results for both $\bar{V}_{fl}$ and n_{fl}.

On the basis of the results the following general conclusions may be drawn concerning the flutter behavior of conical shells:

(1) The flutter phenomenon of conical shells is basically the same as that of cylindrical shells.

(2) The computational labor for this case, due to the ignorance of the true natural frequencies and mode shapes, is more involved than in the case of the cylinder.

(3) The primary effect of taper is most probably to raise the flutter speed and to lower the value of n at flutter.

(4) The method developed for the flutter analysis of conical shells seems to work satisfactorily. Better accuracy in the results can be obtained by using the same method with a larger number of assumed modes. This can be easily done provided adequate computational facilities and time are available.

CHAPTER 7

THERMAL EFFECTS ON PLATE VIBRATIONS BEFORE AND AFTER BUCKLING

7.1 Introduction

The analyses presented so far in this work were limited to problems free of any additional effects. The reasons for this are quite clear. These phenomena must first be understood under free conditions before any heating, acceleration or other linear or nonlinear effects are included. Analogously, the study of these additional effects should begin with simple configurations in order to gain a basic understanding of the way in which they affect the problem, before it is extended to the more complicated cases. This is especially true in the case of nonlinear effects, since the necessary approximations can best be evaluated when applied to simple problems first.

With the increasing flight speeds of air vehicles and the resulting thermal environment, the effects of thermal stresses on the dynamic characteristics of the structural components have become important. The changes in frequencies and mode shapes that take place due to the thermal stresses affect considerably the various static and dynamic aeroelastic instabilities. These changes, for the case of a flat plate, are the subject of this chapter.

The problem to be treated is the following: A thermally thin, rectangular flat plate supported at its four edges is

subjected to a uniform temperature rise. If the side supports remain at low temperature, a compressive stress is induced in the plate which, for some value of the temperature increment, will cause a finite-deflection buckling pattern to form, which introduces an element of nonlinearity into the problem. The purpose of this study is to investigate the vibration characteristics of the plate in its pre- and post-buckling states as functions of the temperature increment.

Previous work on this problem was done by Bisplinghoff and Pian [56] and by Gale [57]. In the former, the plate was considered as completely simply supported and free to displace laterally (in the y-direction, cf. Fig. 7.1). Agreement between theory and experiment was good, any deviations being due mainly to initial imperfections of the plate. The same boundary conditions were considered by Gale, but the plate was completely restrained from lateral displacements. In this case, however, agreement between theory and experiment was rather poor. (It may be significant that the analytical treatment corresponded to the applied boundary condition of a specified displacement at one edge of the plate, which was done in the experiment, and not to the problem meant to be solved-- a uniformly heated plate completely restrained laterally). Both of these analyses are simple cases of the more general problem of the plate restrained both rotationally and tangentially at all of its four edges. Before proceeding to tackle the general case, we remark briefly on the general relationship between the normal vibration problem and the elastic instability problem of plates.

Massonet [58], and later Lurie [59] and others have shown that there exists an intimate relationship between the two seemingly different problems of the normal vibrations and the instability of elastic systems. The differential equations for the two problems are similar, and for some cases identical. For such cases the eigenvalues for the two problems are the

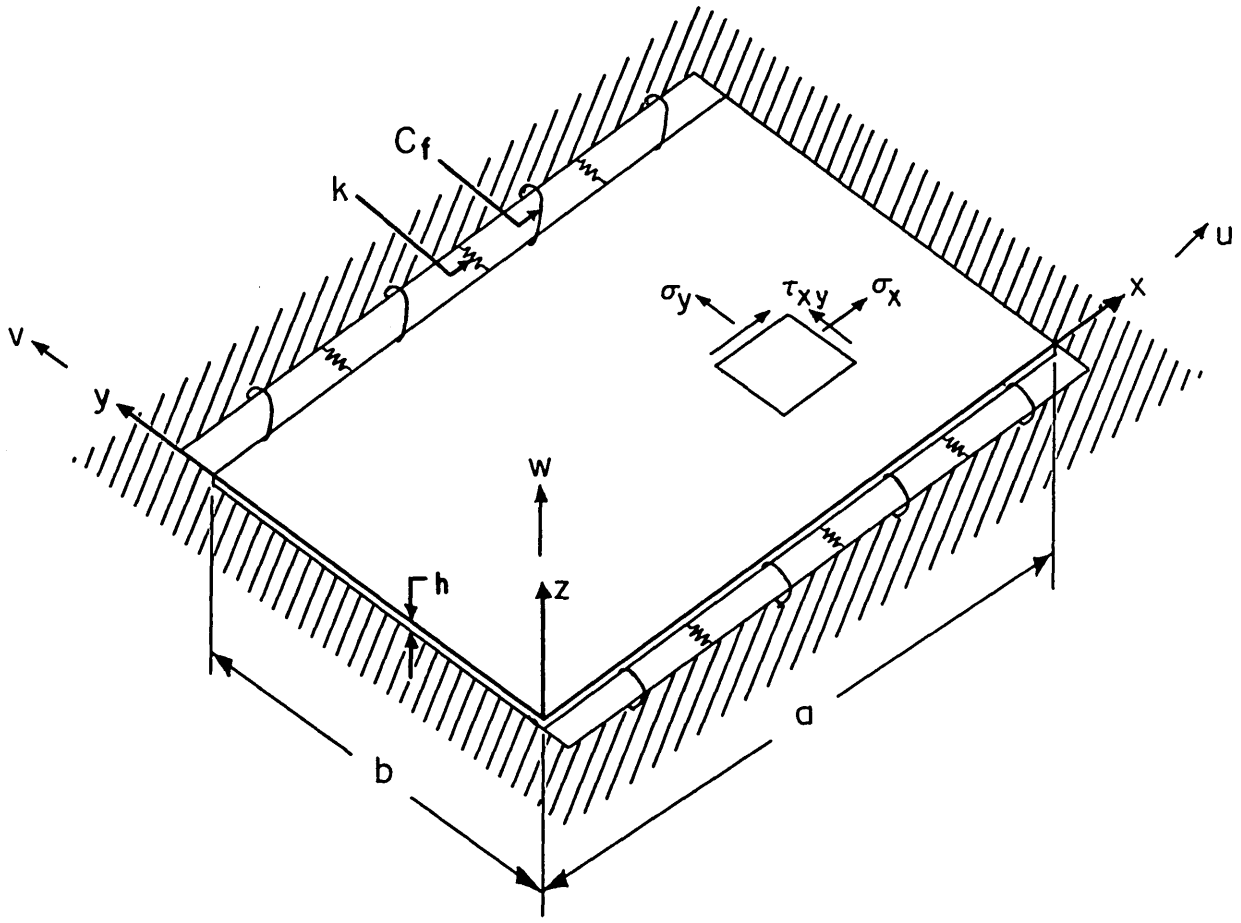

FIG. 7.1 PLATE COORDINATE SYSTEM

same, and therefore so are the characteristic mode shapes. For axially-loaded rectangular plates, it is shown [58] that these cases are: (1) All plate boundaries are simply supported and the plate may be subjected to forces in either or both axial directions at once, (2) The plate is loaded in one axial direction, the loaded edges are simply supported, the unloaded edges being arbitrarily rotationally restrained. In both cases the natural vibration modes of the plate retain their shape with increasing load and are identical to the buckling mode shapes. For such cases the squares of the natural frequencies vary linearly with the load until they vanish at the corresponding buckling load. This property is used in some instances to predict the buckling load by extrapolation of a few points obtained experimentally at relatively low loads on the frequency squared-load curve.

When any of the conditions of the two cases is not fulfilled, the modes do not retain their shape and the frequency squared does not vary linearly with the load. In many cases, however, the variation from linearity is very small, so that a linear relationship may be assumed in practice with a negligible error. Both of the analyses of Refs. [56] and [57] fall into the linear category.

In the following analysis the problem is generalized so that arbitrary support conditions at the longitudinal edges can be accounted for. The linear pre-buckling behavior is investigated first, then the non-linear aspect of the problem is solved by confining the non-linearity to the buckling deflection and assuming small vibration about this equilibrium position.

7.2 Equations of Motion and Boundary Conditions

Shell problems, some of which were analyzed in the previous chapters, are characterized by the fact that even for small deflections, the equations of compatibility and trans-

verse equilibrium are coupled. For flat plates, however, this coupling occurs only when large deflections are taken into account, in which case the coupling terms are non-linear. For a thermally thin plate under inertia loading, the equations, which bear von-Kármán's name, are given by,

$$\nabla^4 F + Eh\alpha\nabla^2 T = Eh[w_{xy}^2 - w_{xx}w_{yy}] \qquad (7\text{-}1a)$$

$$D\nabla^4 w + \rho h\ddot{w} = F_{yy}w_{xx} + F_{xx}w_{yy} - 2F_{xy}w_{xy} \qquad (7\text{-}1b)$$

where F is the Airy function for the stress resultants.

These equations indicate that the transverse displacement and the in-plane stresses are mutually dependent. In the small deflection case the non-linear terms on the right hand side of Eq.(7-1a) are neglected, in which case F can be solved for first, and the result substituted in Eq.(7-1b) which is then solved for w.

It is immediately appreciated that whereas in the latter case an exact solution is possible in many cases, the non-linear case must be solved by an approximate method. Marguerre's method, which was utilized in Section 3.3, will again be used here. In the non-linear case, this method calls for F to satisfy the boundary conditions on the average rather than at each point.

Since the analysis presented here is intended to be applicable to plates with various edge supports, the boundary conditons are formulated for general support conditions at the longitudinal edges.

Due to the fact that both in-plane and transverse displacements must be considered, four boundary conditions must be specified at each of the four edges of the plate, as per schedule given in Section 2.2. Considering the moment conditions first, we note that restraint against plate rotation

can take many forms in practice. The support might consist of a torque-tube, for instance, which provides a restoring moment per unit length proportional to the tube's torsional rigidity GJ and to the rate of change of its twist rate,

$$M_R = \frac{\partial}{\partial x}(GJ \frac{\partial \phi}{\partial x}) \qquad (7\text{-}2)$$

For a uniform support, and since the condition of continuity demands that the twist angle of the tube must be equal to the plate slope $\frac{\partial w}{\partial y}$ at any point x along the edge, the restoring moment for this case is:

$$M_R = GJ \frac{\partial^3 w}{\partial x^2 \partial y} \qquad (7\text{-}3)$$

Another form of rotational restraint is one where the restoring moment per unit length is proportional to the local angle of twist,

$$M_R = C_f \frac{\partial w}{\partial y} \qquad (7\text{-}4)$$

Such restraint is provided, for instance, by spiral springs distributed uniformly along the edges, of stiffness C_f.

For the sake of simplicity, while still retaining generality, the latter case is chosen in this study, i.e. the plate is assumed to be elastically restrained along its longitudinal edges by uniformly distributed torsional springs. This boundary condition is given by,

$$D\left(\frac{\partial^2 w}{\partial y^2} + \nu \frac{\partial^2 w}{\partial x^2} \right) = \mp C_f \frac{\partial w}{\partial y} \quad \text{at } y=0,b \qquad (7\text{-}5)$$

Along the other two edges the moment is assumed to vanish. This condition is given by,

$$D\left(\frac{\partial^2 w}{\partial x^2} + \nu \frac{\partial^2 w}{\partial y^2} \right) = 0 \qquad \text{at } x = 0, a \tag{7-6}$$

Next we assume that the vertical supports are non-yielding, in which case,

$$w = 0 \quad \text{at} \quad x = 0, a \quad \text{and} \quad y = 0, b \tag{7-7}$$

This completes the statement of the conditions on w. We next consider the conditions on the in-plane displacements and stress resultants. In general, restraint against in-plane displacements can be thought of as being afforded by distributed springs along the edges, of uniform stiffness, k. The boundary condition for such a support expresses the equilibrium between the springs' restoring force and the plate lateral force,

$$N_i \pm k_i u_i = 0 \qquad i = x, y \tag{7-8}$$

We now assume that the lateral edges are immovable, i.e. $k_x = \infty$, but the longitudinal edges are assumed flexible. These boundary conditions are therefore given by,

$$u = 0 \qquad \text{at } x = 0, a \tag{7-9}$$

$$\overline{\frac{\partial^2 F}{\partial x^2}} \pm k_y v = 0 \qquad \text{at } y = 0, b \tag{7-10}$$

where the bar denotes that this condition applies to the average stress.

Finally, the assumption of no shear at the edges is expressed as,

$$\overline{\frac{\partial^2 F}{\partial x \partial y}} = 0 \qquad \text{at } x = 0,\ a \qquad \text{and } y = 0,\ b \qquad (7\text{-}11)$$

Regrouping all the boundary conditions, we then have after some simplifications,

$$\text{At } x = 0,\ a: \quad u = 0,\ w = 0,\ \bar{F}_{xy} = 0,\ w_{xx} = 0, \qquad (7\text{-}12a)$$

$$\text{At } y = 0: \quad \bar{F}_{xx} + k_y v = 0,\ w = 0,\ \bar{F}_{xy} = 0,\ \zeta \frac{b}{2} w_{yy} + w_y = 0 \qquad (7\text{-}12b)$$

$$\text{At } y = b: \quad \bar{F}_{xx} - k_y v = 0,\ w = 0,\ \bar{F}_{xy} = 0,\ \zeta \frac{b}{2} w_{yy} - w_y = 0 \qquad (7\text{-}12c)$$

$$\text{where} \quad \zeta = \frac{2D}{bC_f} = \text{coefficient of rotational restraint} \qquad (7\text{-}13)$$

The parameter ζ varies between 0 and ∞ as the rotational restraint changes from complete fixity to complete freedom.

Similarly, the coefficient of lateral restraint is defined by

$$\delta = \frac{1}{1 + \dfrac{k_y b(1-\nu^2)}{2Eh}} \qquad (7\text{-}14)$$

The parameter δ varies between 0 and 1 as the lateral restraint changes from complete immovability to complete yielding.

By varying the values of ζ and δ, the solution may be applied to problems with a wide range of conditions at the longitudinal supports.

For the problem under investigation it is assumed that the plate is subjected to a uniform temperature difference

relative to the supports. This assumption implies that the edges are perfectly insulated and that a steady-state condition has been reached. In practice these conditions may not strictly hold, but this simplified analysis will reveal the main features of the problem. Under this assumption the $\nabla^2 T$ term in Eq.(7-1a) vanishes.

7.3 Effect of Temperature on Vibrations Prior to Buckling

We investigate first the case in which the temperature increment is below its critical value. In this case small-deflection theory is applicable. Then the solution of Eq.(7-1a) subject to Eqs.(7-12) is given by,

$$N_x = \frac{\partial^2 F}{\partial y^2} = -\frac{Eh\alpha\Delta T}{1-\nu}(1-\delta\nu) \tag{7-15a}$$

$$N_y = \frac{\partial^2 F}{\partial x^2} = -\frac{Eh\alpha\Delta T}{1-\nu}(1-\delta) = \bar{\delta}N_x \tag{7-15b}$$

$$N_{xy} = -\frac{\partial^2 F}{\partial x \partial y} = 0 \tag{7-15c}$$

where

$$\bar{\delta} = \frac{1-\delta}{1-\delta\nu} \tag{7-16}$$

Substituting Eqs.(7-15) into Eq.(7-1b) we have,

$$D\nabla^4 w + \frac{Eh\alpha\Delta T}{1-\nu}(1-\delta\nu)[w_{xx}+\bar{\delta}w_{yy}] + \rho h\ddot{w} = 0 \tag{7-17}$$

The solution of Eq.(7-17) subject to Eqs.(7-12) is,

$$w = \sum_p \bar{w}_p \sin\frac{p\pi}{a}x \left[\cos\beta_1\left(\frac{y}{b}-\frac{1}{2}\right) - \sqrt{\kappa}\cosh\beta_2\left(\frac{y}{b}-\frac{1}{2}\right)\right] e^{i\omega^{(p)}t} \tag{7-18}$$

The characteristic equation is given by,

$$\beta_1 \tan\frac{\beta_1}{2} + \beta_2 \tanh\frac{\beta_2}{2} + \frac{\zeta}{2}(\beta_1^2 + \beta_2^2) = 0 \qquad (7\text{-}19)$$

where,

$$\beta_{1,2} = \frac{p\pi}{\lambda}\left\{\gamma_n \frac{n}{p}\left[(1-\bar{\delta})r + \left(\frac{\bar{\delta}n}{2p}\gamma_n\right)^2 r^2 + \left(\frac{\bar{\omega}_o^{(p)}}{\gamma_n}\frac{p}{n}\right)^2 \Omega^{(p)2}\right]^{\frac{1}{2}}\right. \qquad (7\text{-}20a)$$

$$\left. \mp \left[1 - \frac{\bar{\delta}}{2}\left(\frac{n}{p}\gamma_n\right)^2 r\right]\right\}^{\frac{1}{2}}$$

$$\sqrt{\mathcal{H}} = \frac{\cos\frac{\beta_1}{2}}{\cosh\frac{\beta_2}{2}} \qquad (7\text{-}20b)$$

and where,

$$\bar{\omega}_o^{(p)} = \left(\frac{a}{p\pi}\right)^2 \sqrt{\frac{\rho h}{D}}\,\omega_o^{(p)} = \text{Eigenvalue for } p^{th} \text{ natural vibration mode of the unstressed plate. Obtained by letting } r=0 \text{ and } \Omega^{(p)}=1 \text{ in Eq.(7-20a).} \qquad (7\text{-}21a)$$

$$\gamma_n = \frac{12\alpha}{h^2}\left(\frac{a}{n\pi}\right)^2(1+\nu)(1-\delta\nu)\Delta T_{cr} = \text{Eigenvalue for lowest buckling mode. Obtained by letting } r=1 \text{ and } \Omega^{(p)}=0 \text{ in Eq.(7-20a).} \qquad (7\text{-}21b)$$

and where n is the value of p for lowest buckling mode, r is the temperature ratio $\Delta T/\Delta T_{cr}$ and $\Omega^{(p)}$ is the frequency ratio $\omega^{(p)}/\omega_o^{(p)}$.

If our attention is restricted to the low frequencies of plates of moderate aspect-ratio λ, then we may limit the consideration to those modes whose y dependence is determined by the first eigenvalue of Eq.(7-19). [For λ of order 1, some modes corresponding to the 2nd eigenvalue for p=1 might be lower than the first eigenvalue for p=3, for example].

Our main interest is in the variation of $\Omega^{(p)}$ with r. In general, there is no explicit expression for $\Omega^{(p)}$ in terms of r, and the exact solution for each r must be obtained numerically. This must be preceded by solving for $\bar{\omega}_o^{(p)}$ and γ_n.

For the case of lateral freedom at the longitudinal edges ($\delta = 1$), Eq.(7-19) had long been solved for various values of the rotational restraint ζ and the aspect ratio λ to yield γ_p, which is equal to $\bar{\omega}^{(p)}$ in this case. The results are given, for example, in Refs.[60] and [61]. Similar results for γ_p may be obtained for other values of δ, either by systematically solving Eq.(7-19) for different values of (p/λ), or by approximate methods.

For one particular case, the plate rotationally free at the longitudinal edges ($\zeta = \infty$), the characteristic equation simplifies into an explicit solution for γ.

$$\gamma_{pq}^2 = \frac{[1+(\frac{q\lambda}{p})^2]^2}{1+\bar{\delta}(\frac{q\lambda}{p})^2} \tag{7-22}$$

where the buckling modes (which are in this case the same as the natural vibration modes, but $\gamma_p \neq \bar{\omega}_o^{(p)}$) are given by,

$$w_{pq} = \sin\frac{p\pi}{a}x \sin\frac{q\pi}{b}y \tag{7-23}$$

It is evident that whereas the effect of rotational restraint is to raise the critical temperature, the effect of lateral restraint is to lower it.

As mentioned above, for $\delta = 1$ ($\bar{\delta} = 0$) the eigenvalues of the buckling and vibration problems are the same, therefore the mode shapes remain unaltered with r. The relationship between $\Omega^{(p)}$ and r in this case is simply given by,

$$\Omega^{(p)^2} = 1 - \left(\frac{n\bar{\omega}_o^{(n)}}{p\bar{\omega}_o^{(p)}}\right)^2 r \qquad (7\text{-}24)$$

Since r, by definition, is the ratio of the actual temperature increment to the lowest critical temperature increment, the coefficient of r in Eq.(7-24) depends on the mode number p. For p = n, i.e. for the vibration mode identical with the lowest buckling mode, its value is 1. For all other values of p, it will be smaller than 1, since unlike the fundamental frequency, which always occurs for p = 1, the value of p corresponding to the lowest critical temperature (p = n) is in general not 1 but an integer close to λ , depending on ζ .

In the general case, when $\zeta \neq \infty$ and $\delta \neq 1$, the y dependence of each vibration mode changes with r, and the linear relationship indicated by Eq.(7-14) does not strictly hold. However, the variation from linearily is quite small for all cases, so that a linear dependence may be assumed. Thus the problem reduces to determining the coefficient of r in the expression. This coefficient, which for each mode p depends on n, λ , ζ and δ, may be determined by either one of the following two methods. In both methods it is assumed that the mode shapes do not vary with r.

In the first method account is taken of the variation of Y with p [where Y denotes the bracketed term in Eq.(7-18), which gives the functional dependence of each mode on y], thus the ratio $\bar{\omega}_o^{(n)} / \bar{\omega}_o^{(p)}$ is replaced by γ_n/γ_p in Eq.(7-24) to yield,

$$\Omega^{(p)^2} = 1 - \left(\frac{n\gamma_n}{p\gamma_p}\right)^2 r \qquad (7\text{-}25)$$

For given boundary conditions this method necessitates as many solutions of the transcendental characteristic equation as the number of modes of interest.

Fig. 7.2 compares Eq.(7-25) with the exact solution for the case $\lambda = 3$, $\delta = .769$, $\zeta = .061$. The excellent agreement is evident. Although this is not an extreme case, similar conclusions are reached for other values of δ.

In the second method all modes are assumed to have the same y dependence as the buckling mode, i.e. for any p, $Y = Y_n$.

Using Rayleigh's method (which is applicable since the modes are uncoupled), with the potential energy given by,

$$V = \frac{D}{2}\int_0^a\int_0^b (\nabla^2 w)^2 dydx + \frac{Eh\alpha\Delta T(1-\delta\nu)}{2(1-\nu)}\int_0^a\int_0^b (w_x^2+\bar{\delta}w_y^2)dydx$$
$$+ \frac{D}{2}(\zeta\frac{b}{2})\int_0^a w_{yy}^2\Big|_{y=0,b} dx \qquad (7\text{-}26)$$

the variation of $\Omega^{(p)}$ with r is obtained as,

$$\Omega^{(p)^2} = 1 - (\frac{n}{p}\gamma_n)^2 \frac{Q_2^{(p)}}{Q_1^{(p)}} r \qquad (7\text{-}27)$$

The p^{th} natural frequency of the unstressed plate is now given by the close approximation,

$$\omega_o^{(p)} = (\frac{\pi}{a})^2 \sqrt{\frac{D}{\rho h}}\sqrt{\frac{Q_1^{(p)}}{T_3}} \qquad (7\text{-}28)$$

where $Q_1^{(p)}$, $Q_2^{(p)}$, T_3 and all subsequent functions which are not defined in the text, are defined in Appendix 7A.

For given boundary conditions this method requires the solution of the characteristic equation just once,

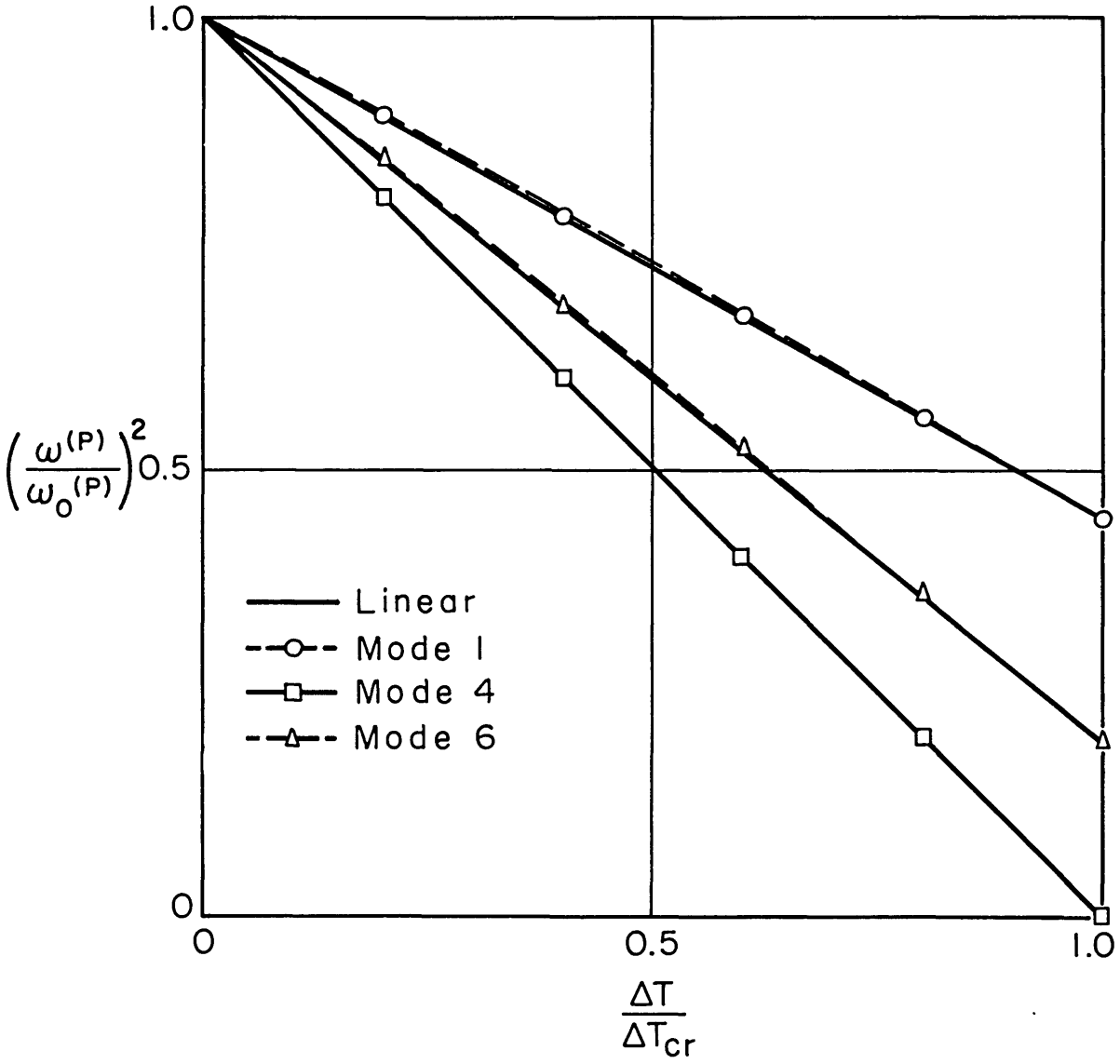

FIG. 7.2- EXACT AND APPROXIMATE VARIATION OF FREQUENCIES WITH TEMPERATURE INCREMENT BEFORE BUCKLING $\lambda = 3$, $\nu = .30$, $\zeta = .0610$, $\delta = .769$.

for p = n. The functions $Q_1^{(p)}$ and $Q_2^{(p)}$ then depend on this solution and the value of p only.

In Table 7.1 the values of γ_p^2 and $Q_1^{(p)}/Q_2^{(p)}$ are compared for the case shown in Fig. 7.2 for which n = 4. The relatively simpler second method is seen to compare well with the first method, the maximum error being 3.4 °/o, the error for most modes being less than 1 °/o.

TABLE 7.1

COMPARISON OF TWO APPROXIMATIONS TO THE PRE-BUCKLING VARIATION OF FREQUENCY WITH TEMPERATURE INCREMENT

$\lambda = 3$, $\delta = .769$, $\zeta = .0610$, $n = 4$, $\nu = .3$

Mode Number	First Method	Second Method	°/o Error
p	γ_p^2	$Q_1^{(p)}/Q_2^{(p)}$	
1	86.86	89.80	3.4
2	15.36	15.55	1.3
3	5.551	5.570	.36
4	3.018	3.020	.07
5	2.094	2.098	.20
6	1.677	1.682	.31

7.4 Vibrations in the Post-Buckling State

We next turn to the investigation of the case in which the temperature increment has exceeded its critical value and the plate has consequently buckled. It is assumed that the motion consists of small vibration of amplitude $\bar{w}_1$ about a finite buckling deflection of amplitude $\bar{w}_o$, where $\bar{w}_o \gg \bar{w}_1$. Whereas the actual amplitude of the vibration modes is arbi-

trary (within the small vibration assumption) the amplitude $\bar{w}_o$ is determined uniquely by the value of r, where now $r > 1$. Since large deflections are involved, the non-linear terms in Eqs.(7-1) must now be retained.

If the vibration modes are chosen as before, the total displacement is of the form,

$$w = [\bar{w}_o \sin\frac{n\pi}{a}x + \bar{w}_1 \sum_p q_p(t)\sin\frac{p\pi}{a}x]\ Y_n \qquad (7\text{-}29)$$

For the purpose of obtaining a relatively simple explicit expression for F, it is useful to expand Y_n in Fourier series.

Therefore, let,

$$Y_n = \cos\beta_1(\frac{y}{b}-\frac{1}{2}) - \sqrt{\varkappa}\cosh\beta_2(\frac{y}{b}-\frac{1}{2}) = \sum_{m\ \text{odd}}^{M} a_m \sin\frac{m\pi}{b}y \qquad (7\text{-}30)$$

where the coefficients a_m are given by,

$$a_m = \frac{4m}{\pi}\cos\frac{\beta_1}{2}\ \frac{(\frac{\beta_1}{\pi})^2 + (\frac{\beta_2}{\pi})^2}{m^4 + [(\frac{\beta_2}{\pi})^2 - (\frac{\beta_1}{\pi})^2]m^2 - (\frac{\beta_1}{\pi})^2(\frac{\beta_2}{\pi})^2} \qquad (7\text{-}31)$$

It is easily seen that $a_m \propto m^{-3}$ for large m; therefore rapid convergence is assured and the upper limit M can be quite low. It is recognized that the moment boundary conditions at y = 0 and y = b are not satisfied, but it is argued that since the expansion closely approximates the actual function Y_n (except <u>at</u> the boundaries) no appreciable error is introduced in calculating the stress function. Furthermore, whenever w appears explicitly, as in the energy expressions, the Fourier expansion is not needed.

The deflection w is therefore written as:

$$w = [\bar{w}_o \sin\frac{n\pi}{a}x + \bar{w}_1 \sum_{p} q_p(t)\sin\frac{p\pi}{a}x] \sum_{m\ \text{odd}}^{M} a_m \sin\frac{m\pi}{b}y \qquad (7\text{-}32)$$

Upon substitution of Eq.(7-32) into Eq.(7-1a) and remembering that for this problem $\nabla^2 T = 0$, the expression for the stress function F is obtained,

$$F = F_1 + F_2 \qquad (7\text{-}33)$$

where,

$$F_1 = Eh\,\lambda^2 \sum_{i=0} \sum_{j=0} \frac{F_{ij}}{(i^2+\lambda^2 j^2)^2} \cos\frac{i\pi}{a}x \cos\frac{j\pi}{b}y \qquad (7\text{-}34a)$$

$$F_2 = \frac{\bar{N}_x}{2} y^2 + \frac{\bar{N}_y}{2} x^2 \qquad (7\text{-}34b)$$

where the average stresses $\bar{N}_x$ and $\bar{N}_y$ depend on the buckling amplitude $\bar{w}_o$ but not on the vibration amplitude $\bar{w}_1$.

The coefficients F_{ij} are given by:

$$F_{0j} = \frac{j^2}{8} G_1(j)\ [\bar{w}_o{}^2 n^2 + 2\bar{w}_o\bar{w}_1 n^2 q_n + \bar{w}_1{}^2 \sum_{p}^{P} p^2 q_p{}^2] \qquad (7\text{-}35a)$$

$$F_{i0} = \frac{i^2}{8} S_1\ [2\bar{w}_o\bar{w}_1(q_{i-n} - q_{n-i} - q_{i+n}) \qquad (7\text{-}35b)$$

$$+ \bar{w}_1{}^2\Big(\frac{q_i{}^2}{2} - 2\sum_{0<p\le P-i} q_p q_{i+p} + 2\sum_{i-P\le p<\frac{i}{2}} q_p q_{i-p}\Big)]$$

$$F_{ij} = \frac{\bar{w}_1^2}{4}\left\{ \frac{i^2}{4} G_2(j) q_{\frac{i}{2}}^2 + \sum_{\substack{0<i\leq P-1 \\ 0<p\leq P-i}} G_3(i,j,p) q_p q_{i+p} \right.$$

$$\left. - \sum_{\substack{2<i\leq 2P \\ i-P\leq p<\frac{i}{2}}} G_4(i,j,p) q_p q_{i-p} \right\} \qquad (7\text{-}35c)$$

$$+ \frac{\bar{w}_o \bar{w}_1}{4}\left\{ G_3(i,j,n) q_{i+n} + G_4(i,j,n)[q_{n-i} - q_{i-n}] \right\}$$

For i = 2n, the following terms should be added:

$$F_{2n,0_{add}} = \frac{\bar{w}_o^2 n^2}{2} S_1 \qquad (7\text{-}35d)$$

$$F_{2n,j_{add}} = \frac{\bar{w}_o^2 n^2}{4} G_2(j) \qquad (7\text{-}35e)$$

The average stresses $\bar{N}_x$ and $\bar{N}_y$ must satisfy the boundary conditions. Using Eqs.(7-12) they are given as,

$$\bar{N}_x = -\frac{Eh}{1-\nu^2}\left[\alpha\Delta T(1+\nu) - \nu\frac{\bar{v}}{b} - \frac{\pi^2\lambda^2}{8a^2}\bar{w}_o^2(S_2+\nu S_1)\right] \qquad (7\text{-}36a)$$

$$\bar{N}_y = -\frac{Eh}{1-\nu^2}\left[\alpha\Delta T(1+\nu) - \frac{\bar{v}}{b} - \frac{\pi^2\lambda^2}{8a^2}\bar{w}_o^2(S_1+\nu S_2)\right] \qquad (7\text{-}36b)$$

where $\bar{v} = v(b)-v(0)$ is the total v displacement of the plate.

Once F is obtained, the relationship between the buckle amplitude $\bar{w}_o$ and the temperature increment ΔT must first be determined. This is done by using the minimum potential energy principle. The potential energy of the buckled plate

is given by,

$$V = \frac{D}{2}\int_0^a\int_0^b (\nabla^2 w)^2 dydx + \frac{D}{2}\zeta\frac{b}{2}\int_0^a w_{yy}^2\Big|_{y=0,b} dx$$
$$+ \frac{1}{2E}\int_0^a\int_0^b [(\nabla^2 F_1)^2 + F_{2_{xx}}^2 + F_{2_{yy}}^2 - 2\nu F_{2_{xx}} F_{2_{yy}}]dydx \qquad (7\text{-}37)$$

Substituting Eq.(7-29) for w and Eqs.(7-33) - (7-35) for F and letting $\bar{w}_1 = 0$, the potential energy in the absence of vibration is obtained in terms of ΔT, $\bar{v}$ and the buckle amplitude $\bar{w}_o$,

$$V = V(\Delta T, \bar{v}, \bar{w}_o) \qquad (7\text{-}38)$$

Application of the minimum condition,

$$\frac{\partial V}{\partial \bar{w}_o}(\Delta T, \bar{v}, \bar{w}_o) = 0 \qquad (7\text{-}39)$$

yields the following relationship between ΔT, $\bar{v}$ and $\bar{w}_o$,

$$\alpha\Delta T(1+\nu)(S_1+S_2) + \frac{\bar{v}}{b}(S_1+\nu S_2) = \frac{\pi^2(1-\nu^2)}{16a^2}\lambda^2\bar{w}_o^2 S_6$$
$$+ \frac{\pi^2 h^2}{12\lambda^2 a^2} Q_1(n) + \frac{\pi^2\lambda^2}{8a^2}\bar{w}_o^2[S_1^2 + 2\nu S_1 S_2 + S_2^2] \qquad (7\text{-}40)$$

Now, using $\bar{N}_y$, as given by Eq.(7-36b), in the boundary conditions on the v displacement, $\bar{v}$ is obtained in terms of ΔT and $\bar{w}_o$ as,

$$\frac{\bar{v}}{b} = \delta\left[\alpha\Delta T(1+\nu) - \frac{\pi^2\lambda^2}{8a^2}\bar{w}_o^2(S_1+\nu S_2)\right] \qquad (7\text{-}41)$$

Substituting Eq.(7-41) in Eq.(7-40) and transposing, we get,

$$\Delta T = \frac{\pi^2 h^2 n^2}{12(1+\nu)(1-\delta\nu)\alpha a^2} \frac{Q_1^{(n)}}{Q_2^{(n)}} \left[1 + \frac{1}{S_8}\left(\frac{\bar{w}_o}{h}\right)^2\right] \qquad (7\text{-}42)$$

When $\bar{w}_o = 0$, Eq.(7-42) must reduce to the expression for the critical temperature, namely,

$$\Delta T_{cr} = \frac{\pi^2 h^2 n^2}{12(1+\nu)(1-\delta\nu)\alpha a^2} \frac{Q_1^{(n)}}{Q_2^{(n)}} \qquad (7\text{-}43)$$

Comparing this expression with the exact one given by Eq.(7-21b), we note that the nature of the approximation in this case is, of course, the same as encountered in Section 7.3, where it was shown that the error is very small. When Eq.(7-42) is solved for $\left(\frac{\bar{w}_o}{h}\right)^2$, we obtain,

$$\left(\frac{\bar{w}_o}{h}\right)^2 = S_8(r-1) \qquad (7\text{-}44)$$

Thus, Eq.(7-44) shows that the square of the buckle amplitude to thickness ratio is linearly dependent on the post-critical temperature ratio.

Using Eq.(7-44) it is now possible to determine the effect of r on the vibration modes and frequencies. The equations of motion are obtained by the energy approach, using Lagrange's equations.

The potential energy for this case takes the form,

$$V = \frac{D}{2}\int_0^a\int_0^b (\nabla^2 w)^2 dydx + \frac{D}{2}\zeta \frac{b}{2}\int_0^a w_{yy}^2\Big|_{y=0,b} dx$$

$$+ \frac{1}{2E}\int_0^a\int_0^b (\nabla^2 F_1)^2 dydx - \frac{1}{2}\int_0^a\int_0^b (\bar{N}_x w_x^2 + \bar{N}_y w_y^2) dydx \qquad (7\text{-}45)$$

where the average stresses $\bar{N}_x$, $\bar{N}_y$, are obtained by substituting Eq.(7-41) into Eqs.(7-36), and are given by,

$$\bar{N}_x = \frac{-Eh}{1-\nu^2}\left\{\alpha\Delta T(1+\nu)(1-\delta\nu) - \frac{\pi^2\lambda^2}{8a^2}\bar{w}_o^2[S_2(1-\delta\nu^2)+S_1(1-\delta)\nu]\right\} \qquad (7\text{-}46a)$$

$$\bar{N}_y = \frac{-Eh}{1-\nu^2}(1-\delta)\left\{\alpha\Delta T(1+\nu) - \frac{\pi^2\lambda^2}{8a^2}\bar{w}_o^2[S_1+\nu S_2]\right\} \qquad (7\text{-}46b)$$

The kinetic energy is given by,

$$T = \frac{\rho h}{2}\int_0^a\int_0^b \dot{w}^2 dydx \qquad (7\text{-}47)$$

By substituting Eq.(7-29) for w, Eqs.(7-34a) and (7-35) for F, and Eqs.(7-46) for $\bar{N}_x$ and $\bar{N}_y$ into Eqs.(7-45) and (7-47), the energy expressions are obtained in terms of the coordinates $q_p(t)$ and the buckle amplitude $\bar{w}_o$. Substituting these expressions into Lagrange's equations, which for this conservative system are given by,

$$\frac{d}{dt}\left(\frac{\partial T}{\partial \dot{q}_p}\right) + \frac{\partial V}{\partial q_p} = 0 \qquad (7\text{-}48)$$

then using Eq.(7-44) and neglecting non-linear terms in the q_p's by virtue of the assumption of small vibrations, the

equations of motion are obtained,

For $p \neq n$

$$\ddot{q}_p + [Q_4^{(p)} + Q_3^{(p)}r]q_p + [Q_5^{(p)}(r-1)][q_{2n-p} - q_{p-2n}] + [Q_6^{(p)}(r-1)]q_{p+2n} = 0 \qquad (7\text{-}49a)$$

For $p = n$

$$\ddot{q}_n + Q_3^{(n)}(r-1)q_n + Q_6^{(n)}(r-1)q_{3n} = 0 \qquad (7\text{-}49b)$$

where,

$$\ddot{q} = \frac{d^2q}{d(\omega_o^{(1)}t)^2} \qquad (7\text{-}50a)$$

$$\omega_o^{(1)} = \sqrt{\frac{Q_1^{(1)}}{T_3}} \quad \frac{\pi^2}{a^2}\sqrt{\frac{D}{\rho h}} = \text{Fundamental frequency of unheated plate} \qquad (7\text{-}50b)$$

Equations (7-49) seem to indicate that the mode $p = n$ is coupled with the mode $p = 3n$. However, since the analysis is limited to the lower modes, say for $p < 2n$, then the results are applicable to those modes only and the higher modes, say for $p > 2n$, should be left out in this case. The equations, therefore, reduce to the form,

For $p \neq n$

$$\ddot{q}_p + [Q_4^{(p)} + Q_3^{(p)}r]q_p + Q_5^{(p)}(r-1)q_{2n-p} = 0 \qquad (7\text{-}51a)$$

For p = n

$$\ddot{q}_n + Q_3^{(n)}(r-1)q_n = 0 \qquad (7\text{-}51b)$$

Since the coefficients of the equations of motion depend strongly on γ_n (through the functions Q_1, Q_2 and others) and since the behavior of the modes for which $p \neq n$ differs from the mode p = n, it is evident that accurate determination of γ_n and n is very important for any particular case.

The frequency chosen for the non-dimensionalization of the equations is the fundamental frequency of the unheated plate. In the literature there are no exact solutions available for the natural frequencies of unloaded plates with an arbitrary edge restraint. In fact exact solutions are available only for a few special cases, such as simple support, etc. Hearmon [62] compiled the available results for different combinations of simply-supported, clamped and free plate boundaries. Most of the results listed in this reference were obtained by the Rayleigh-Ritz method, Ref. [63] being an example. The fact that the published results for ζ other than $\zeta = \infty$ were obtained by an approximate manner when the exact solutions of Eq.(7-19) had been available for some time is somewhat surprising. As shown in Section 7.3 the solutions of that equation are applicable not only to the buckling problem for which they were obtained originally, but also to the vibration problem of the unheated plate. Therefore the results as given in Ref. [61] for example may be applied to the vibration problem. Apparently no published results are available for the higher eigenvalues for each value of p. These may be easily solved for, thus the higher frequencies may be obtained.

The fundamental frequency for the case $\lambda = 3$, $\zeta = 0$ is given in Ref. [62] as $\omega_o^{(1)} = 20.96(\frac{\pi}{a})^2 \sqrt{\frac{D}{\rho h}}$. The assumed modes

in that case consisted of sums of polynomials and trigonometric functions. The accuracy of this result, when compared to the exact solution of Eq.(7-19) is better than .05 $^{o}/o$. No results are given for the higher frequencies.

7.5 Application to a Particular Case

The results are applied now to a particular example. The plate to be considered is made of aluminum alloy, measures 24'' x 8'' and is 0.05'' thick. The value of the spring constant k_y is 31,700 lbs/in per running inch, the rotational restraint ζ is assumed to be such as to cause 4 longitudinal half-waves to occur in the buckling mode at the minimum critical temperature.

We have, then,

$$\lambda = 3; \quad n = 4; \quad \delta = .769; \quad \sqrt{\frac{D}{\rho h}} = 3000 \text{ in}^2/\text{sec}$$

Using the method given in Appendix 7C, we get $\gamma_n = 1.7374$ and $\zeta = .0610$. From Eq.(7-21b) we get $\Delta T_{cr} = 12.1\ ^{o}F$. Equation (7-31) is used to get the coefficients a_m's,

$$a_1 = .958047$$
$$a_3 = -.106954$$
$$a_5 = -.024615$$

The equations of motion for the first symmetrical mode and the first three antisymmetrical modes become (for $r > 1$),

$$\ddot{q}_1 + [.36037 + .10068\ r]\ q_1 = 0 \qquad (7\text{-}52a)$$

$$\ddot{q}_4 + 5.09352\ (r\text{-}1)\ q_4 = 0 \qquad (7\text{-}52b)$$

$$\ddot{q}_2 + [-.11703 + .38607\ r]\ q_2 + .41844\ (r\text{-}1)\ q_6 = 0 \qquad (7\text{-}52c)$$

$$\ddot{q}_6 + [-2.19525 + 3.52115\ r]\ q_6 + .41844\ (r-1)\ q_2 = 0 \qquad (7\text{-}52d)$$

The relationship between the buckle amplitude and the temperature ratio is,

$$\left(\frac{\bar{w}_o}{h}\right)^2 = .38771\ (r-1) \qquad (7\text{-}53)$$

Prior to buckling, $(r < 1)$, the equations read,

$$\ddot{q}_1 + [1.00000 - .53895\ r]\ q_1 = 0 \qquad (7\text{-}54a)$$

$$\ddot{q}_2 + [1.20955 - .94051\ r]\ q_2 = 0 \qquad (7\text{-}54b)$$

$$\ddot{q}_4 + 2.54676\ [1-r]\ q_4 = 0 \qquad (7\text{-}54c)$$

$$\ddot{q}_6 + [6.54976 - 5.22386\ r]\ q_6 = 0 \qquad (7\text{-}54d)$$

For this case $\omega_o^{(1)} = 19.0\ \frac{\pi^2}{a^2}\ \sqrt{\frac{D}{\rho h}} = 155.4$ cps.

The frequencies of the various modes are plotted as functions of the temperature ratio, the results shown in Fig. 7.3.

7.6 Concluding Remarks

Equations of motion have been derived for thermally stressed plates both before and after initial buckling. These equations yield the free vibration characteristics of these plates for the two equilibrium states as affected by the temperature rise. The results are valid for uniformly heated plates with two opposite edges simply supported and with generalized support conditions on the other two edges.

The following general observations may be made:

(1) The initial buckling mode has a profound effect on the plate's behavior in the post-buckling range.

(2) All of the plate's vibration frequencies decrease with

the temperature rise before buckling occurs.

(3) The vibration mode associated with the initial buckling mode is the mode affected most strongly by the temperature rise. The square of its frequency varies linearly with temperature rise, its rate of increase after buckling being twice as much as its rate of decrease before buckling for all cases.

(4) In the post buckling state, each vibration mode is composed of two pre-buckling vibration modes, the degree of coupling among them being dependent on the edge conditions. The sum of the number of half waves of the two modes is always twice the number of half waves in the buckling mode, thus no coupling exists between symmetrical and antisymmetrical modes.

(5) The square of the buckle-amplitude-to-thickness ratio is a linear function of the temperature rise; the coefficients of this function depend on the nature of the edge-supports.

In Appendix 7B, a generalized analysis of the problem of a plate subjected to a specified compressive displacement at one of the lateral edges rather than a temperature rise is presented. This corresponds to the case treated in Ref. [57]. It is shown that the results for this problem are quite different from the results for the problem treated above. In particular, stronger coupling among the modes exists in the post-buckling range. In Appendix 7C a method is presented by which the buckling temperature may be obtained in practice in certain cases.

This analysis was restricted to the following two idealized conditions: (a) Perfectly flat plates; (b) A uniform temperature distribution. The effects of initial deformations and non-uniform temperature distribution may be treated rigorously as modifications to this analysis.

The effects of initial deformations may be expected to be: a) To alter the functional relationship between the buckle amplitude and the temperature rise, so as to tend to increase the deflection at any temperature; b) To cut down the reduction in the frequencies of the lower modes in the pre-buckling state near the critical temperature.

The primary effect of a non-uniform temperature distribution is to alter the stress-function's spatial distribution. Therefore, the relationship between the buckle amplitude and the temperature rise is expected to change, thus affecting the frequencies through a change in the coefficients of the equations of motion.

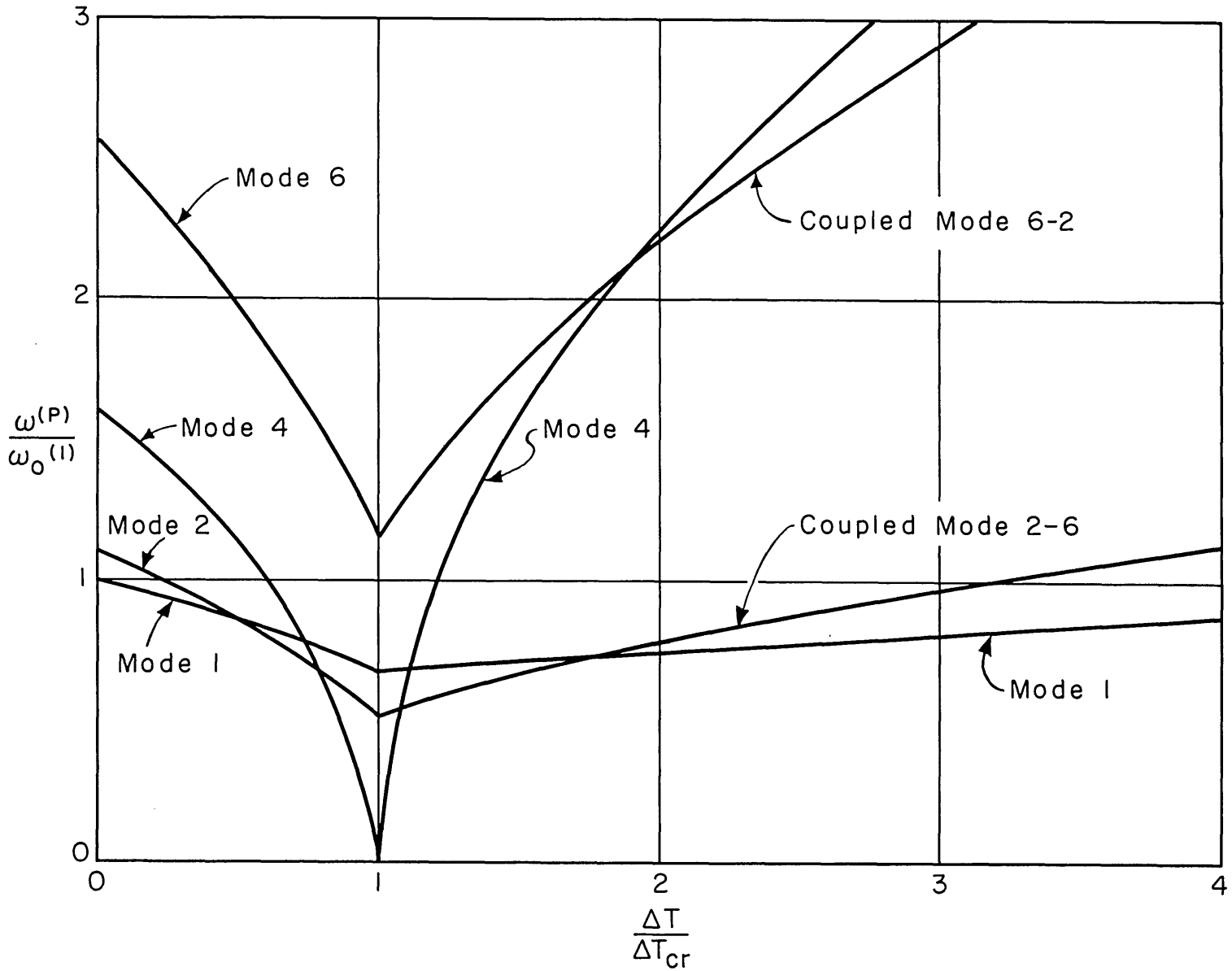

FIG. 7.3- VIBRATION FREQUENCIES vs. TEMPERATURE INCREMENT $\lambda = 3$, $\nu = .30$, $\zeta = .0610$, $\delta = .769$ $n = 4$.

APPENDIX 7A

DEFINITION OF FUNCTIONS

The following are functions of n:

$$T_1 = [1+\frac{\sin\beta_1}{\beta_1}] - \frac{2}{\beta_1^2+\beta_2^2}[\beta_1\sin\beta_1+\kappa\beta_2\sinh\beta_2]$$

$$T_2 = \kappa[1+\frac{\sinh\beta_2}{\beta_2}] - \frac{2}{\beta_1^2+\beta_2^2}[\beta_1\sin\beta_1+\kappa\beta_2\sinh\beta_2]$$

$$T_3 = \frac{2}{b}\int_0^b Y_n^2 dy = T_1 + T_2$$

$$T_4 = 2b\int_0^b Y_n'^2 dy = [1-\frac{\sin\beta_1}{\beta_1}]\beta_1^2 - [1-\frac{\sinh\beta_2}{\beta_2}]\kappa\beta_2^2 + \frac{4\beta_1\beta_2}{\beta_1^2+\beta_2^2}[\beta_2\sin\beta_1 - \kappa\beta_1\sinh\beta_2]$$

$$S_1 = \sum_{m\ \text{odd}}^{M} m^2 a_m = \frac{1}{\pi^2} T_4$$

$$S_2 = (\frac{n}{\lambda})^2 \sum_{m\ \text{odd}}^{M} a_m^2 = (\frac{n}{\lambda})^2 T_3$$

$$S_3 = (\frac{n}{\lambda})^4 \sum_j [G_1(j)]^2$$

$$S_4 = 2\left(\frac{n}{\lambda}\right)^4 \sum_j \frac{[G_2(j)]^2}{[4(\frac{n}{\lambda})^2+j^2]^2}$$

$$S_5 = \left(\frac{n}{\lambda}\right)^4 \sum_j \frac{G_2(j)G_3(2,j,1)}{[4(\frac{n}{\lambda})^2+j^2]^2}$$

$$S_6 = S_1^2 + S_3 + S_4$$

$$S_7 = (1-\delta)S_1^2 + 2\nu(1-\delta)S_1S_2 + (1-\delta\nu^2)S_2^2$$

$$S_8 = \frac{2Q_1(n)}{3\lambda^4(S_7 + \frac{1-\nu^2}{2} S_6)}$$

The following are functions of n and p, except as noted:

$$Q_1(p) = p^4 \left\{T_1[(\frac{\beta_1}{p\pi})^2+1]^2 + T_2[(\frac{\beta_2}{p\pi})^2-1]^2\right\}$$

$$Q_2(p) = p^4 [T_3 + \bar{\delta}(\frac{\lambda}{p\pi})^2 T_4]$$

$$Q_3(p) = \frac{Q_1(n)}{Q_1(1)[S_6+\frac{2}{1-\nu^2} S_7]} \left\{4S_1^2+R_1+\frac{S_1\bar{\delta}}{S_1\bar{\delta}+S_2}[\frac{2S_2}{1+\nu}(S_1-S_2) - S_6]\right\} + (\frac{p}{n})^2\left\{S_3-\frac{S_2\bar{\delta}}{S_1\bar{\delta}+S_2}[\frac{2S_1}{1+\nu}(S_1-S_2)+S_6]\right\}$$

$$Q_3(n) = 2\frac{Q_1(n)}{Q_1(1)}$$

$$Q_4(p) = \frac{Q_1(p)}{Q_1(1)}[1 - (\frac{n\gamma_n}{p})^2 \frac{Q_2(p)}{Q_1(p)}] - Q_3(p)$$

$$Q_5^{(p)} = \frac{Q_1^{(n)}}{Q_1^{(1)}[S_6+\frac{2}{1-\nu^2}S_7]}[3S_1^2+R_3-R_5]$$

$$Q_6^{(p)} = \frac{Q_1^{(n)}}{Q_1^{(1)}[S_6+\frac{2}{1-\nu^2}S_7]}[-3S_1^2-R_2+R_4]$$

$$Q_6^{(n)} = \frac{3Q_1^{(n)}}{Q_1^{(1)}[S_6+\frac{2}{1-\nu^2}S_7]}[-S_1^2+S_5]$$

In the following expressions, the summations over $a_m a_{j-m}$ have the limits: $j-M \leq m < j/2$, $2 < j \leq 2M$, the summations over $a_m a_{j+m}$ have the limits: $0 < m \leq M-j$, $0 < j \leq M-1$.

$$G_1(j) = a_{j/2}^2 + 2\sum_m a_m a_{j-m} - 2\sum_m a_m a_{j+m}$$

$$G_2(j) = \sum_m (j+2m)^2 a_m a_{j+m} - \sum_m (j-2m)^2 a_m a_{j-m}$$

$$G_3(i,j,k) = \frac{(i+2k)^2}{4} j^2 a_{j/2}^2 + \sum_m [(mi+jk)^2 + (mi-ij-jk)^2] a_m a_{j-m} - \sum_m [(mi-jk)^2 + (mi+ij+jk)^2] a_m a_{j+m}$$

$$G_4(i,j,k) = \frac{(i-2k)^2}{4} j^2 a_{j/2}^2 + \sum_m [(mi-jk)^2 + (mi-ij+jk)^2] a_m a_{j-m} - \sum_m [(mi+jk)^2 + (mi+ij-jk)^2] a_m a_{j+m}$$

$$R_1(p) = \sum_j \left\{ \frac{[G_3(p-n,j,n)]^2}{[(p-n)^2+\lambda^2 j^2]^2} + \frac{[G_4(p+n,j,n)]^2}{[(p+n)^2+\lambda^2 j^2]^2} \right\}$$

$$R_2(p) = \sum_j \frac{G_3(p+n,\ j,n) G_4(p+n,j,n)}{[(p+n)^2+\lambda^2 j^2]^2}$$

$$R_3(p) = \sum_j \frac{G_3(p-n,j,n) G_4(p-n,j,n)}{[(p-n)^2+\lambda^2 j^2]^2}$$

$$R_4(p) = n^2 \sum_j \frac{G_2(j) G_3(2n,j,p)}{[4n^2+\lambda^2 j^2]^2}$$

$$R_5(p) = n^2 \sum_j \frac{G_2(j) G_4(2n,j,p)}{[4n^2+\lambda^2 j^2]^2}$$

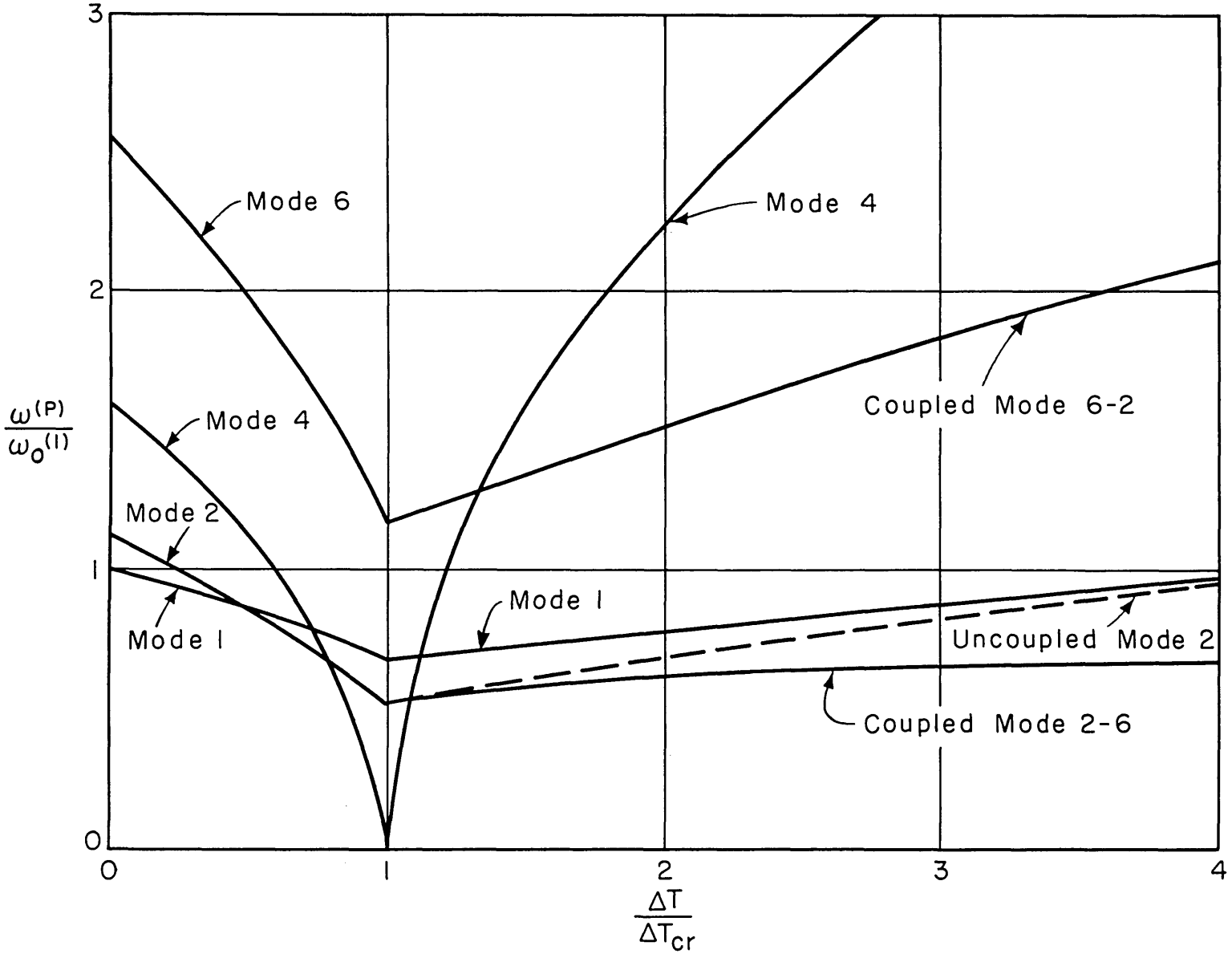

FIG. 7.4 - VIBRATION FREQUENCIES vs. TEMPERATURE INCREMENT FOR CASE TREATED IN APPENDIX 7B.

APPENDIX 7B

ANALYSIS OF A PLATE SUBJECTED TO A SPECIFIED DISPLACEMENT AT ONE EDGE

The case treated by Gale [57] is generalized in this Appendix. The problem is similar to the one treated in the body of this chapter, except that the plate is subjected to an applied compressive displacement u_a at the edge $x = a$ instead of being heated uniformly. For this case the boundary conditions of Eq.(7-12a) read,

$$\text{At } x = 0,\ u = 0,\ w = 0,\ \bar{N}_{xy} = 0,\ \frac{\partial^2 w}{\partial x^2} = 0 \qquad (7B\text{-}1a)$$

$$\text{At } x = a,\ u = -u_a,\ w = 0,\ \bar{N}_{xy} = 0,\ \frac{\partial^2 w}{\partial x^2} = 0 \qquad (7B\text{-}1b)$$

and the stresses $\bar{N}_x$ and $\bar{N}_y$ of Eqs.(7-15) now are,

$$N_x = -\frac{Ehu_a}{a}\,\frac{1-\delta\nu^2}{1-\nu^2} \qquad (7B\text{-}2a)$$

$$N_y = -\frac{Ehu_a}{a}\,\frac{1-\delta}{1-\nu^2}\,\nu \qquad (7B\text{-}2b)$$

In the pre-buckling range, the equations for this problem (problem II) are identical to those of the main problem (problem I) if the factor $\bar{\delta}$ is replaced by $\bar{\nu}$, where,

$$\bar{\nu} = \frac{1-\delta^*}{1-\delta^*\nu^2}\,\nu \qquad (7B\text{-}3)$$

and where δ^* denotes the coefficient of lateral restraint for problem II. If $\bar{\nu}$ is set equal to $\bar{\delta}$, then,

$$\frac{1-\delta}{1-\delta\nu} = \frac{1-\delta^*}{1-\delta^*\nu^2}\nu \qquad (7B\text{-}4)$$

from which follows,

$$\delta = \frac{1+\delta^*\nu}{1+\nu} \qquad (7B\text{-}5)$$

This means that for any problem II with a given value of δ^* there exists a corresponding problem I with a value of δ given by Eq.(7B 5) (but not vice-versa, since for $\delta < \frac{1}{1+\nu}$, the corresponding value of δ^* in negative; this case, however, may correspond to a lateral pre-stretching of the plate), the frequency results for both problems being the same in the pre-buckling state. (The other parameters must be equal for both problems).

In the post-buckling state, no such direct correspondence exists. For problem II, the relationship between the applied displacement u_a and the buckle amplitude reads,

$$u_a = \frac{\pi^2 h^2 n^2}{12(1-\delta^*\nu^2)a} \frac{Q_1^{(n)}}{Q_2^{(n)}}\left[1 + \frac{1}{S_8}\left(\frac{\bar{w}_o}{h}\right)^2\right] \qquad (7B\text{-}6)$$

where the functions Q_i, S_i are the same as for problem I if $\bar{\delta}$ is replaced by $\bar{\nu}$.

The equations of motion for problem II are the same as for problem I, except that in this case $Q_3^{(p)}$ is replaced by,

$$Q_3^{(p)*} = \frac{Q_1^{(n)}}{Q_1^{(1)}(S_6+\frac{2}{1-\nu^2}S_7)}\Big\{[4S_1^2 + R_1 + \frac{S_1\bar{\nu}}{S_1\bar{\nu}+S_2}(\frac{2S_1S_2}{\nu}-S_6)] \tag{7B-7}$$

$$+ (\frac{p}{n})^2[S_3 - \frac{S_2}{S_1\bar{\nu}+S_2}(2\frac{\bar{\nu}}{\nu}S_1^2 + S_7)]\Big\}$$

the other coefficients remaining the same.

Fig. 7.4 shows that results for problem II with a value of δ^* ($\delta^* = 0$) "matched" to the value of δ of the example of problem I given in Section 7.5, all other parameters remaining the same. A comparison of Figs. 7.3 and 7.4 shows that while the pre-buckling behavior of all modes and the post-buckling behavior of mode 4 are the same, the post-buckling behavior of all other modes is quite different. In particular, the coupling effect is stronger in this case.

APPENDIX 7C

A METHOD OF DETERMINING THE BUCKLING TEMPERATURE IN CERTAIN CASES

When the value of ζ is unknown for any particular case (e.g. its estimate is difficult or its experimental evaluation is impractical) but the value of n is known experimentally, then the following method may be used to solve for γ_n and to obtain ζ.

If the assumption is made that the value of ζ is such that the critical temperature is a minimum for the given δ, λ and n, then we have,

$$\frac{\partial \Delta T_{cr}}{\partial \left(\frac{\lambda}{n}\right)} = 0 \qquad (7C\ 1)$$

Substituting Eq.(7-21b) into Eq.(7C-1), the latter can be written as,

$$\frac{\partial \gamma}{\partial \left(\frac{\lambda}{n}\right)} = \frac{\gamma}{\left(\frac{\lambda}{n}\right)} \qquad (7C\text{-}2)$$

where the subscript n has been dropped. For the general case γ is not an explicit function of $\left(\frac{\lambda}{n}\right)$. However, if Eq.(7-19) is solved for ζ we have,

$$\zeta = -\frac{\left(\frac{\lambda}{n}\right)}{\pi\gamma\bar{\beta}}\left[\bar{\beta}_1 \tan\frac{\beta_1}{2} + \bar{\beta}_2 \tanh\frac{\beta_2}{2}\right] \qquad (7C\text{-}3)$$

where,

$$\bar{\beta}_1 = \frac{\lambda}{n\pi}\,\beta_1 \tag{7C-4a}$$

$$\bar{\beta}_2 = \frac{\lambda}{n\pi}\,\beta_2 \tag{7C-4b}$$

$$\bar{\beta} = \sqrt{1 - \bar{\delta} + \frac{\bar{\delta}^2}{4}\gamma^2} \tag{7C-4c}$$

Then, for a fixed value of $\bar{\delta}$,

$$d\zeta = \frac{\partial \zeta}{\partial \left(\frac{\lambda}{n}\right)}\, d\left(\frac{\lambda}{n}\right) + \frac{\partial \zeta}{\partial \gamma}\, d\gamma \tag{7C-5}$$

For any fixed value of ζ, $d\zeta = 0$, and we have,

$$\frac{\partial \gamma}{\partial \left(\frac{\lambda}{n}\right)} = - \frac{\partial \zeta / \partial \left(\frac{\lambda}{n}\right)}{\partial \zeta / \partial \gamma} \tag{7C-6}$$

Combining Eqs. (7C-2) and (7C-6), we get the condition for minimum ΔT_{cr} as,

$$\left(\frac{\lambda}{n}\right) \frac{\partial \zeta}{\partial \left(\frac{\lambda}{n}\right)} + \gamma \frac{\partial \zeta}{\partial \gamma} = 0 \tag{7C-7}$$

Using Eq. (7C-3) to evaluate the derivatives, we obtain, finally,

$$\gamma\left[1 - \bar{\delta}\left(1 - \frac{1-\frac{\bar{\delta}}{2}}{\bar{\beta}}\gamma\right)\right]\frac{1}{\beta_1}\tan\frac{\beta_1}{2}$$

$$+ \gamma\left[1 - \bar{\delta}\left(1 + \frac{1-\frac{\bar{\delta}}{2}}{\bar{\beta}}\gamma\right)\right]\frac{1}{\beta_2}\tanh\frac{\beta_2}{2} \qquad (7C\text{-}8)$$

$$+ \left[1 - \frac{\gamma}{2}\left(2\bar{\beta} - 1 + \bar{\delta} - \frac{\bar{\delta}^2}{2}\gamma^2\right)\right]\sec^2\frac{\beta_1}{2}$$

$$+ \left[-1 - \frac{\gamma}{2}\left(2\bar{\beta} - 1 + \bar{\delta} - \frac{\bar{\delta}^2}{2}\gamma^2\right)\right]\mathrm{sech}^2\frac{\beta_2}{2} = 0$$

For any given values of $\bar{\delta}$, λ and n, therefore, Eq.(7C-8) may be solved for γ, thus the critical temperature is obtained and the value of ζ is determined using Eq.(7C-3). If, however, the value of ζ is actually such that the critical temperature is not a minimum for the given δ, λ and n, then this method is inapplicable.

CHAPTER 8

CONCLUSIONS

The purpose of this chapter is to compile and present a summary of the major conclusions drawn from the various phases of this study.

The investigation of the free vibration problem of conical shells has indicated the existence of an optimum method which satisfactorily accounts for the opposing effects of taper on membrane and bending frequencies. It was shown that this method may be used to obtain better approximations to the frequencies by the process of including more expansion modes in the analysis. This can be easily done provided adequate computational facilities, such as the IBM 704 computer for example, are available. The numerical calculations performed in this study have yielded first approximations to the frequencies for a wide range of the relevant parameters.

The study of the general shell and panel flutter problem has indicated the general characteristics of the phenomenon, which are common to a wide variety of structural components of different geometry and stiffness characteristics. The role of the initial frequency distribution of the shell (or panel) was shown to have a deciding influence on its behavior. Application of the Galerkin method to the panel flutter problem, which was questioned in the past, was shown to be valid, provided the results are interpreted correctly.

The investigation of the flutter problem of cylindrical

shells has revealed the important fact that the flutter speed and frequency of the shell reach a minimum for a particular mode number n. This mode number is different from the one associated with the minimum frequency of the shell. The flutter speeds obtained in this study were considerably lower than those obtained previously. It was shown that this was due to the neglect of axial bending stiffness of the shell in the previous study. An approximate criterion was developed which indicates the flutter mode. Using this criterion the computational labor involved in an extensive parametric study of this problem can be reduced considerably.

The study of the conical shell flutter problem has shown that the effect of taper is to increase the flutter speed of the shell. A method was developed by which reliable approximate results may be obtained. It was shown that this problem, as the free vibration problem, must depend for its satisfactory solution on the availability of a large scale computational facility.

The effects of thermal stresses on the vibration characteristics of plates of arbitrary support conditions were determined. It was shown that these effects are different, depending on whether the plate has buckled or not. It was shown that the effect of buckling is to increase the stiffness of all the modes and to cause coupling to occur among the modes in a particular manner. It was shown that the manner in which the plate is supported strongly affects its pre- and post-buckling dynamic behavior.

REFERENCES

1. Bisplinghoff, R.L., "Some Structural and Aeroelastic Considerations of High-Speed Flight", (Nineteenth Wright Brothers Lecture), JAS 23,4, pp. 289-330, 1956.

2. Mar, J.W., Schmit, L.A. et al, "The Influence of Aerodynamic Heating on the Structural Design of High-Speed Aircraft", Parts I-VIII, ASRL TR 55.1-55.3, 73.1-73.5, 1955-1958.

3. Budiansky, B., and Mayers, J., "Influence of Aerodynamic Heating on the Effective Torsional Stiffness of Thin Wings", JAS 23, 12, pp. 1081-1093, 1956.

4. Singer, J., and Hoff, N.J., "Effect of the Change in Thermal Stresses due to Large Deflections on the Torsional Rigidity of Wings", JAS 24, 4, Reader's Forum, 1957.

5. Bisplinghoff, R.L., and Dugundji, J., "Influence of Aerodynamic Heating on Aeroelastic Phenomena", paper presented at College of Aeronautics, Cranfield, England, August 1956.

6. Heldenfels, R.R., and Vosteen, L.F., "Approximate Analysis of Effects of Large Deflections and Initial Twist on Torsional Stiffness of a Cantilever Plate Subjected to Thermal Stresses", NACA Rep. 1361, 1958.

7. Crisp, J.D.C., "The Equation of Energy Balance for Fluttering Systems with Some Applications in the Supersonic Regime", paper presented at the IAS 27th Annual Meeting, N.Y. Jan. 1959.

8. Donnell, L.H., "Stability of Thin-Walled Tubes Under Torsion", NACA Rep. 479, 1933.

9. Marguerre, K., "Zur Theorie der Gekrümmten Platte Grosser Formänderung", Fifth International Congress for Applied Mechanics, Cambridge, Mass., 1938.

10. Wang, C.T., "Applied Elasticity", McGraw-Hill, New York, 1953.

11. Reissner, E., "On a Variational Theorem in Elasticity", Journal of Mathematics and Physics, 29, 2, 1950.

12. Federhofer, K., "Eigenschwingungen der Kegelschale", Ingenieur-Archiv, 9, pp. 288-304, 1938.

13. Goldberg, J.E., "Axisymmetric Oscillations of Conical Shells", Proceedings of the Ninth International Congress of Applied Mechanics, Brussels, Belgium, Vol. VII, September 1956, pp. 333-343.

14. Grigolyuk, E.I., "Small Vibrations of Thin Elastic Conical Shells", Izvestia AN, USSR Otdelnye Tekhnicheski Nauk, No. 6, pp. 35-44, 1956.

15. Herrmann, G., and Mirsky, I., "On Vibrations of Conical Shells", JAS 25, 7, pp. 451-458, 1958.

16. Flügge, W., "Statik und Dynamik der Schalen", Julius Springer, Berlin, 1934.

17. Mushtari, Kh., and Sachenkov, A.V., "Stability of Cylindrical and Conical Shells of Circular Cross Section, with Simultaneous Action of Axial Compression and External Normal Pressure", NACA TM 1433, 1958.

18. Ramakrishna, B.S., "Transient Response of Speakers and Vibrations of Conical Shells", Ph.D. Thesis, Ill. Inst. of Tech. 1949.

19. Partridge, G.R., "Modes of Vibrations of a Loudspeaker Cone", Ph.D. Thesis, Yale, 1950.

20. Jahnke, E., and Emde, F., "Tables of Functions", Dover Publications, N.Y., 1945.

21. Bisplinghoff, R.L., Ashley, H., and Halfman, R.L., "Aeroelasticity", Addison-Wesley, Cambridge, 1955.

22. Sylvester, M.A., and Baker, J.E., "Some Experimental Studies of Panel Flutter at Mach Number 1.3", NACA TN 3914, 1957.

23. Eisley, J.G., "The Flutter of a Two-Dimensional Buckled Plate with Clamped Edges in a Supersonic Flow", AFOSR TN 56-296, 1956.

24. Mitchell, D.H., "Flutter of a Buckled Plate", S.M. Thesis, M.I.T., 1957.

25. Martin Co. Dynamics Research Staff, "Flutter of Thin Panels at Subsonic and Supersonic Speeds", AFOSR TR 57-65, 1957.

26. Jordan, P.F., "The Physical Nature of Panel Flutter", Aero Digest, pp. 34-38, February 1956.

27. Miles, J.W., "Dynamic Chordwise Stability at Supersonic Speeds", North-American Aviation Rep. AL-1140, 1950.

28. Shen, S.F., "Flutter of a Two-Dimensional Simply-Supported Uniform Panel in a Supersonic Stream", MIT ASRL Rep. No. 25.10, 1952.

29. Nelson, H.C., and Cunningham, H.J., "Theoretical Investigation of Flutter of Two-Dimensional Flat Panels with One Surface Exposed to Supersonic Potential Flow", NACA Rep. 1280, 1956.

30. Goland, M., and Luke, Y.L., "An Exact Solution for Two-Dimensional Linear Panel Flutter at Supersonic Speeds", JAS, 21, 4, pp. 275-276, 1954.

31. Hedgepeth, J.M., "Flutter of Rectangular Simply Supported Panels at High Supersonic Speeds", JAS, 24, 8, pp. 563-573, 1957.

32. Eisley, J.G., "The Flutter of Simply Supported Rectangular Plates in Supersonic Flow", AFOSR TN 55-236, 1955.

33. Luke, Y.L., and St. John, A., "Supersonic Panel Flutter", WADC TR 57-252, 1957.

34. Movchan, A.A., "Ob ustoichivosti paneli, dvizhushcheisia v gaze", (On the Stability of a Panel Moving in a Gas), Prikladnaia Matematika i Mekhanika, 21, 2,1957. (Recently translated and issued as NASA RE 11-21-58W).

35. Houbolt, J.C., "A Study of Several Aerothermoelastic Problems of Aircraft Structures", Doctoral Thesis, E.T.H., Zurich, 1958.

36. Ashley, H., and Zartarian, G., "Piston Theory - A New Aerodynamic Tool for the Aeroelastician", JAS, 23, 12, pp. 1109-1118, 1956.

37. Pines, S., "An Elementary Explanation of the Flutter Mechanism", Proceedings of the National Specialists' Meeting on Dynamics and Aeroelasticity, IAS, pp. 52-58, November 1958.

38. Stepanov, R.D., "On the Flutter of Cylindrical Shells and Panels Moving in a Flow of Gas", NACA TM 1438, 1958.

39. Movchan, A.A., "O kolebaniiakh plactinki dvizhushcheisia v gaze", (On Vibrations of a Plate Moving in a Gas), Prikladnaia Matematika i Mekhanika, 20, 2, 1956. (Recently translated and issued as NASA RE 11-22-58W).

40. Fung, Y.C., "On Panel Flutter", JAS, 25, 3, pp. 145-160, 1958.

41. Miles, J.W., "On the Aerodynamic Stability of Thin Panels", JAS, 23, 8, pp. 771-780, 1956.

42. Miles, J.W., "Supersonic Panel Flutter of a Cylindrical Shell", JAS 24, 2, pp. 107-118, 1957. Also, "Supersonic Flutter of a Cylindrical Shell-II", JAS, 25, 5, pp. 312-316, 1958.

43. Leonard, R.W., and Hedgepeth, J.M., "On Panel Flutter and Divergence of Infinitely Long Unstiffened and Ring-Stiffened Thin-Walled Circular Cylinders", NACA Rep. 1302, 1957.

44. Kopzon, G.I., "Vibration of Thin-Walled Elastic Bodies in a Gas Flow", Doklady AN USSR, 107, 2, pp. 217-220, 1956. Also "Vibrations of a Shallow Wing-Shell in a Gas Flow", Doklady, AN USSR, 107, 3, pp. 377-380, 1956.

45. Holt, M., "Aerodynamic Forces on a Cylindrical Shell in Panel Flutter", AFOSR TN 58-974, 1958.

46. Murnaghan, F.D., "Introduction to Applied Mathematics", John Wiley and Sons, N.Y., 1948.

47. Flax, A.H., "Aeroelastic Problems at Supersonic Speeds", Proceedings of the 2nd International Aeronautical Conference, N.Y., pp. 322-359, 1949.

48. Wielandt, H., "The Method of Iteration for Non-Self-Adjoint Linear Eigenvalue Problems", Aerodynamische Versuchsanstalt Göettingen, 1943. Translation published by the Ministry of Aircraft Production, Great Britain, as MAP-VG-155.

49. Nielsen, J.M., "Quasi-Cylindrical Theory of Wing-Body Interference at Supersonic Speeds and Comparison with Experiment", NACA Rep. 1252, 1955.

50. Hayes, W.D., "A Buckled Plate in a Supersonic Stream", North-American Aviation Report AL-1029, 1950.

51. Love, A.E.H., "A Treatise on the Mathematical Theory of Elasticity", Fourth Edition, Dover Publications, N.Y., 1944.

52. Vlasov, V.S., "Basic Differential Equations in General Theory of Elastic Shells", NACA TM 1241, 1951.

53. Timoshenko, S., "Theory of Plates and Shells", McGraw-Hill, N.Y., 1940.

54. Goldenveiser, A.L., "Teoria uprugikh tonkikh obolochek", (Theory of Elastic Thin Shells), Gosizdat tekhnikoteoretich. literatury, Moscow, 1953.

55. Leonard, R.W., and Hedgepeth, J.M., "On the Flutter of Infinitely Long Panels on Many Supports", JAS, 24, 5, pp. 381-383, 1957.

56. Bisplinghoff, R.L., and Pian, T.H.H., "On the Vibrations of Thermally Buckled Bars and Plates", Proceedings of the 9th International Congress of Applied Mechanics, Brussels, Belgium, Vol. VII, September 1956, pp. 307-318.

57. Gale, A.P., "A Further Study of the Vibrations of a Thermally Buckled Plate", S.M. Thesis, M.I.T., Feb. 1957.

58. Massonnet, Ch., "Les Relations entre les Modes Normaux de Vibration et la Stabilité des Systèmes Elastiques", Bulletin des Cours et des Laboratoires d'Essais des Constructions du Génie Civil, Universite de Liége, Vol. 1, 1940.

59. Lurie, H., "Lateral Vibrations as Related to Structural Stability", Journal of Applied Mechanics, Vol. 19, No. 2, June 1952, pp. 195-204.

60. Bleich, F., "Buckling Strength of Metal Structures", McGraw-Hill, N.Y., 1952.

61. Lundquist, E.E., and Stowell, E.Z., "Critical Compressive Stress for Flat Rectangular Plates Supported Along all Edges and Elastically Restrained Against Rotation Along the Unloaded Edges", NACA TR 733, 1942.

62. Hearmon, R.F.S., "The Frequency of Vibration of Rectangular Isotropic Plates", Journal of Applied Mechanics, Vol. 19, No. 3, September 1952, pp. 402-403.

63. Iguchi, S., "Die Eigenwerte Probleme für die Elastische Rechteckige Platte", Memoirs of the Faculty of Engineering, Hokkaido Imperial University, Vol. 4, 1938, p. 305.

BIOGRAPHICAL NOTE

Yechiel Shulman was born in Tel-aviv, Israel, on January 28, 1930, received his primary and secondary education at the "Herzlia" Hebrew Gymnasium in that city and graduated in the Science Course in 1947. The next three years were spent in the Armed Services of Isreal and in 1950 he came to the U.S., where he attended the University of California at Berkeley for one semester, following which he came to M.I.T. As a member of the Honors Group in the Department of Aeronautical Engineering he received the Bachelor's and Master's degrees in June 1954. At the same time he completed the requirements for, and received a Bachelor's degree from the School of Industrial Management at M.I.T.

Following graduation, he joined the Aeroelastic and Structures Research Laboratory in the Department of Aeronautical Engineering, serving as a Research Engineer and as a Project Leader on various research Projects. In 1956 he became a Research Assistant in the Department of Aeronautical Engineering and enrolled as a Doctoral Candidate.

He was the recipient of the Richard C. DuPont Memorial Fellowship during the academic year 1953-54 and again during 1956-57. He is a member of Tau Beta Pi, Sigma Xi, Sigma Gamma Tau, and a member of the Institute of Aeronautical Sciences.

His publications include:

(1) "Stability of Flexible Helicopter Rotor Blades in Forward Flight", Journal of the Aeronautical Sciences, 23,7, 1956.

(2) "Wind Tunnel Investigation of the Response of Rigid and Elastic Helicopter Rotors to Control Forces and Inflow Variations", MIT ASRL TR 59-1, 1956.

(3) "On the Vibration of Thermally Stressed Plates in the Pre-Buckling and Post-Buckling States", MIT ASRL TR 25-25, 1958.